

Studies in Polymerizations Comprising Supramolecular Complexes

A THESIS SUBMITTED TO

PUNE UNIVERSITY

FOR THE DEGREE OF
DOCTOR OF PHILOSOPHY
(CHEMISTRY)

BY

SUNITA SURYAKANT SATAV
(M. Sc. ORGANIC CHEMISTRY)

UNDER THE GUIDANCE OF
DR. MOHAN G. KULKARNI

POLYMER SCIENCE AND ENGINEERING DIVISION
NATIONAL CHEMICAL LABORATORY
PUNE 411008 (INDIA)

18 JULY, 2007

CERTIFICATE

Certified that the work incorporated in the thesis entitled “**Studies in Polymerizations Comprising Supramolecular Complexes,**” submitted by Sunita Suryakant Satav, was carried out under my supervision. Such material as has been obtained from other sources has been duly acknowledged in the thesis.

Date: 18 July, 2007
National Chemical Laboratory,
Pune 411008.

Dr. M. G. Kulkarni
(Research Guide)

DECLARATION

I hereby declare that the work presented in the thesis entitled “**Studies in Polymerizations Comprising Supramolecular Complexes,**” submitted for Ph.D. degree to the University of Pune, has been carried out by me at the National Chemical Laboratory, Pune, under the supervision of Dr. M. G. Kulkarni. The work is original and has not been submitted in part or full by me for any degree or diploma to this or any other university.

Date: 18 July, 2007

National Chemical Laboratory,

Pune 411008.

Sunita S. Satav

(Research Student)

Acknowledgements

I am thankful to Dr. M. G. Kulkarni for being a great mentor, good friend and offering advice and encouragement whenever I need. He taught me useful skills for research, technical writing and presentations throughout the course of this doctoral research. I consider myself to be fortunate to work under his guidance. His kind and all-aspect help has made the past years an ever-good memory in my life.

It is my pleasure to acknowledge Dr. S. Sivaram, Director, National Chemical Laboratory, for permitting me to present this work in the form of thesis and also for creating DIRC, a perfect place to read and write effectively.

I am grateful to Dr. G. N. Sastry and Mr. M. Nagaraju for their help for Molecular modeling simulation.

My sincere thanks to Dr. R. N. Karmalkar, Ms. D. A. Dhobale, Dr. M. V. Badiger, Mr. M. J. Thakar, Dr. R. Rajmohanan, Dr. U. K. Kharul, Dr. K. V. Pandare, and Dr. G. V. N. Rathna for their suggestions and encouragement.

I would like to thank all my colleagues and friends, who not only helped in the lab, but also helped to shape the person I have become through this degree. It was a great pleasure to work with my colleagues who always kept me in the lively working environment and make each and every moment ever memorable. I am also thankful to Mr. Dhavale, Mr. Kokane, Mr. Bharati and Mr. Mahajan for their assistance.

I would like to acknowledge the financial support received from CSIR in the form of Junior and Senior Research Fellowship.

I am glad to dedicate this thesis to my teachers and family for continuous guidance and support.

Sunita S. Satav

18 July, 2007

Table of Content

	Page No.
List of Figures	vi
List of Tables	x
List of Schemes	xii
Abbreviations and Symbols	xiii
Abstract	xv
Chapter 1	
Literature Review	1-39
1.1 Introduction	1
1.2 Cyclodextrin Chemistry	3
1.2.1 Discovery of Cyclodextrins	5
1.2.2 Structure of Cyclodextrins	5
1.2.3 Inclusion Complexes of Cyclodextrins	7
1.2.3.1 Cyclodextrin Inclusion Complexes in Organic Chemistry	7
1.2.3.2 Cyclodextrin Inclusion Complexes in Polymer Science	8
1.2.3.3 Experimental Evidences for the Inclusion Complex Formation	14
1.2.3.4 Industrial Applications of Cyclodextrin Inclusion Complexes	17
1.3 Free Radical Polymerization of Multivinyl Monomers	18
1.3.1 Mechanism of Network Formation	18
1.3.2 Prior Approaches	20
1.3.2.1 Soluble Linear Polymers and Pendant Group Functionalization	20
1.3.2.2 Polymerization of Divinyl Monomers	21
1.4 Molecular Imprinting and Drug Delivery	24
1.4.1 General Principles of Molecular Imprinting	24
1.4.1.1 Covalent Imprinting	25
1.4.1.2 Non-covalent Imprinting	26
1.4.1.3 Semi-covalent Imprinting	27
1.4.2 Newer Approaches for Imprinting	27
1.4.2.1 Molecular Imprinting: Monolith to Nanomaterials	27
1.4.2.2 Novel Functional Cross-linkers	29
1.4.2.3 Two Stage Approach / Processable Imprinting	30

1.4.2.4	Stimuli Responsive Imprinted Polymers	32
1.4.3	Imprinted Polymers for Drug Delivery	33
Chapter 2		
Objective and Scope of the Work		40 - 43
Chapter 3		
Supramolecular Inclusion Complex: Synthesis		44 - 64
3.1	Introduction	45
3.2	Experimental	46
3.2.1	Materials	46
3.2.2	Measurements	46
3.2.3	Monomers Synthesis	46
3.2.3.1	Ethylene Glycol Methacrylate 4-Vinyl Benzoate (EGMAVB)	46
3.2.3.2	Trimethylolpropane Diacrylate 4-Vinyl Benzoate (TMPDAVB)	48
3.2.4	Inclusion Complex: Preparation	49
3.2.4.1	Precipitation Method	49
3.2.4.2	Solvent Evaporation Method	50
3.3	Results and Discussion	50
3.3.1	Inclusion Complex: Preparation	50
3.3.2	Inclusion Complex: Characterization	50
3.3.2.1	NMR of Inclusion Complex	50
3.3.2.2	FTIR of Inclusion Complex	56
3.3.2.3	XRD of Inclusion Complex	58
3.3.3	Molecular Modeling Calculations of Inclusion Complexes	59
3.3.3.1	Divinyl Monomers	59
3.3.3.2	Trivinyl Monomers	60
3.4	Conclusions	62
Chapter 4		
Supramolecular Inclusion Complex: Homopolymerization		63 - 89
4.1	Introduction	64
4.2	Experimental	65
4.2.1	Materials	65

4.2.2	Measurements	65
4.2.3	Inclusion Complex: Homopolymerization	66
4.2.3.1	EGDMA- β -CD IC (Polymerization in DMF)	66
4.2.3.2	EGDMA- β -CD IC (Polymerization in DMSO)	66
4.2.3.3	EGDMA-DM- β -CD IC (Polymerization in Chloroform)	66
4.2.3.4	EGDMA-DM- β -CD IC (Polymerization in Water)	67
4.2.3.5	Polymerization of EGMAVB Monomer	67
4.2.3.6	Comparative Experiments	67
4.2.4	Second Stage Polymerization	68
4.2.4.1	Intermolecular Cross-linking	68
4.2.4.2	Intramolecular Cross-linking	68
4.3	Results and Discussion	68
4.3.1	Inclusion Complex: Homopolymerization	68
4.3.2	Homopolymers: Characterization	70
4.3.2.1	FTIR of Homopolymers	70
4.3.2.2	NMR of Homopolymers	74
4.3.2.3	Intrinsic Viscosity of Homopolymers	80
4.3.2.4	Molecular Weight of Homopolymers by MALLS and GPC	85
4.3.3	Second Stage Polymerization	86
4.3.3.1	Intermolecular Cross-linking	86
4.3.3.2	Intramolecular Cross-linking	88
4.4	Conclusions	89

Chapter 5

Supramolecular Inclusion Complex: Copolymerization	90 - 112	
5.1	Introduction	91
5.2	Experimental	92
5.2.1	Materials	92
5.2.2	Measurements	92
5.2.3	Monomers Synthesis	92
5.2.3.1	Ethylene Glycol Isobutyrate Methacrylate (EGIBMA)	92
5.2.3.2	Trimethylolpropane Methacrylate (TMPMA)	93
5.2.3.3	Trimethylolpropane Diisobutyrate Methacrylate (TMPDIBMA)	93

5.2.4	Inclusion Complex: Copolymerization	94
5.2.5	Co-monomer Reactivity Ratio	95
5.2.6	Second Stage Polymerization	95
5.2.6.1	Intermolecular Cross-linking	95
5.2.6.2	Intramolecular Cross-linking	96
5.3	Results and Discussion	96
5.3.1	Inclusion Complex: Copolymerization	96
5.3.2	Copolymers: Characterization	96
5.3.2.1	FTIR of Copolymers	96
5.3.2.2	NMR of Copolymers	97
5.3.2.3	Intrinsic Viscosity of Copolymers	98
5.3.3	Co-monomer Reactivity Ratio	99
5.3.4	Second Stage Polymerization	110
5.3.4.1	Intramolecular Cross-linking	110
5.4	Conclusions	112

Chapter 6

Molecularly Imprinted Nanoparticles for Drug Delivery	113-140	
6.1	Introduction	114
6.2	Experimental	115
6.2.1	Materials	115
6.2.2	Measurements	115
6.2.3	Functional Copolymers: Synthesis	115
6.2.4	Functional Copolymers: THP Interaction Study (UV and FTIR)	116
6.2.5	THP Imprinted Nanoparticles: Synthesis	117
6.2.6	THP Imprinted Nanoparticles: Rebinding	117
6.2.7	THP Imprinted Nanoparticles: Selectivity	118
6.2.8	THP Imprinted Nanoparticles: Release	118
6.3	Results and Discussion	119
6.3.1	Functional Copolymers: Synthesis	119
6.3.2	Functional Copolymer: THP Interaction Study	120
6.3.3	THP Imprinted Nanoparticles: Synthesis	125
6.3.4	THP Imprinted Nanoparticles: Rebinding	128
6.3.4.1	Effect of Cross-link Density	129

6.3.4.2	Effect of THP to Carboxyl Ratio	131
6.3.4.3	THP Imprinted Nanoparticles: Binding Isotherm	133
6.3.5	THP Imprinted Nanoparticles: Selectivity	135
6.3.6	THP Imprinted Nanoparticles: Release Study	137
6.3.6.1	Effect of Cross-link Density	137
6.3.6.2	Effect of THP Loading	139
6.3.6.3	Effect of THP to Carboxyl Ratio	140
6.4	Conclusions	140
Chapter 7		
Conclusions and Recommendations for Future Research		141-146
7.1	Introduction	142
7.2	Significant Findings	142
7.3	Recommendations for Future Research	144
References		147-157
Publications		158
Curriculum Vitae		169-163

List of Figures

Chapter 1

Literature Review

1.1	Cyclodextrin structures	6
1.2	Structure of β -cyclodextrin	6
1.3	Anisole- α -CD IC and mechanism for its 'p' chlorination	8
1.4	Structure of PEG- α -CD inclusion complex	9
1.5	Cyclodextrin initiated polymerization of lactones	10
1.6	Cyclodextrin mediated aqueous polymerization	11
1.7	Interlocked cross-linked polymers from IC of divinyl monomers	13
1.8	Inclusion complex mediated controlled polymerization	14
1.9 A	X-ray diffractogram of a. free α -CD, b. valeric acid- α -CD IC, c. poly (oxyethylene)- α -CD IC	15
1.9 B	Schematic of a. channel type, b. cage herringbone type, c. cage brick type crystal structures formed by crystalline ICs	15
1.10	Solid-state ^{13}C CP/MAS NMR spectra of a. α -CD, b. PEA- α -CD IC (MW = 1200)	16
1.11	Reactions involved in polymerization of divinyl monomer	19
1.12	Process for covalent and non-covalent molecular imprinting	25
1.13	Synthesis of imprinted core-shell nanoparticles by emulsion polymerization	28
1.14	Novel cross-linkers for molecular imprinting	30
1.15	Preparation of imprinted nanospheres from diblock copolymers	31
1.16	pH responsive imprinted polymer synthesis	33
1.17	Molecularly imprinted polymers: drug loading and release	34
1.18	Enantioselective release	36
1.19	Template responsive drug release	37

Chapter 3

Supramolecular Inclusion Complex: Synthesis

3.1	^1H NMR of EGDMA- β -CD (1:1) IC	51
3.2	^1H NMR of EGDMA-DM- β -CD (1:1) IC	52

3.3	^1H NMR of EGMAVB- β -CD (1:1) IC	52
3.4	^1H NMR of TMPTMA- β -CD (1:2) IC	52
3.5	^1H NMR of TMPTA- β -CD (1:1) IC	53
3.6	^1H NMR of TMPDAVB- β -CD (1:2) IC	53
3.7	Solid state CP/MAS ^{13}C NMR of a. β -CD, b. EGDMA- β -CD (1:1) IC	55
3.8	Solid state CP / MAS ^{13}C NMR spectra of a. β -CD, b. TMPTMA- β -CD (1:2) IC, c. TMPTA- β -CD (1:1) IC	56
3.9	FTIR spectra of a. EGDMA- β -CD IC, b. TMPTA- β -CD IC	58
3.10	X-ray diffractogram of a. EGDMA- β -CD IC, b. EGMAVB- β -CD IC	59
3.11	X-ray diffractogram of a. TMPTA- β -CD IC, b. TMPDAVB- β -CD IC	59
3.12	Conformational studies a. EGDMA- β -CD IC, b. EGMAVB- β -CD IC	60
3.13	Hydrogen bonding in bent and stretched conformation of TMPTA	61
3.14	MD simulations of TMPTMA, TMPTA, and TMPDAVB conformations	62

Chapter 4

Supramolecular Inclusion Complex: Homopolymerization

4.1	FTIR spectra a. poly (EGDMA), b. poly (EGMAVB)	72
4.2	FTIR spectra of poly (TMPTMA) a. in presence, b. after removal of β -CD	72
4.3	FTIR spectra of poly (TMPTA) a. in presence, b. after removal of β -CD, c. expanded ester carbonyl region of poly (TMPTA)	73
4.4	FTIR spectra poly (TMPDAVB) a. in presence, b. after removal of β -CD	73
4.5	^1H NMR of poly (EGDMA)	74
4.6	^{13}C NMR of poly (EGDMA)	75
4.7	^{13}C NMR spectrum, expanded in (-OCH ₂ -CH ₂ O-) region	75
4.8	^1H NMR of poly (EGMAVB) by IC polymerization	76
4.9a	^1H NMR of poly (EGMAVB) by monomer polymerization	77
4.9b	Poly (EGMAVB): expanded spectrum	77
4.10	^1H NMR of poly (TMPTMA)	78
4.11	Structure of poly (TMPTA)	78
4.12	^1H NMR of poly (TMPTA) a. whole spectrum b. expanded region	79

4.13	¹ H NMR of poly (TMPDAVB)	80
4.14	Reduced viscosity and polymer concentration a. poly (EGDMA), b. poly (TMPTMA)	81
4.15	Structure of polymer a. poly (EGDMA) b. poly (TMPTMA)	82
4.16	Intrinsic viscosity <i>versus</i> molecular weight plots for ■ poly (TMPTMA), ◆ linear poly (EGDMA), and ▲ hyperbranched poly (EGDMA)	84
4.17	Mark-Houwink-Sakurada parameters of a. linear poly (EGDMA), b. hyperbranched poly (EGDMA), c. poly (TMPTMA)	84
4.18	TGA scans before and after second stage polymerization a. poly (EGDMA), b. poly (TMPTMA)	86
4.19	Thermogram of poly (EGDMA) and poly (TMPTMA) a. first, b. second heating cycle	87
4.20	FTIR spectra of poly (EGDMA) a. before b. after cross-linking	88

Chapter 5

Supramolecular Inclusion Complex: Copolymerization

5.1	FTIR of poly (TMPTMA-co-MMA)	96
5.2	¹ H NMR of poly (EGDMA-co-MMA)	97
5.3	¹ H NMR of poly (EGMAVB-co-MMA)	98
5.4	¹ H NMR of poly (TMPTMA-co-MMA)	98
5.5	Intrinsic viscosity <i>versus</i> molecular weight plots for ■ poly (EGDMA-co-MMA) (60:40), ● linear poly (EGDMA) and ▲ hyperbranched poly (EGDMA)	99
5.6	Mark - Houwink - Sakurada exponent for poly (EGDMA-co-MMA) (60:40)	99
5.7	FR and KT plots to calculate co-monomer reactivity ratio	104-106

Chapter 6

Molecularly Imprinted Nanoparticles for Drug Delivery

6.1	Plot of $1/\Delta A$ <i>versus</i> $1/b_0$ at 288 nm a. poly (EGDMA-co-MAA) (50:50), b. (EGDMA+MAA) (50:50), c. poly (TMPTMA-co-MAA) (30:70), d. (TMPTMA+MAA) (30:70)	122
6.2	Spectral shifts due to interactions between THP and functional	123

	copolymer	
6.3	a. FTIR spectra of poly (EGDMA-co-MAA) (50:50), THP and different molar ratios of THP to –COOH of polymer, 1:1, 1:2, 1:3 and 1:4 concentration, b. spectra in N-H region, c. spectra in C=O and C=N region	124
6.4 A	a. Poly (EGDMA-co-MAA), b. NIP nanoparticles, c. MIP nanoparticles after extraction of THP	128
6.4 B	a. MIP nanoparticles after THP extraction, b. MIP nanoparticles after THP rebinding	128
6.5	The FTIR spectra in the carbonyl region after subtracting the THP spectra from the THP to carboxyl mixture 1:1 to 1:4	132
6.6	THP binding on a. poly (EGDMA-co-MAA) (30:70) and b. poly (TMPTMA-co-MAA) (30:70) nanoparticles	133
6.7	Freundlich Fit for poly (EGDMA-co-MAA) (30:70) nanoparticles	134
6.8	Structure of theophylline and caffeine	137
6.9	Fractional release of THP from a. poly (EGDMA-co-MAA) 50:50 and 90:10, b. poly (TMPTMA-co-MAA) 30:70 and 70:30 nanoparticles	138

List of Tables

Chapter 1

Literature Review

1.1	Cyclodextrin: discovery to application	3-5
-----	--	-----

Chapter 3

Supramolecular Inclusion Complex: Synthesis

3.1	Stoichiometry of ICs	54-55
3.2	FTIR of ICs	57

Chapter 4

Supramolecular Inclusion Complex: Homopolymerization

4.1	FTIR of IC, polymer	71
4.2	Molecular weight and intrinsic viscosity of poly (EGDMA)	83
4.3	Molecular weight and intrinsic viscosity of poly (TMPTMA)	83
4.4	Properties of poly (EGDMA) and poly (TMPTMA)	85
4.5	Thermal properties of poly (EGDMA)	86
4.6	Thermal properties of poly (TMPTMA)	87
4.7	Particle size of nanoparticles	89

Chapter 5

Supramolecular Inclusion Complex: Copolymerization

5.1	FR and KT parameters to calculate co-monomer reactivity ratio	101-104
5.2	Reactivity ratios evaluated by FR and KT methods	107
5.3	Copolymers: varying multivinyl monomer	110
5.4	Copolymers: varying molecular weights	111

Chapter 6

Molecularly Imprinted Nanoparticles for Drug Delivery

6.1	Functional co-polymers: properties	119
6.2	Association constants	121
6.3	FTIR of THP, polymer and their stoichiometric mixtures	123

6.4	Poly (EGDMA-co-MAA) and poly (TMPTMA-co-MAA) nanoparticles	127
6.5	THP rebinding on nanoparticles	129
6.6	THP rebinding on nanoparticles: effect of THP to carboxyl ratio	131
6.7	Effect of cross-linking density on heterogeneity index (m) and median binding affinity (K_0) of nanoparticles	134
6.8	Effect of THP to carboxyl ratio on rebinding parameters	135
6.9	THP-imprinted nanoparticles: selectivity	137
6.10	THP release from poly (EGDMA-co-MAA) (50:50) nanoparticles	140

List of Schemes

Chapter 1 Literature Review

1.1	Synthesis of poly (HEMA-co-t-BMA) and post functionalization	20
1.2	Cobalt mediated polymerization of EGDMA	22
1.3	Synthesis of hydrogel for p-amino benzoic acid release by hydrolytic cleavage	38

Chapter 3

Supramolecular Inclusion Complex: Synthesis

3.1	EGMAVB monomer synthesis	47
3.2	TMPDAVB monomer synthesis	48
3.3	EGDMA- β -CD IC preparation	49
3.4	TMPTMA- β -CD IC preparation	49

Chapter 4

Supramolecular Inclusion Complex: Homopolymerization

4.1	Polymerization of EGDMA- β -CD IC	69
4.2	Polymerization of TMPTMA- β -CD IC	69

Chapter 5

Supramolecular Inclusion Complex: Copolymerization

5.1	EGIBMA monomer synthesis	92
5.2	TMPMA and TMPDIBMA monomers synthesis	93
5.3	Copolymerization of EGDMA- β -CD IC	94

Chapter 6

Molecularly Imprinted Nanoparticles for Drug Delivery

6.1	Synthesis of poly (EGDMA-co-MAA)	119
6.2	Synthesis of THP imprinted nanoparticles	126

Abbreviations and Symbols

AIBN	Azobisisobutyronitrile
BMA	Butyl methacrylate
CAF	Caffeine
CD	Cyclodextrin
β -CD	β -Cyclodextrin
α -CD	α -Cyclodextrin
γ -CD	γ -Cyclodextrin
CHCl ₃	Chloroform
DM- β -CD	Dimethyl- β -cyclodextrin
DMF	N,N Dimethyl formamide
DMSO	Dimethyl sulphoxide
dL/g	Deciliter per gram
DSC	Differential scanning calorimetry
DRS	Diffuse reflectance spectroscopy
EGDMA	Ethylene glycol dimethacrylate
EGMAVB	Ethylene glycol methacrylate 4-vinyl benzoate
EGIBMA	Ethylene glycol isobutyrate methacrylate
FTIR	Fourier transform infrared spectroscopy
GPC	Gel permeation chromatography
h	hours
HEMA	2-Hydroxyethyl methacrylate
H ₂ O	Water
IC	Inclusion complex
IV	Intrinsic viscosity
K _D	Dissociation constant
K _a	Association constant
LS	Light scattering
MALLS	Multi angle laser light scattering
MEK	Methyl ethyl ketone
MMA	Methyl methacrylate
MAA	Methacrylic acid
MIP	Molecularly imprinted polymers
M _w	Weight average molecular weight
M _n	Number average molecular weight
N ₂	Nitrogen
[η]	Intrinsic viscosity
NMR	Nuclear magnetic resonance spectroscopy
NIP	Non imprinted polymer
NVIm	N-vinyl imidazole
O ₂	Oxygen
poly	Polymer
RT	Room temperature
TMPDAVB	Trimethylolpropane diacrylate 4-vinyl benzoate
TMPTMA	Trimethylolpropane trimethacrylate
TMPTA	Trimethylolpropane triacrylate
TMPTM	Trimethylolpropane methacrylate
TMPIBMA	Trimethylolpropane isobutyrate methacrylate
TGA	Thermo gravimetric analysis

Temp.	Temperature
THP	Theophylline
THF	Tetrahydrofuran
UV	Ultra violet spectroscopy
XRD	X-ray diffraction

Abstract

Studies in Polymerizations Comprising Supramolecular Complexes

Polymer architecture governs its properties and performance.¹ Cross-linked polymers obtained by simultaneous polymerization / cross-linking of monomers containing multiple double bonds find a wide range of applications such as ion exchange resins, adsorbents, molecularly imprinted polymers, supports for reagents in organic synthesis, enzyme immobilization and drug delivery systems.² A sequential approach wherein a soluble linear polymer is first synthesized, converted into desirable form and then cross-linked, offers significant advantages in most of these applications.³ This has been hitherto achieved by a) conjugation of vinyl monomers with polymers containing pendant functional groups,^{3a-d} and b) co-polymerization with cross-linkers containing multiple unsaturated groups differing in reactivity.^{3e} The first approach is limited by the choice of monomers while the later is limited by the choice of cross-linkers. Clearly, there is a need for a single step method for the synthesis of soluble polymers containing unsaturation, which can be cross-linked in a subsequent step, and is independent of the nature of the monomer as well as the cross-linkers.

Cyclodextrins (CD) form host-guest complexes with a variety of organic compounds and polymers.^{4a-g} CD is cyclic oligosaccharides composed of six (α), seven (β) or eight (γ) glucopyranose ring units, which are joined together by α (1-4) linkage forming torus shaped ring structure. The primary hydroxyl groups of glucose ring are exterior to the cavity, which makes it soluble in water whereas the hydrophobic interior cavity facilitates formation of an inclusion complex (IC) by hydrophobic interactions. The ability of CD to form IC and to shield the included part of the molecule from the chemical attack has been exploited in highly selective organic synthetic procedures,⁵ whereas in polymer synthesis use of CD ICs to solubilize the hydrophobic methacrylate or methacrylamide monomers in aqueous media is reported.⁶ Sarvothaman and Ritter⁷ reported the formation of IC containing diacrylate and dimethacrylate of 1, 4 butane diol and 1, 6 hexane diol with α -CD and dimethyl- β -CD (DM- β -CD). Diacrylate completely penetrated the CD cavity when it formed a complex with DM- β -CD,

whereas in case of dimethacrylate, the CD ring was located at the terminal end of the monomer. The polymerization of these ICs in water resulted in cross-linked polymers. Our research work demonstrates the use of CD host-guest chemistry to control the reactivity of multivinyl monomers during free radical polymerization. Divinyl as well as trivinyl monomers form stoichiometric IC with CD and undergo selective polymerization wherein only one of the vinyl unsaturations takes part in polymerization to yield soluble polymers comprising pendant unsaturations per repeat unit. Thus, the study includes the formation of ICs of various multivinyl monomers with CD and their characterization by instrumental as well as molecular modeling calculations. Homo and copolymerization of included multivinyl monomers and structural elucidation of formed polymers was also carried out. The application of polymers formed in molecular imprinting and drug delivery is demonstrated.

The research work undertaken is divided into seven chapters and a brief outline of each chapter is given below:

Chapter 1 Literature Review

This chapter begins with an introduction of CD host-guest chemistry and its applications in organic and polymer chemistry. Various examples of use of CD to control the reactivity of included guest molecule in synthetic organic chemistry as well as to solubilize hydrophobic monomers in polymerization are cited.

The free radical polymerization of multivinyl monomers yields three-dimensional cross-linked network which find applications in super absorbents, ion exchange resins, molecularly imprinted polymers, photoresists, optical waveguides, contact lenses, optical fibers and controlled drug delivery, etc. Significant research effort is devoted towards the synthesis of linear polymers containing pendant vinyl unsaturations. These include controlling the reactivity of divinyl monomers using polymerization techniques such as atom transfer radical polymerization, transition metal mediated polymerization, group transfer polymerization etc. A sequential approach wherein a soluble linear polymer is first synthesized, condensed with functional monomers and then cross-linked is elaborated. The limitations of these approaches are also discussed.

This is followed by a brief description of the objective of our research to control the reactivity of multivinyl monomers to obtain soluble linear polymers containing pendant vinyl unsaturations.

A brief introduction of molecular imprinting and drug delivery and the need for new materials in these areas is also discussed. The utility of the new methodology in molecular imprinting and drug delivery is also discussed.

Chapter 2 Objectives and Scope of the Work

The literature survey revealed the need for a simple methodology to control the reactivity of multivinyl monomers to obtain latent cross-linkable polymers in view of limitations of prior efforts made in this direction. Literature also demonstrated the use of CD to control the reactivity of included guest molecules. Thus the main objective of the present research work is to control the reactivity of multivinyl monomers via their IC mediated polymerization and to study the properties and performance of ICs and polymers. This includes the following:

1. Synthesis and characterization of supramolecular ICs of multivinyl monomers with CD and its derivatives.
2. Homopolymerization of IC and its structural evaluation.
3. Co-polymerization of IC with various co-monomers and study the co-polymerization behavior.
4. Explore the possibility of cross-linking the polymers containing pendant unsaturations by thermal and photo irradiation.
5. To evaluate the application of self cross-linked nanoparticles in molecular imprinting and controlled drug delivery.

Chapter 3 Supramolecular Inclusion Complex: Synthesis

This chapter deals with the synthesis of ICs of multivinyl monomers and their characterization. ICs of multivinyl monomers such as ethylene glycol dimethacrylate (EGDMA), ethylene glycol methacrylate 4-vinyl benzoate (EGMAVB), trimethylol propane trimethacrylate (TMPTMA), trimethylolpropane triacrylate (TMPTA), trimethylol propane diacrylate 4-vinyl benzoate (TMPDAVB) with CD and its derivatives were obtained by precipitation and solvent evaporation methods respectively. The ICs were characterized by instrumental techniques such as FTIR,

NMR and XRD as well as molecular modeling calculations. FTIR showed the stable IC formation between the multivinyl monomer and CD due to hydrogen bonding between the carbonyl group of monomer and secondary -OH groups of CD rim. The ^1H NMR characterization is useful to establish the stoichiometry of IC. The divinyl monomers such as EGDMA and EGMAVB formed 1:1 IC confirming unequivocal inclusion of methacrylate group into the cavity of β -CD. In case of trivinyl monomers the intramolecular hydrogen bonding in monomer governs the stoichiometry of the IC. The trivinyl monomers TMPTMA and TMPDAVB formed 1:2 and TMPTA formed 1:1 IC with β -CD due to absence of and presence of intramolecular hydrogen bonding in the former and the later respectively. The XRD characterization of all the ICs showed a cage type structure. The molecular modeling calculations also corroborated the formation and observed stoichiometry of IC.

Chapter 4 Supramolecular Inclusion Complex: Homopolymerization

Homopolymerization of IC was carried out by free radical solution polymerization. The polymers obtained are soluble in common organic solvents such as chloroform (CHCl_3), tetrahydrofuran (THF), dimethyl sulfoxide (DMSO) and N, N dimethyl formamide (DMF). The homopolymers were characterized by instrumental techniques such as FTIR, NMR, gel permeation chromatography (GPC), intrinsic viscosity (IV), multi angle laser light scattering (MALLS). The FTIR analysis of the homopolymers showed the presence of unreacted vinyl unsaturations and absence of CD in polymer. ^1H NMR analysis of the homopolymers showed presence of double bonds in the polymer structure consistent with the stoichiometry of the complex. The intrinsic viscosity and molecular weight correlation of the homopolymers showed a linear dependence between the two. The Mark-Houwink-Sakurada exponent of poly (TMPTMA) is 0.39, while the corresponding values for linear poly (EGDMA) and hyperbranched poly (EGDMA) are 0.29 and 0.14 respectively. The values of M_w obtained by multi-angle laser light scattering (2.16×10^5) and by GPC (2.46×10^5) are comparable. In contrast, the values differ by an order of magnitude for the branched polymers. The value of the second virial coefficient ($3.5 \times 10^{-4} \text{ mol mL/g}^2$) for poly (EGDMA) of $M_w 2.16 \times 10^5$ is closer to that for linear polystyrene ($4.4 \times 10^{-4} \text{ mol mL/g}^2$) of $M_w 2.9 \times 10^5$ than for the

hyperbranched poly (EGDMA) (7.5×10^{-6} mol mL/g²) of Mw 7.68×10^5 . All these results confirm linear structure of polymer obtained by IC mediated polymerization.

The pendant vinyl groups of the homopolymers were subsequently reacted by inter or intramolecular cross-linking. The intermolecular cross-linking yielded three dimensional cross-linked products whereas intramolecular cross-linking yielded self cross-linked nanoparticles. The type of multivinyl monomer and molecular weight of the precursor polymer control the particle size of nanoparticles between 20-140 nm. Thus this chapter discusses the polymerization of complexed multivinyl monomers, structural elucidation of polymer, second stage cross-linking of pendant vinyl groups and their potential applications in various fields.

Chapter 5 Supramolecular Inclusion Complex: Copolymerization

Co-polymerization allows the synthesis of a wide range of polymers by variations in the choice and composition of the monomers. The co-polymerization thus helps to broaden the range of applications compared to the homopolymers. All the copolymers were soluble in organic solvents and contained pendant vinyl unsaturations as established by FTIR and NMR characterization.

The comonomer reactivity ratios of MMA with the multivinyl monomers in the form of and in absence of IC and the structurally similar monovinyl monomers were evaluated. The reactivity ratios were calculated by Fineman Ross and Kelen Tudos methods. The following systems were investigated.

- EGDMA- β -CD-MMA
- EGDMA-MMA
- EGIBMA- β -CD-MMA
- EGIBMA-MMA
- EGMAVB- β -CD-MMA
- EGMAVB-MMA
- TPM-MMA
- TMPTMA-MMA
- TMPIBMA- MMA
- TMPTMA- β -CD-MMA

The results showed decrease in reactivity of divinyl monomer due to complexation with β -CD. In the co-polymerization of EGDMA with MMA, ($r_{\text{EGDMA}} = 0.52$, $r_{\text{MMA}} = 0.28$) Reactivity of EGDMA was twice that of MMA but after formation of IC, EGDMA- β -CD and MMA ($r_{\text{EGDMA-}\beta\text{-CD}} = 0.50$, $r_{\text{MMA}} = 0.85$). The complexed EGDMA showed lower reactivity as compared to MMA. Results with other monovinyl, divinyl and trivinyl monomers showed similar trends.

Further this chapter also deals with the synthesis and characterization of self cross-linked nanoparticles. The copolymers of EGDMA-*co*-MMA and TMPTMA-*co*-MMA varying in molecular weight and co-monomer compositions were prepared. The polymers were then cross-linked intramolecularly in dilute solutions to obtain self cross-linked nanoparticles. The particle size measurement shows the dependence of particle size on various parameters such as molecular weight, solvent concentration during cross-linking etc.

Chapter 6 Molecularly Imprinted Nanoparticles for Drug Delivery

The copolymers of EGDMA-*co*-MAA and TMPTMA-*co*-MAA of various co-monomer compositions were prepared to obtain the polymers with latent cross-linkable groups as well as recognition site. The template theophylline was complexed with the carboxylic groups of polymer and the pendant vinyl groups were cross-linked intramolecularly to yield theophylline-imprinted nanoparticles. Similarly, non-imprinted nanoparticles were prepared in absence of theophylline. Imprinted and non-imprinted nanoparticles were evaluated for the binding study in acetonitrile after extraction of theophylline. The binding efficiency of imprinted nanoparticles for theophylline was found to be higher as compared to non-imprinted nanoparticles and increased with increase in percentage of cross-linker in precursor copolymer. Thus theophylline-binding capacity of imprinted nanoparticles prepared from EGDMA-*co*-MAA (10:90) was 0.66 mg/g whereas that of EGDMA-*co*-MAA (50:50) was 1.23 mg/g. The corresponding values for non-imprinted polymers were 0.33 mg/g and 0.53mg/g respectively. The imprinted nanoparticles showed the selectivity towards theophylline as compared to caffeine. The release study of theophylline loaded on imprinted as well as non-imprinted nanoparticles showed that theophylline from non-imprinted nanoparticles was completely released in 6 hrs whereas from the imprinted polymer only 40 % was released in the same time span.

Chapter 7 Conclusions and Recommendation for Future Research

This investigation has led to the functional soluble polymers from the cross-linkers by exploiting host-guest chemistry. Using this methodology it is possible to obtain polymers containing pendant vinyl unsaturations, which can be subsequently, reacted to yield the cross-linked materials. Also the work showed the application of these polymers to obtain the functional nanoparticles for molecular imprinting and controlled drug delivery. The methodology can be extended in future to the areas listed below,

- The extension of this methodology to control the reactivity of hydrophilic multivinyl monomers, which will widen the scope of applications in biosensors (enzyme immobilization).
- The co-polymerization of IC with functional monomers and evaluation of their applications in microlithography, molecular imprinting, controlled drug delivery, biodegradable polymer synthesis and nanocomposites etc.
- Synthesis of functional nanoparticles and binding them with active reagents such as drug, enzyme etc or use of the functional nanoparticles as catalyst support in organic reactions.

References:

- (1) (a) Tomalia, D. A. *Prog. Polym. Sci.* **2005**, *30*, 294-324. (b) Frauenrath, H. *Prog. Polym. Sci.* **2005**, *30*, 325-384.
- (2) Zhu S.; Hamielec A.E. *Makromol. Chem., Macromol. Symp.* **1993**, *69*, 247-256.
- (3) (a) Liu, J-H.; Lin, S-H.; Shih, J-C. *J. Appl. Polym. Sci.* **2001**, *80*, 328-333. (b) Koo, J-S.; Smith, P. G. R.; Williams, R. B.; Grossel, M. C.; Whitcombe, M. *J. Chem. Mater.* **2002**, *14*, 5030-5036. (c) Li, Z.; Day, M.; Ding, J.; Faid, K. *Macromolecules* **2005**, *38*, 2620-2625. (d) Mecerreyes, D.; Lee, V.; Hawker, C. J.; Hedrick, J. L.; Wursch, A.; Volksen, W.; Magbitang, T.; Huang, E.; Miller, R. D. *Adv. Mater.* **2001**, *13* (3), 204-208. (e) Nagelsdiek, R.; Mennicken, M.; Maier, B.; Keul, H.; Hocker, H. *Macromolecules* **2004**, *37*, 8923-8932.
- (4) a) Harada, A.; Li, J.; Kamachi, M. *Macromolecules* **1993**, *26*, 5698-5703. (b) Li, J.; Yan, D.; Jiang, X.; Chen, Q. *Polymer* **2002**, *43*, 2625-2629. (c) Harada, A.;

- Nishiyama, T.; Kawaguchi, Y.; Okada, M.; Kamachi, M. *Macromolecules* **1997**, *30*, 7115-7118. (d) Jiao, H.; Goh, S. H.; Valiyaveetil, S. *Macromolecules* **2001**, *34*, 8138-8142. (e) Rusa, C. C.; Bullions, T. A.; Fox, J.; Porbeni, F. E.; Wang, X.; Tonelli, A. E. *Langmuir* **2002**, *18*, 10016-10023. (f) Harada, A.; Kamachi, M. *Macromolecules* **1990**, *23*, 2823-2824. (g) Wen, X.; Liu, Z.; Zhu, T. *Chem. Phys. Lett.* **2005**, *405*, 114-117.
- (5) Takahashi, K. *Chem. Rev.* **1998**, *98*, 2013-2033.
- (6) Ritter, H.; Tabatabai, M. *Prog. Polym. Sci* **2002**, *27*, 1713-1720.
- (7) Sarvothaman, M. R.; Ritter, H. *Macromol. Rapid Commun.* **2004**, *25*, 1948-1952.

Chapter 1
Literature Review

1.1 Introduction

Supramolecular chemistry has attracted considerable attention from researchers in diverse disciplines over recent years because of its interdisciplinary nature and potential applications (Lehn 1995, Fyfe and Stoddart 1997). In this approach, supramolecular architectures are created through a wide range of non-covalent interactions such as ion-ion, ion-dipole, dipole-dipole, hydrophobic, hydrogen bonding, cation- π , π - π stacking and van der Waals forces (Lehn 1995). These interactions are mainly host - guest type, in which the supramolecule acts as a host and has convergent binding site whereas the guest molecule has divergent binding site and forms the other component of the complex (Szejtli 1998).

Cyclodextrin (CD) is one of the host molecules widely studied because of its easy availability and complex formation ability with a variety of organic guest molecules (Szejtli 1998). The physical properties such as solubility, stability and volatility of the guest molecule included are modified without affecting its chemical structure. These inclusion complexes (ICs) have numerous practical applications in synthetic organic and polymer chemistry.

The present research work demonstrates the use of CD host-guest chemistry to control the reactivity of multivinyl monomers in free radical polymerization to yield latent cross-linkable polymers. The study includes the formation of ICs of various divinyl and trivinyl monomers with CD, their characterization by instrumental as well as molecular modeling calculations, homo and copolymerization of ICs comprising multivinyl monomers and structural elucidation of polymers formed. The methodology of controlled polymerization of multivinyl monomer was coupled with molecular imprinting and intramolecular cross-linking to obtain imprinted nanoparticles for sustained drug delivery.

This chapter presents an overview of the developments in CD chemistry from its discovery to applications in synthetic organic and polymer chemistry. General aspects of free radical polymerization of multivinyl monomers and applications of latent cross-linkable polymers in upcoming areas such as molecular imprinting, optical waveguides, microlithography, nanotechnology and controlled drug delivery, have been reviewed. The prior efforts as well as their limitations in the synthesis of latent cross-linkable

polymers are summarized. A brief introduction of molecular imprinting and its application in drug delivery is discussed with appropriate examples. This is followed by a description of the objective of our research investigation and approach to obtain latent cross-linkable polymers from multivinyl monomers and to explore their application in various areas such as nanotechnology, molecular imprinting and controlled drug delivery. The coverage in the literature review is illustrative rather than encyclopedic.

1.2 Cyclodextrin Chemistry

The important milestones in CD chemistry are summarized in Table 1.1. There are three stages in the development of CD chemistry, discovery period (1891 to 1930s), systematic studies on CDs and ICs (1930s to 1970s) and their industrial production and utilization (1970s onward).

Table 1.1: Cyclodextrin: Discovery to Application

Year	Researchers / Group	Important Findings
1891	Villiers	Isolated crystalline compound from “ <i>Bacillus amylobacter</i> ” culture contaminated with “ <i>Bacillus macerans</i> ”
1903-1911	Schardinger	Extensive study on the isolation and characterization of crystalline dextrin
1928, 1932	Pringsheim	The crystalline dextrans and their acetates were shown to form complexes with various organic compounds
1930	Freudenberg and Coworkers, Karrer, Miekeley	The crystalline dextrans were built from maltose units and contained only α -1, 4-glycosidic linkages. The first scheme for the isolation of homogeneous and pure fractions was described
1936	Freudenberg and coworkers	Postulated the cyclic structure of crystalline dextrans
1948-1950	Freudenberg and Cramer	Discovery of γ -CD and structure elucidated
	French et al and	Enzymatic production of pure CDs

	Cramer et al	French reported even larger CDs Cramer's group reported the IC forming properties of CDs
1953	Freudenberg, Cramer, and Plieninger	First patent on application of CDs in drug formulations
Upto 1960		Methodologies for laboratory-scale preparation of CDs, their structure, physical and chemical properties, as well as their IC forming properties
1969	Breslow and Campbell	CD-ICs in selective organic synthesis
1973	Griffiths and Bender	CD-ICs as catalyst in organic synthesis
1976	Ogata et al	Polymerization of CD complexed monomers (Polyamides synthesis by condensation of dibasic acid chlorides and CD complexed diamine)
1979	Maciejewski et al	Polymerization of CD complexed monomers to obtain polyrotaxanes (Radical polymerization)
1991	Born and Ritter	Comb-like rotaxane polymers containing non-covalently bound CDs in the side chains
1990	Harada et al	CD-IC with low molecular weight
1994		hydrophilic and hydrophobic polymers
1996	Lau Leyrer et al	CD-IC with of long chain hydrophobic monomers in emulsion polymerization
1998	Tonelli and coworkers	CD-IC with high molecular weight polymers
1998	Jeromin and Ritter	CD-IC mediated aqueous polymerization of hydrophobic methacrylate and methacrylamide monomers
1999	Rimmer and coworkers	Use of CD as emulsifier in emulsion polymerization
2004	Sarvothaman and	CD-IC mediated aqueous polymerization of

	Ritter	dimethacrylate and diacrylate to form interlocked polyrotaxanes
2004	Harada et al	CD initiated polymerization of lactones
2006	Chen et al	CD-IC to obtain linear polymers by condensation polymerization

1.2.1 Discovery of CDs

In 1891, Villiers isolated a crystalline compound from *Bacillus amylobacter* a culture contaminated with *Bacillus macerans* and named it “cellulosines” as it resembled cellulose. Freudenberg (1930) established the true structure of CDs with the help of the observations made by Karrer and Miekeley. Freudenberg, Cramer and Plieninger (1953) obtained first patent on the ICs comprising CDs and variety of drug molecules. They demonstrated that the stabilization, volatility reduction, and solubility changes of the drug molecules occurred as a result of complexation. The structure and IC formation properties of CDs are discussed in the following sections.

1.2.2 Structure of CDs

CDs are obtained by degradation of starch. They are cyclic oligosaccharides composed of six (α), seven (β) or eight (γ) glucopyranose ring units, which are joined together by α (1-4) linkage forming torus shaped ring structure (Figure 1.1). Recently derivatives of CDs containing nine to thirteen glucose units have been reported (Szejtli 1998). However, they have a collapsed cylinder structure, and their internal cavities are even smaller than that of γ -CD. They are less stable and do not exhibit good complex formation ability and hence have not been extensively investigated (Szejtli 1998).

The glucopyranose units of CD have 4C_1 chair conformation forming torus shaped ring structure. The primary hydroxyl groups of glucopyranose units are located at the narrow side of the torus, whereas the secondary hydroxyls are located at the wider side of the torus (Figure 1.2). The C₂-OH group of one glucopyranose unit can form hydrogen bond with the C₃-OH group of the adjacent glucopyranose unit. In β -CD these hydroxyls form a complete secondary belt on the molecule and impart greater rigidity to the structure. In α -CD this hydrogen bond is incomplete because one of the glucopyranose units out of six is distorted. In γ -CD hydrogen bonding is absent due to

its more flexible, non-coplanar structure. β -CD has therefore lowest water solubility amongst α , β and γ -CD.

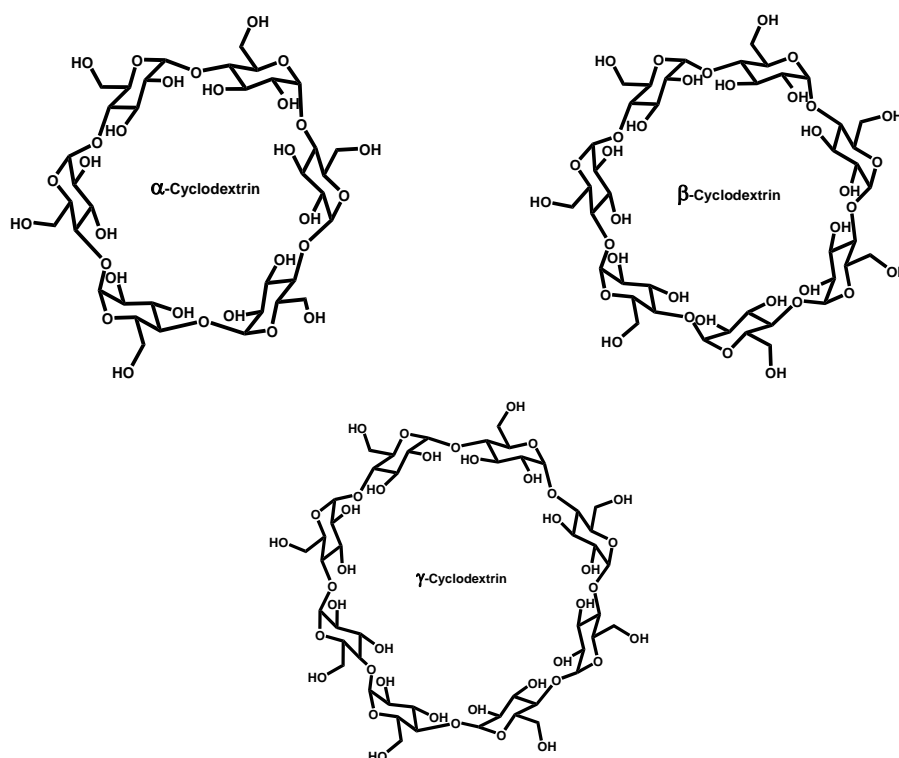


Figure 1.1: Cyclodextrin structures

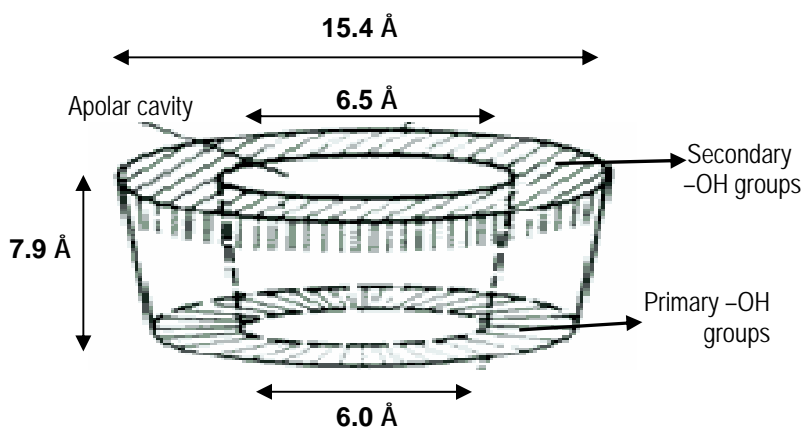


Figure 1.2: Structure of β -cyclodextrin

Among all CDs β -CD is the most commonly utilized derivative because of its suitable cavity dimensions, which can form IC with wide range of organic as well as inorganic guest molecules and ease of isolation and production.

1.2.3 Inclusion Complexes of CDs

CDs form ICs with a variety of organic and inorganic molecules. The complex formation takes place without formation or breaking of covalent bonds. The presence of polar hydrophilic outer shell and relatively hydrophobic cavity enables CDs to build host-guest complexes in water through non-covalent interactions. In an aqueous solution, the apolar CD cavity is occupied by water (polar) molecules, which is an energetically unfavoured condition (apolar-polar interaction) and water molecules can be easily displaced by relatively less polar i.e. hydrophobic guest molecules, (apolar - apolar interaction) (Szejtli 1998). Thus the complex formation decreases the CD ring strain resulting in more stable energy state (Szejtli 1998). The presence of water plays a key factor in the formation of IC. It acts as a driving force for the hydrophobic interaction of the guest with the cavity of the CD. In some cases, water is required to stabilize the ICs, since water molecules can form a bridge between the hydroxyl groups of adjacent molecules of CD to form a cage structure (Hedge 1998). ICs can be prepared using co-precipitation, slurry, paste, dry mixing, and solvent evaporation methods. Among these the co-precipitation is the most commonly used method to prepare the ICs of native CDs, whereas the solvent evaporation methodology is utilized to obtain the ICs of CD derivatives.

The inclusion of guest into the CD cavity significantly influences the physicochemical properties of guest molecules that are not achievable otherwise (Schmid 1989). These properties are: solubility enhancement of highly insoluble guests, stabilization of labile guests against degradative effects of oxidation, visible or UV light and heat, control of volatility and sublimation, physical isolation of incompatible compounds, chromatographic separations, taste modification by masking of flavors, unpleasant odors and controlled release of drugs and flavors (Hedges 1998; Barse et al., 2003).

1.2.3.1 CD ICs in Organic Chemistry

The ICs of CDs are utilized in highly selective organic synthetic reactions since the formation of an IC alters the reactivity and selectivity of included guest molecules

(Takahashi 1998). Breslow and Campbell (1969) were the first to demonstrate the use of CD-ICs to control the aromatic substitution reactions. Complexation of anisole with α -CD suppressed the reaction at the 'o' position and enhanced the *p/o* ratio of the chlorinated product from 1.48 to 21.6. Figure 1.3 illustrates the mechanism for the 'p' chlorination of anisole.

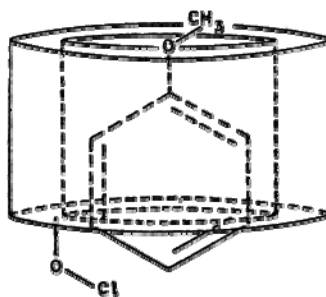


Figure 1.3: Anisole- α -CD IC and mechanism for its 'p' chlorination
(From Breslow and Campbell 1969)

Similarly, the use of CDs in other aromatic substitution (Hirai et al., 1993, 1995 and 1996), selective asymmetric induction (Fornasier et al., 1991), reductive ring opening epoxidation (Hu et al., 1990; and Hu et al., 1991), asymmetric oxidation of sulfides (Czarnik 1984), intermolecular Diels-Alder reactions (Schneider 1986), isomerization (Tian, 1995), photochemical reactions (Bortolus, 1996.) has been reported (Takahashi 1998).

1.2.3.2 CD ICs in Polymer Science

In polymer science, complexes of CD are being used for variety of applications e.g. to prepare supramolecular architectures such as polyrotaxanes and pseudorotaxane either by *insitu* polymerization or by threading of CDs on the preformed polymers, to enhance the solubility of the hydrophobic monomers to mediate their aqueous polymerization reactions, as well as in various other polymerization reactions as a mediator for polymerization.

Ogata et al (1976) reported the synthesis of CD polyrotaxanes. CD was threaded on the aliphatic or aromatic diamine monomer in water. The interfacial or solution polymerization of CD complexed diamine with diacid chloride yielded the polyamide rotaxane. These polymers were named "tunnel polymers" as the resulting polyamide is

covered with many β -CD molecules and polyamide is like a train going through these tunnels.

In 1979 Maciejewski prepared the polyrotaxanes by *in situ* radical polymerization of β -CD complexed monovinyl monomers such as methyl acrylate, methacrylonitrile, vinyl chloride and styrene. The ICs of β -CD and the monomer were prepared in water. The polymerization of these ICs was carried out in N, N dimethyl formamide (DMF) at higher temperature to yield the polyrotaxanes. The author reported that the monomer-CD IC was stable under the polymerization conditions and does not dissociate rather continue to form in DMF.

Harada et al., (1990) reported that the CD not only formed the IC with small guest molecules but can be used to form complex with preformed polymer chains. The complex formation between the CD and the polymer chain strongly depends on the nature of the polymer i.e. hydrophilic or hydrophobic, molecular weight of the guest polymer, the functional groups on the polymer backbone and the size of the CD cavity (Harada, 1996, Okumura et al., 2000).

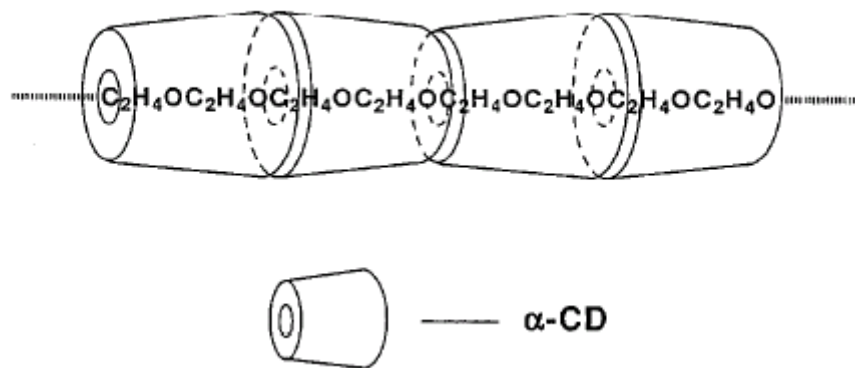


Figure 1.4: Structure of PEG- α -CD inclusion complex
(From Harada 1996)

Reports from Harada et al., (1993, 1996) on the IC formation between the water soluble non-ionic polymers and CD revealed that α -CD formed a crystalline complex with poly (ethylene glycol) (PEG) of various molecular weights whereas the other derivatives of CDs, β -CD and γ -CD failed to form the complex. The yield of the complex increased with increase in the molecular weight of PEG. Further study on the effect of PEG chain

end groups on polyrotaxane formation demonstrated that the presence of small substituents, methyl, dimethyl and amino groups increased the yield of IC as compared to the PEG. PEG chain comprising bulky substituents or bulky end groups did not form any complexes with the α -CD. Harada and coworkers also evaluated the formation of polyrotaxane containing other hydrophilic and hydrophobic polymers as well as inorganic polymers (Harada et al., 1996).

Rusa et al., (2000, 2001) investigated the formation of polyrotaxane between the CD and high molecular weight polymers. Jiao et al., (2000) reported the formation of CD complexes with multiarm poly (ethylene glycol) (PEG) polymers. The star shaped PEG with three, four and six arms formed stoichiometric crystalline ICs with α -CD and γ -CD but did not form the complex with β -CD.

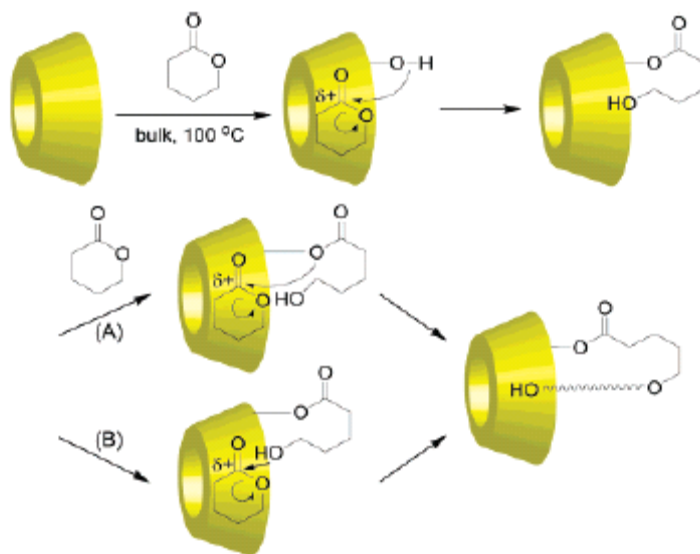


Figure 1.5: Cyclodextrin initiated polymerization of lactones

(From Harada et al., 2004)

Recently, Takashima et al., (2004) reported the use of CD to initiate the polymerization of cyclic esters i.e. lactones. Poly (δ -valerolactone) i.e. poly (δ -VL) was obtained on heating the mixture of δ -VL and β -CD at 100 °C whereas in absence of CD, δ -VL did not give any polymer. The use of γ -CD or α -CD gave lower yield of the polymer and the use of CDs derivatives such as 2, 6-Di-*O*-methyl- β -CD and 2, 3, 6-tri-*O*-acetyl- β -CD showed no reactivity in lactones polymerization. This indicated that the cavity size

of CD and the presence of hydroxyl at C2 carbon of glucose ring play an important role in initiating the polymerization. The possible mechanism involved in the polymerization of lactones is shown in Figure 1.5.

The idea of exploiting CDs to mediate aqueous polymerization of hydrophobic monomers has been mooted recently. Ritter and coworkers (1999) reported the use of CDs as emulsifier in heterogeneous polymerization of butyl acrylate. The authors studied the effect of addition of CD during emulsion polymerization both in presence and in absence of other ionic emulsifier. They observed an increase in molecular weight of the polymers on addition of CD, in absence of ionic emulsifier. In contrast, in presence of ionic emulsifier very little effect on number and weight average molecular weight as well as average particle size of latex was observed.

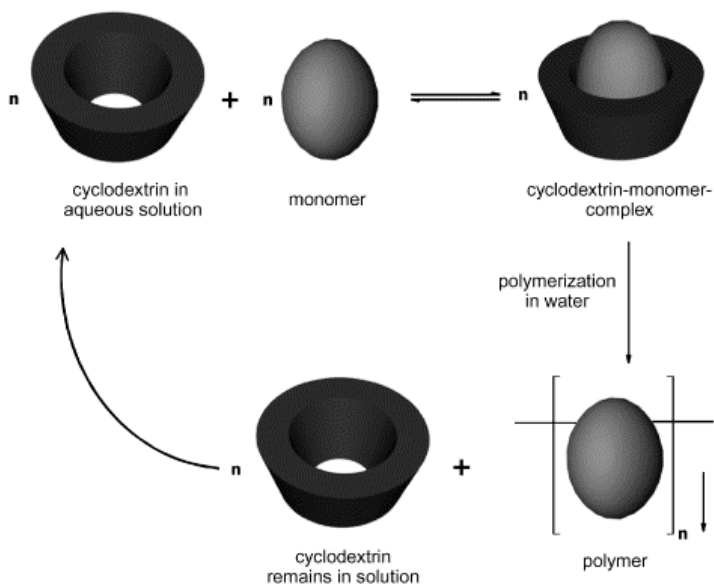


Figure 1.6: Cyclodextrin mediated aqueous polymerization

(From Ritter and Tabatabai 2002)

Ritter and coworkers reported the use of CDs to alter the solubility of included hydrophobic monomers in water to mediate their polymerization in aqueous media. This group has published a series of papers covering various aspects of CD mediated aqueous polymerization of hydrophobic monovinyl monomers.

The complex formation between phenyl, cyclohexyl methacrylate and N-methacryloyl-11-aminoundecanoic acid with CD derivative (Dimethyl- β -CD, DM- β -CD) and

unmodified CD (β -CD) respectively enhanced their solubility in water (Jeromin and Ritter 1998, 1999). Water-soluble free radical initiator then initiated polymerization of these complexed monomers in an aqueous medium. During the polymerization of included monomer, the resulting polymer gradually precipitated out leaving behind water soluble CD in aqueous medium (Figure 1.6).

Glockner and Ritter (1999) reported the copolymerization behavior of complexed monomers. The co-monomer reactivity ratios of DM- β -CD complexed monomers, isobornyl acrylate and n-butyl acrylate ($r_{\text{isobornyl acrylate-}\beta\text{-CD}} = 0.3 \pm 0.1$; $r_{\text{n-butyl acrylate-}\beta\text{-CD}} = 1.7 \pm 0.1$) differ significantly from those of uncomplexed monomers in organic medium ($r_{\text{isobornyl acrylate}} = 1.3 \pm 0.1$; $r_{\text{n-butyl acrylate}} = 1.0 \pm 0.1$). These authors also reported the influence of chain transfer agent on the degree of polymerization. The ICs, methyl methacrylate-DM- β -CD and styrene-DM- β -CD were polymerized in aqueous medium in presence of 0 to 3.0 mole % water soluble chain transfer agent, N-acetyl-L-cysteine. The higher chain transfer constant values were obtained for complexed monomers (Cs for MMA-DM- β -CD = 1.7 ± 0.3 and Cs for Styrene-DM- β -CD = 2.6 ± 0.3) as compared to the polymerization of uncomplexed monomers (Cs for MMA = 0.7 ± 0.1 and Cs for Styrene = 0.7 ± 0.1) in organic solvent. This indicated that the degree of polymerization could be controlled effectively using water-soluble chain transfer agent.

Bernhardt et al., (2001) reported the effect of hydrophilic character of the included guest on the initial rate of polymerization. The increase in the hydrophilic nature of the included guest decreases the initial rate of polymerization. The author suggested that the increase in hydrophobic character of the included guest increases the local concentration of complexes close to the active radical chain end of the phase separated polymer and thus leads to higher values of the initial polymerization rate.

Recently, Sarvothaman and Ritter (2004) reported the IC mediated polymerization of dimethacrylate and diacrylate with an idea to develop a new class of mutually interlocked molecules. The author aimed at the synthesis of polyrotaxane structures having different physical and mechanical properties because of different topology as compared to the classical polymers. Diacrylate and dimethacrylate of 1, 4 butane diol and 1, 6-hexane diol were complexed with DM- β -CD as well as α -CD. CDs showed the

discriminating behavior during complex formation between the diacrylate and dimethacrylate. Diacrylate formed a true inclusion complex in which CD was completely threaded on the diacrylate molecule whereas dimethacrylate showed the partial inclusion in CD where the CD sits at the terminal position. Aqueous polymerization of these complexes resulted in the formation of interlocked polymer architectures because of dethreading of CD ring and cross-linking of the exposed double bonds (Figure 1.7). The FTIR and thermal analysis of these polymers showed the evidence for the presence of polyrotaxane architecture.

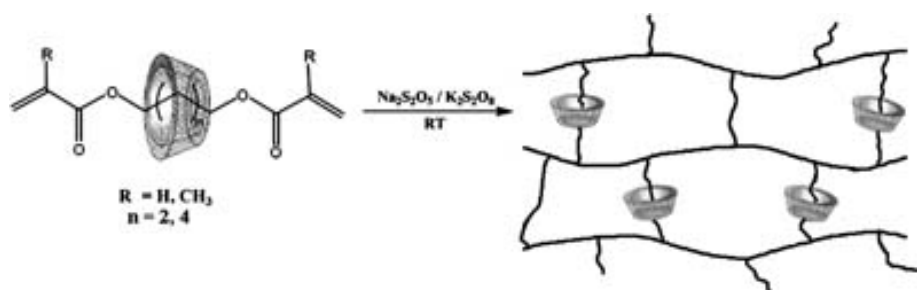


Figure 1.7: Interlocked cross-linked polymers from IC of divinyl monomers
(From Sarvothaman and Ritter 2004)

The amount of β -CD controlled the branching in poly (sulfone-amine) chains. β -CD did not take part in polymerization but remained in the form of complex on the molecule during polymerization. Thus CD threaded onto to the polymer chains after polymerization. The Figure 1.8 illustrates the concept of controlled polymerization using CD.

Chen et al., (2006) explored the use of CD to control polymer topology in the condensation polymerization. The polycondensation-addition reaction of 1-(2-aminoethyl) piperazine, a BB'_2 monomer and divinylsulfone, an A_2 monomer resulted into the formation of hyperbranched structures by monomer-coupling methods. This was due to the difference in reactivity between primary amino and secondary amino groups of 1-(2-aminoethyl) piperazine monomer which form an $AabB'_2$ -type intermediate and further polymerization yields hyperbranched poly (sulfone-amine) (PSA). 1-(2-aminoethyl) piperazine formed stable complex with β -CD because of the presence of intermolecular hydrogen bonding interactions between the amino and

hydroxyl groups of 1-(2-aminoethyl) piperazine and β -CD respectively. Polymerization of 1-(2-aminoethyl) piperazine- β -CD IC and divinylsulfone yielded linear polymers having higher decomposition temperature than pure poly (sulfone-amine). The higher stability of polymer chain was attributed to the presence of complexed β -CD rings.

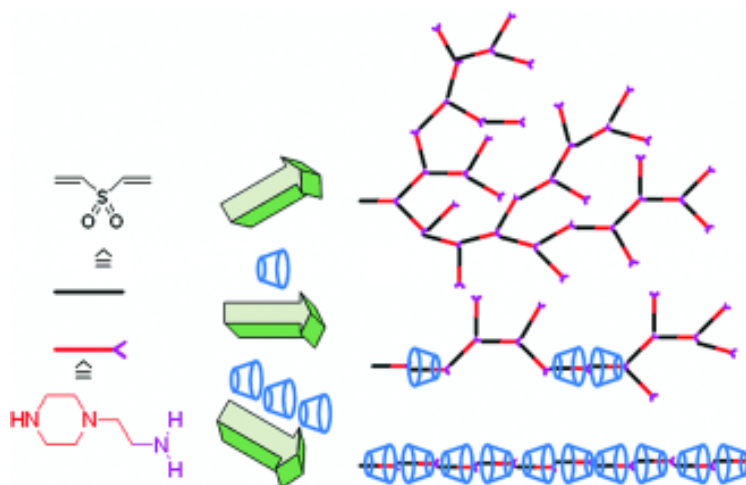


Figure 1.8: Inclusion complex mediated controlled polymerization
(From Chen et al., 2006)

The computational analysis revealed that the 1-(2-aminoethyl) piperazine molecule after encapsulating into the CD cavity, behaves as a bifunctional monomer during polymerization to yield a linear polymer with divinyl sulfone.

1.2.3.3 Experimental Evidences for the IC Formation

Most of the inclusion complexes are obtained by precipitation method. In this CD rings are threaded on the guest molecule and whole complex precipitates out from water. The precipitation of the inclusion complex indicates the geometrical fit of the guest into CD cavity. Synthesizing stoppers at both the ends of the polymer chain generally obtain the additional evidence for the formation of IC in polymers. If the stoppers prevent the formation of an IC then one can conclude that the inclusion must have taken place in absence of stoppers. The yield of the complex depends on the molar concentration of CD and added guest molecules. CD always forms stoichiometric complexes with the guest molecules.

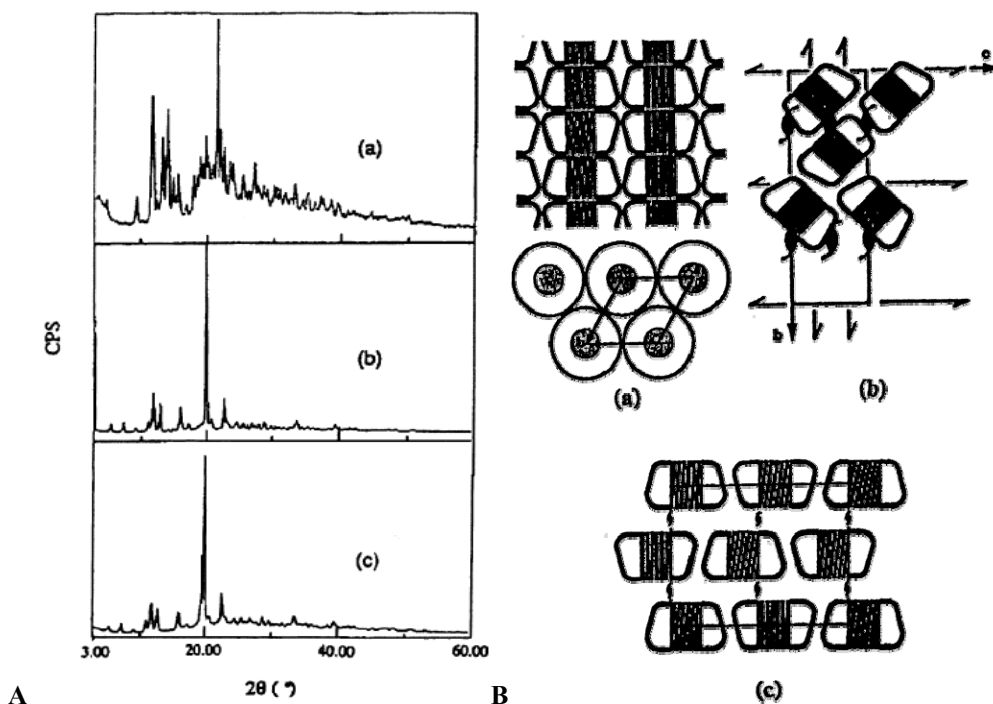


Figure 1.9 A. X-ray diffractogram of a. free α -CD, b. valeric acid- α -CD IC, c. poly (oxyethylene)- α -CD IC (From Harada et al., 1993)

Figure 1.9 B Schematic of a. channel type, b. cage herringbone type, c. cage brick type crystal structures formed by crystalline ICs (From Rusa et al., 2001)

X-ray crystal structural analysis of is one of the critical methods to characterize the CD complex. Since it is difficult to grow a single crystal of complex, this method is seldom used. Therefore the crystal structures of very few CD complexes are available. However, X-ray powder diffractograms are generally useful to characterize the complexes of small organic molecules as well as the large polymer chains. The diffractograms provide enough evidence to differentiate the structural arrangement of CDs complexes such as herringbone and channel type packing (Figure 1.9).

CDs in absence of inclusion complexation remains in cage type structure have lower symmetry and show a great number of reflections. This causes the presence of many peaks in X-ray powder diffractogram. In contrast the presence of long chain polymer in cavity, CDs adopts a channel type structure and has fewer reflections, with characteristic strong reflection at $\theta = 20^\circ$ in diffractogram (Figure 1.9 A).

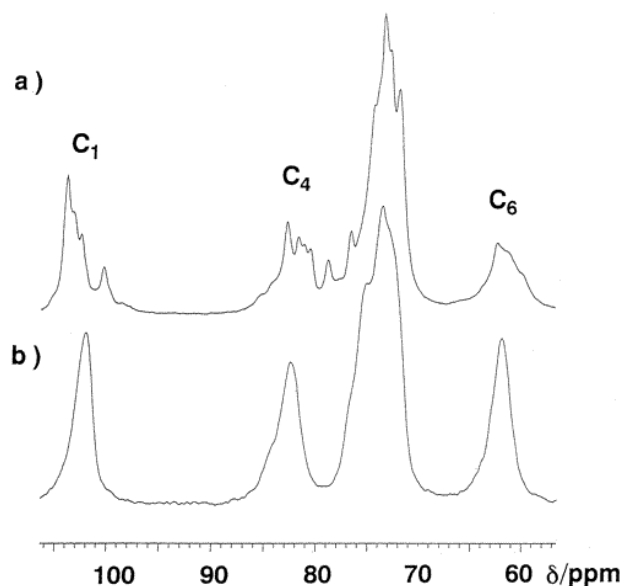


Figure 1.10 Solid-state ¹³C CP/MAS NMR spectra of a. α-CD, b. α-CD-PEA IC (MW = 1200) complex (From Harada et al 1997)

Solution NMR spectroscopy is not really useful to characterize the ICs for the interactions present in between the guest and CD cavity. As in polar solvents such as DMSO the ICs rapidly undergo dethreading but the compositions can be calculated. ¹³C CP/MAS solid state NMR spectroscopy provides valuable structural information about the CD complexes. The inclusion of guest into the CD cavity gives it a symmetrical cyclic conformation. This can be concluded from the solid state CP/MAS NMR spectra of CD before and after inclusion of the guest. The spectrum of free CDs shows the presence of multiple signals for each carbon of glucose ring. In contrast, after inclusion of guest into the CD cavity each carbon appears as a singlet. These sharp carbon signals are clear evidence in favor of inclusion of guest into CD cavity (Figure 1.10).

FTIR analysis of ICs provides useful information about the interacting groups of guest molecule and hydroxyl groups of CDs. The presence and extent of intermolecular interactions can be observed from the relative shift in the peak positions of CD and guest molecules. In the FTIR spectrum of free CD molecules the hydroxyl groups appear as a broad peak and after formation of an inclusion complex the same results in a sharp signal. This indicates the breaking of intramolecular hydrogen bonding

interactions of hydroxyl groups of CD and the formation of intermolecular hydrogen bonding with the functional groups of the guest molecules.

1.2.3.4 Industrial Applications of CD ICs

CD has a wide range of industrial applications and the market for them is growing continuously because of their unique complex formation properties as well as de-complexation kinetics.

Pharmaceutical Applications

The complex formation ability of CDs is broadly utilized in pharmaceutical industry and drug delivery systems. CDs may act as protecting agent for certain drug molecules by forming complex and thus prevent their premature metabolism. CDs are also utilized to enhance the solubility of poorly soluble drug without any chemical modification. The complex formation ability of CDs is utilized to mask the unpleasant taste and malodors of the drug molecules.

Analytical Separation

Analytical chemistry is one of the major areas of CDs application. CD is being used mainly in chromatographic methods such as thin layer chromatography, gas chromatography, capillary electrophoresis and high-pressure liquid chromatography (HPLC). CDs are used as complexing agent for the analytes under study. The presence of CDs or their derivatives in the mobile phase or as chemical bonded to the stationary phase improve the separation efficiency and the speed of analysis and thus lead to the separations of isomers as well as closely related compounds. This is a low cost alternative to the HPLC separation of enantiomer using chiral columns having high cost for stationary phase.

Foods and Flavor Industry

CDs are used in food industry because of their high temperature stability during food processing. Complexation of expensive flavor of oils and spices, such as apple, citrus, cinnamon, garlic, ginger, and menthol with CDs reduces the amounts that required adding to achieve the required flavor strength. The inclusion of flavor protects the flavoring from oxidation, photochemical degradation, thermal decomposition or loss by sublimation etc. Complexation of volatile oils with CDs converts them into the fine powder thus reduces their handing, packaging and storage costs as well as reduces their

microbial contaminations. CDs are also utilized to selectively remove cholesterol from the products like milk, butter and eggs.

Agricultural Applications

In agriculture CDs are used to encapsulate the herbicides, pesticides, insecticides, fungicides, repellent, growth regulators etc. The inclusion increases their stability as well as water solubility.

Cosmetics, Personal Care and Toiletry

The main advantages of ICs of CD in this field are to improve the process aid after conversion of liquid ingredient into the solid form, their stabilization and odor control. The applications include toothpaste, skin creams, liquid and solid fabric softeners, and deodorant etc.

1.3 Free Radical Polymerization of Multivinyl Monomers

Free radical polymerization of multivinyl monomers leads to the formation of cross-linked materials. Polymeric networks thus synthesized have a wide range of specialized applications such as superabsorbents, ion exchange resins, column packing material for size exclusion chromatography, photoresist, optical fiber coating, dental materials, contact lenses, and controlled release delivery systems (Zhu and Hamielec 1993).

1.3.1 Mechanism of Network Formation

The multivinyl monomer undergoes various reactions during polymerization in presence of free radical initiator. These are presented in Figure 1.11. During polymerization the polymer radical propagates with a double bond on a divinyl monomer, the unreacted double bond on the same monomer molecule becomes pendant on the polymer chain (Zhu and Hamielec 1993). The reactivity of this pendant double bond decides the fate of polymerization product such as its cross-link density, sol fraction, and critical conversion for gelation (Landin and Macosko 1988). If the growing polymer radical adds to the double bond of another monomer, then the linear polymer containing pendant double bonds will be formed (intermolecular propagation). If the growing polymer radical adds to the pendant double bond of previously formed polymer chain, cross-linking would take place. Thus tetra branched polymer chains are formed which on further branching lead eventually to cross-linking (intermolecular cross-linking) (Zhu and Hamielec 1993).

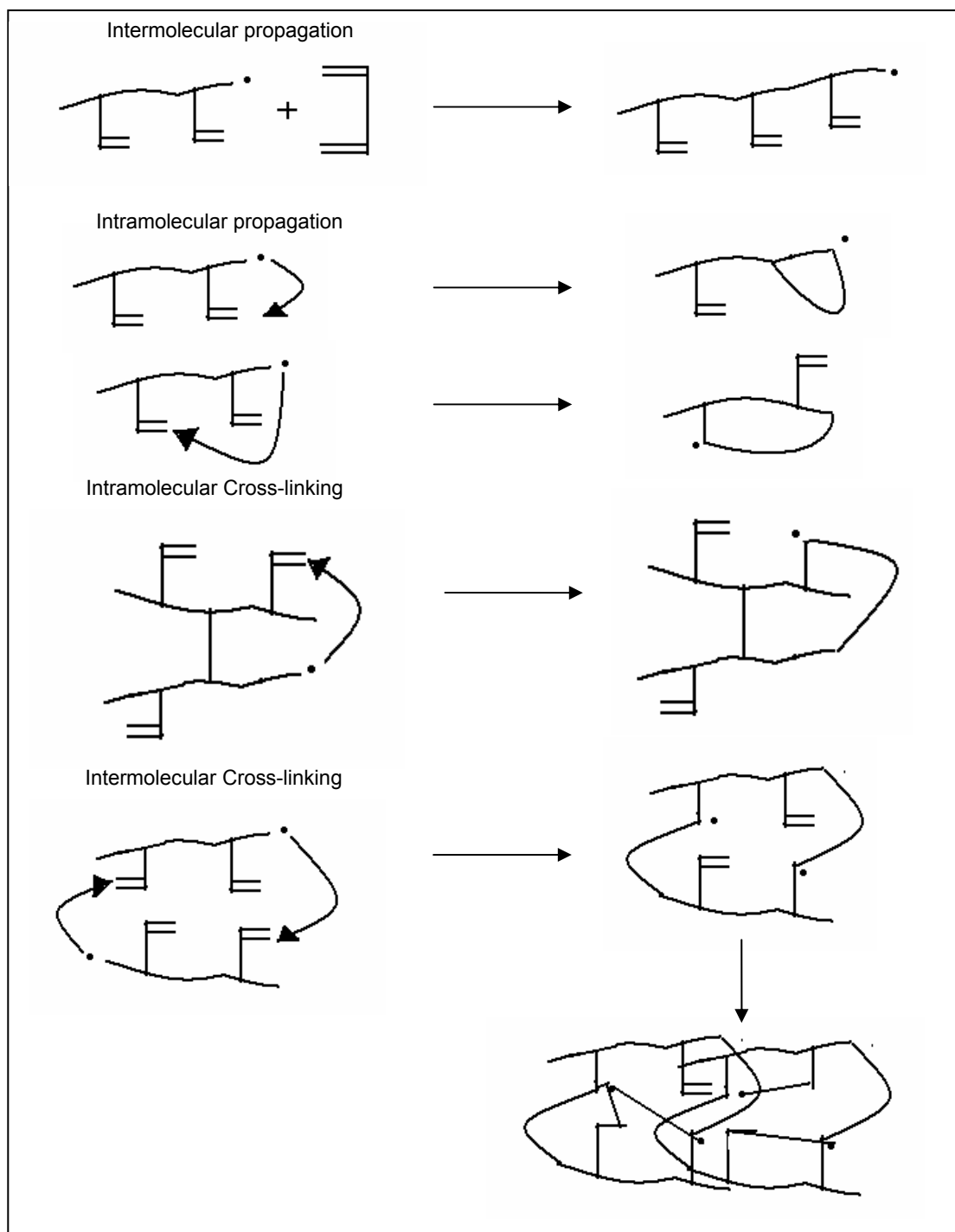


Figure 1.11: Reactions involved in polymerization of divinyl monomer

In contrast if the growing polymer radical reacts with the pendant double bond present on the same polymer chain, a cyclized product would be formed (intramolecular propagation) (Landin and Macosko, 1988). Most of the polymerization reactions of

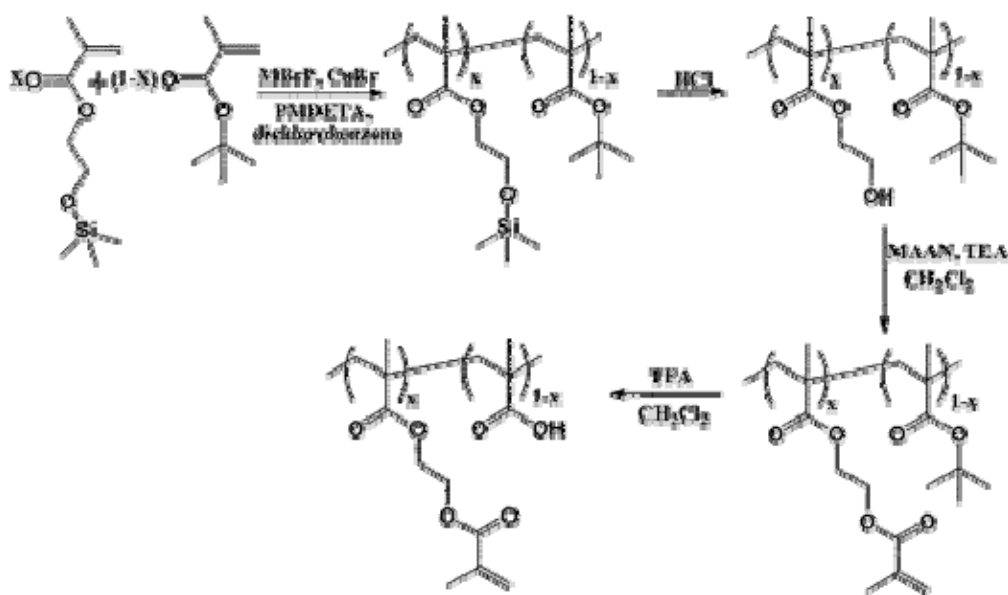
divinyl or trivinyl monomers the intermolecular cross-linking as well as intramolecular cyclization reactions occur simultaneously, which dramatically changes the network properties (Elliott and Bowman 2002).

Thus understanding the behavior of pendant double bonds is a key to study the network formation by addition polymerization involving multifunctional monomers (Landin and Macosko 1988).

Significant synthetic efforts are being devoted to control network formation. This is because applications of cross-linked products in emerging areas such as biosensors, optical waveguides, processable molecularly imprinted polymers, and microlithography demand non cross-linked soluble polymers having pendant vinyl functionally which can undergo cross-linking when desired (e.g. by irradiation or thermal treatment) (Li et al., 2005, 2006, Nagelsdiek et al., 2004, Koo et al 2002, Liu et al 2001). These materials offer dual advantage of solvent processability as well as fine-tuning of the properties of the final product over the cross-linked products obtained by the conventional methods.

1.3.2 Prior Approaches

1.3.2.1 Soluble Linear Polymers and Pendant Group Functionalization



Scheme 1.1 Synthesis of poly (HEMA-*co*-t-BMA) and post functionalization

(From Li et al., 2005)

This methodology involves the synthesis of linear, soluble copolymers containing pendant hydroxyl functionality and its subsequent modification. e.g. the free radical copolymerization of 2-hydroxyethyl methacrylate (HEMA) or silyl protected HEMA i.e. HEMA-TMS with various co-monomers such as glycidyl methacrylate (GMA), methyl methacrylate (MMA), t-butyl methacrylate (t-BMA), n-butyl acrylate (n-BA), t-butyl methacrylate (t-BMA), acrylic acid (AA) was carried out over a range of co-monomer feed ratios. The pendant hydroxyl groups of these co-polymers were then functionalized using methacryloyl / acryloyl chloride or methacrylic anhydride to obtain polymers containing pendant double bonds. These polymers were shown to be useful as a positive photoresist (Liu et al., 2001), in wave-guide applications (Koo et al., 2002), for the synthesis of functional self cross-linked nanoparticles (Mecerreyes et al., 2001; Jiang and Thayumanavan, 2005) and as molecularly imprinted polymers (Li et al., 2005), etc.

Limitations

- Methacryloylation using methacryloyl chloride
The results of pendant group functionalization are not consistent, and the product, which varied in nature from a free flowing powder to a contaminated sticky solid, was difficult to isolate (Koo et al., 2002).
- Methacryloylation using methacrylic anhydride
Methacrylic anhydride is less reactive than methacryloyl chloride and is suitable for the preparation of esters only under mild conditions (Koo et al., 2002).
- In both cases stabilizers e.g. *p*-benzoquinone need to be added during the reaction to inhibit the cross-linking. But there are problems in removing the stabilizer. Also the presence of stabilizers lowers the rate of polymerization
- Incomplete conversion of pendant groups, homo polymerization of modifier as well as cross-linking of the already functionalized polymers.

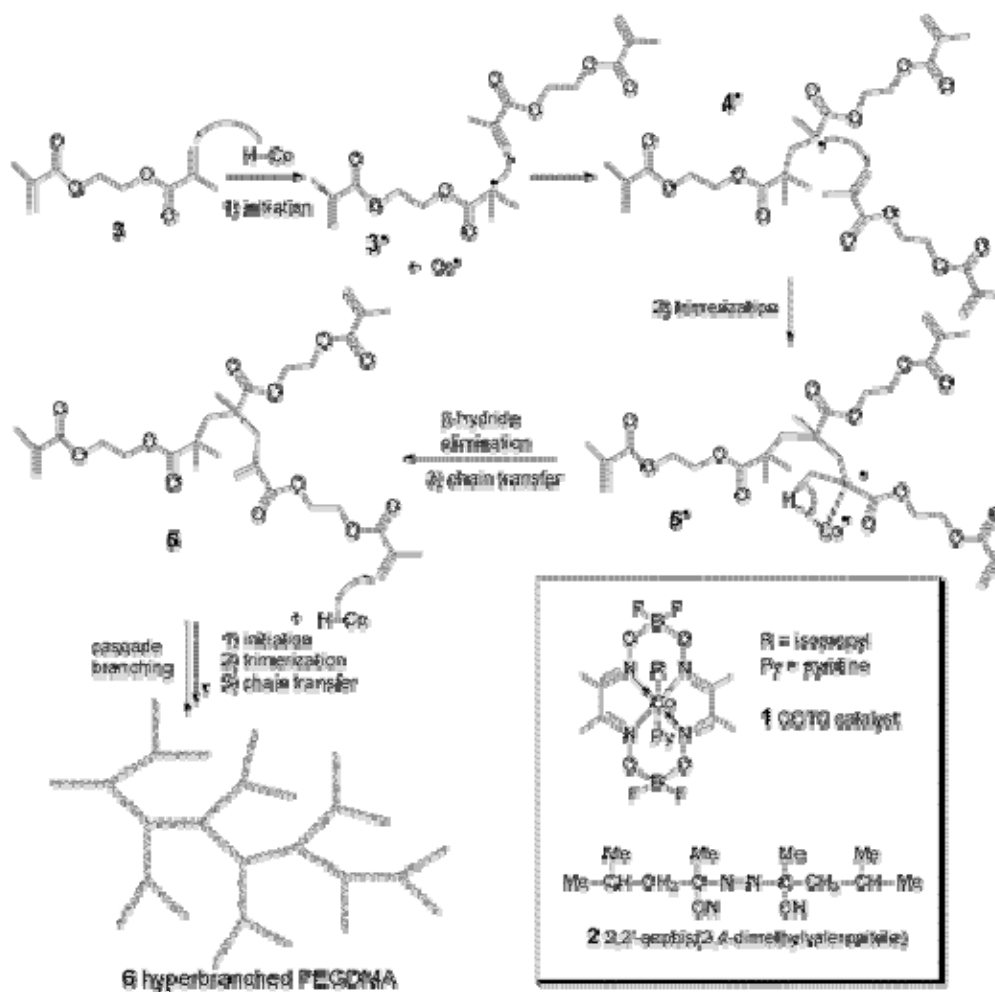
1.3.2.2 Polymerization of Divinyl Monomers

Atom Transfer Radical Polymerization (ATRP)

In this method the polymerization of divinyl monomer containing the double bonds differing in reactivity e.g. allyl methacrylate (AMA) was carried out. Soluble polymers were synthesized by adjusting the degree of polymerization of AMA using appropriate monomer / initiator ratio, which is the crucial parameter governing cross-linking

reaction. Nagelsdiek et al (2004) reported the synthesis of various homo polymers and co polymers of AMA by this method.

Transition Metal Mediated Polymerization



Scheme 2: Cobalt mediated polymerization of EGDMA

(From Guan 2002)

Guan (2002) reported a new approach to control polymer topology through transition metal mediated radical polymerization. In this approach, hyperbranched polymers of EGDMA were synthesized using free radical polymerization by controlling the competition between propagation and chain transfer catalyst.

In this study, a cobalt chain transfer catalyst (CCTC) was used to control the propagation of free radical polymerization of divinyl monomer. The cobalt complexes

bind reversibly to the growing radical centers, and this leads to β -hydride abstraction to terminate the propagating chains while generating cobalt-hydride species to reinitiate new propagating chains. If a dimethacrylate monomer is used and if the CCTC is chosen at the concentration for termination of methacrylate at the trimer stage, the repetitive trimerization of a dimethacrylate monomer leads to hyperbranched polymer.

Group Transfer Radical Polymerization (GTP)

Isaure et al., (2004) reported a facile, generic and cost effective route to branched vinyl polymers via conventional free radical polymerization using a multi-functional vinyl comonomer as the branching species. In this case, the presence of chain transfer agent or catalytic chain transfer species inhibited gelation. With appropriate choice of reaction conditions, copolymerization of methyl methacrylate and ethylene glycol dimethacrylate using Cu based ATRP or GTP methodologies yields soluble branched polymers in facile one-pot reactions.

Initiator Fragment Incorporation Radical Copolymerization

Free radical polymerization of divinyl monomers yields cross-linked materials because of infinitely high molecular weight of the polymers. In the conventional radical polymerization an increase in initiator concentration causes a decrease in the molecular weight of the polymer because of enhanced termination rate. Thus the use of higher initiator concentration in the polymerization of divinyl monomers results in decrease in the polymer molecular weight and resulting polymer becomes soluble.

Sato et al., 2004 reported a methodology to obtain soluble hyperbranched copolymers from divinyl monomer, ethylene glycol dimethacrylate (EGDMA) using high concentration of initiator. In this case the copolymerization of EGDMA with comonomers such as N-methylmethacrylamide, 1,1-diphenylethylene, di α -ethyl β -N-(α' -methylbenzyl) itaconamates (RS- and S-EMBI) derived from (RS)- and (S)- α -methylbenzylamines was conducted at 70 and 80 $^{\circ}$ C using dimethyl 2,2'-azobis isobutyrate as initiator at concentration as high as 0.35 to 0.70 moles/lit. The use of large amount of initiator results in its incorporation in copolymer through initiation and primary radical termination and yields the soluble hyperbranched polymers.

Limitations of Existing Techniques

- Require extreme reaction conditions

(Dry solvents, highly pure reactants & moisture free reaction environment)

- Percentage of double bonds available for post modification is low.
- Incorporation of high concentration of chain transfer agents or initiator in polymer structure changes the properties of the final polymers.

These limitations highlight the need to develop simple methodology to control the reactivity of multivinyl monomer in free radical polymerization independent of choice of multivinyl monomers.

1.4 Molecular Imprinting and Drug Delivery

1.4.1 General Principles of Molecular Imprinting

Molecular imprinting is a technique for the creation of materials having highly specific molecular recognition ability (Komiyama et al., 2002). This involves the copolymerization of functional monomers and multivinyl monomers in presence of molecular template, which imprints the structural information into the resulting polymers. The process of molecular imprinting involves the following steps (Komiyama et al., 2002)

- i. Formation of covalent linkage or non-covalent complex between the template molecule and functional monomers.
- ii. Polymerization of the monomer-template complex in presence of high amount of cross-linker.
- iii. Extraction of template from the cross-linked polymer matrix.

The imprinted polymers after template extraction exhibit a memory for the size, structure, and the interactions such as hydrogen bonding, hydrophobic with the template, and thus bind the template molecule efficiently and selectively (Komiyama et al., 2002).

There are two distinct approaches namely covalent (Wulff and coworkers 1995) and non-covalent (Mosbach and coworkers 2000) to obtain the molecularly imprinted polymers.

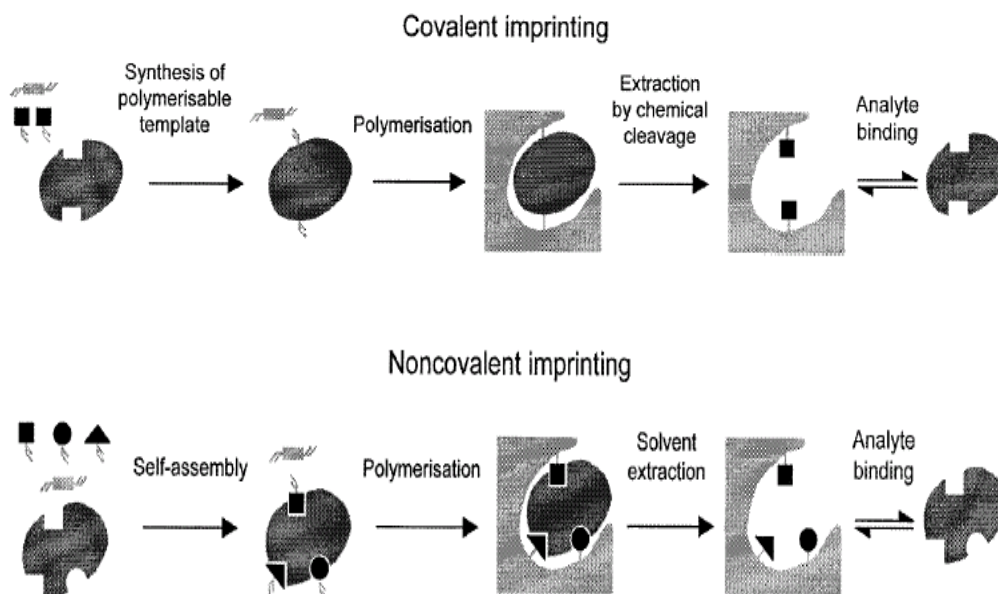


Figure 1.12: Process for covalent and non-covalent molecular imprinting
(From Haupt and Mosbach, 2000)

1.4.1.1 Covalent Imprinting

In this approach the functional monomer and template are bound to each other by covalent linkage. Template bound functional monomers and cross-linkers are then co polymerized under the conditions where the covalent linkage is intact. After the polymerization, the covalent linkage between the template and cross-linked polymer matrix is cleaved to remove the template from the polymer matrix. During rebinding the template is recognized by functional co-monomer of the polymer matrix. The success of this approach largely depends on the choice of the covalent linkage that connects a functional monomer and template molecules. These linkages must be stable under the conditions of polymerization and also must be easily cleaved under mild condition without affecting the properties of imprinted cavity. Also to bind the template molecule and release it, both the formation and dissociation of the covalent linkage must be fast. Wulff and coworkers (1977) reported the use of boronic acid ester linkage to obtain the imprinted polymers. 4-Nitrophenyl α -D-mannopyranoside was covalently linked with the two molecules of p-vinyl benzene boronic acid, and co polymerized with methyl methacrylate and ethylene glycol dimethacrylate. After the polymerization the boronic acid ester linkage was cleaved by hydrolysis and thus 4-nitrophenyl α -D-

mannopyranoside was removed from the cross-linked matrix. The imprinted polymer matrix strongly and selectively bound to 4-nitrophenyl α -D-mannopyranoside as the boronic acid groups were suitably frozen to remember the structure of the sugar molecule.

The other covalent linkages satisfying the conditions of thermodynamic and dynamic requirements include the carbonate esters (Whitcombe et al., 1995), acetals, ketals (Shea and Dougherty, 1986), Schiff bases (Wulff and Vietmeirer, 1989), disulfide bonds (Mukawa et al., 2002) and coordination bonds (Takeuchi et al., 2001; Matsui et al., 1996).

1.4.1.2 Non-covalent Imprinting

In this approach the functional monomer and template molecule are bound together through the non-covalent interactions such as hydrogen bonding, electrostatic or hydrophobic interactions. Thus the functional monomer and template are simply mixed together in a suitable solvent and the polymerization is carried out in the presence of cross-linker. After polymerization the template is removed by extractions of polymer in appropriate solvent. Thus the choice of solvent is critical in non-covalent imprinting. It must dissolve the functional monomer, cross-linker and template and also should not affect the hydrogen bonding or other non-covalent interactions between the functional monomer and template molecules. In all non-covalent interactions, hydrogen bonding is the most commonly employed interaction as it depends on the distance and direction between the functional monomer and template. Thus for the non-covalent imprinting the functional monomers comprising either carboxyl (Vlatakis et al., 1993), amino (Jie and Xiwen 1999), pyridine (Haupt et al., 1998), hydroxyl and amide (Li et al., 2006) groups and the template of complementary functionality are utilized. Some of the functional monomers and templates having multiple sites to form the hydrogen bond, result in more stable and highly efficient imprinting (Turkewitsch et al., 1998; Li et al., 2006). This approach is widely used in chromatographic separation, catalysis, solid phase extraction, biomimetic sensors, and drug delivery because of its flexibility in choice of functional monomer as well as possible template molecules (Sellergren, 2001; Lanza and Sellergren 2001; Mosbach and Ramstrom 1996; Komiyama et al., 2002; Haupt and Mosbach 2000; Wulff 1995; Zimmerman and Lemcoff 2004).

1.4.1.3 Semi-covalent Imprinting

This is a hybrid approach, which combines the advantages and minimizes the disadvantages of covalent and non-covalent molecular imprinting. In this approach the template is covalently bound to the polymerizable groups and therefore after its release the cavity comprises only the specific functionality. The rebinding of the template takes place by non-covalent interactions. Sellergren and Andersson (1990) were the first to report true semi-covalent approach for the imprinting of p-aminophenylalanine ethyl ester. A structural analogue p-aminophenylalanine ethyl ester comprising two polymerizable groups attached via ester linkages were used during the synthesis. The carboxylic groups were left in the cavity after hydrolyzing the template. The rebinding of template was take place by using the hydrogen bonding as well as electrostatic interactions. The other examples of the templates for semi-covalent imprinting include testosterone (Sneshkoff et al., 2002), phenol and bisphenol A (Joshi et al., 1998-2000) and nitro phenol (Caro et al 2002).

1.4.2 Newer Approaches for Imprinting

In view of applications of the molecularly imprinted polymers in various fields, new strategies are developed to improve their properties and performance. Some of these are summarized below.

1.4.2.1 Molecular Imprinting: Monolith to Nonomaterial

Nanotechnology is driving the attention of the researchers because of enhanced properties and functionalities of nanomaterials, which could not be achieved with the bulk materials (Jiang and Thayumanavan 2005, Chronakis et al 2006). The traditional molecular imprinting approach yields microporous monoliths as it involves the bulk polymerization of functional monomer-template complex (formed by covalent or non-covalent interactions) and high concentration of cross-linker initiated by thermal or irradiation methods. These monoliths were then crushed and sieved to fine powder yielding particles of irregular size and shape. However in most of the applications, the imprinted polymers of specific size and shape are required to achieve the enhanced performance and properties such as higher affinity, selectivity, capacity and the accessibility for recognizing the target molecules. Therefore substantial research efforts continue to be devoted to downsizing i.e. minimizing the size of the molecularly

imprinted polymers into sub-micrometer to nanometer range (Perez et al., 2000, Biffis et al., 2001, Vaihinger et al., 2002, Yang et al., 2004, Ciardelli et al., 2004, Li et al., 2006).

Ye et al., (1999) reported the synthesis of monodisperse, spherical micron sized polymer particles in good yield by novel precipitation polymerization. Theophylline and 17β -estradiol imprinted polymers were synthesized by polymerizing the functional monomer-template complex and cross-linker under high dilution conditions. The specific binding sites in precipitated monodisperse particles have higher load capacities compared to the classical particles obtained by grinding the imprinted monolith.

In classical free radical polymerization of monovinyl and divinyl monomers increase in solvent concentration causes the formation of intramolecularly cross-linked microgel particles. Biffis et al (2001) utilized the concept to obtain the imprinted microgel particles from homogeneous polymerization solution. Sugar imprinted microgel particles of methyl methacrylate and ethylene glycol dimethacrylate (containing 50 % of cross-link density) were obtained by free radical solution polymerization in dilute solution. The rebinding experiments demonstrated the presence of specific cavities in the microgel particles, which recognize the print molecules and bind selectively.

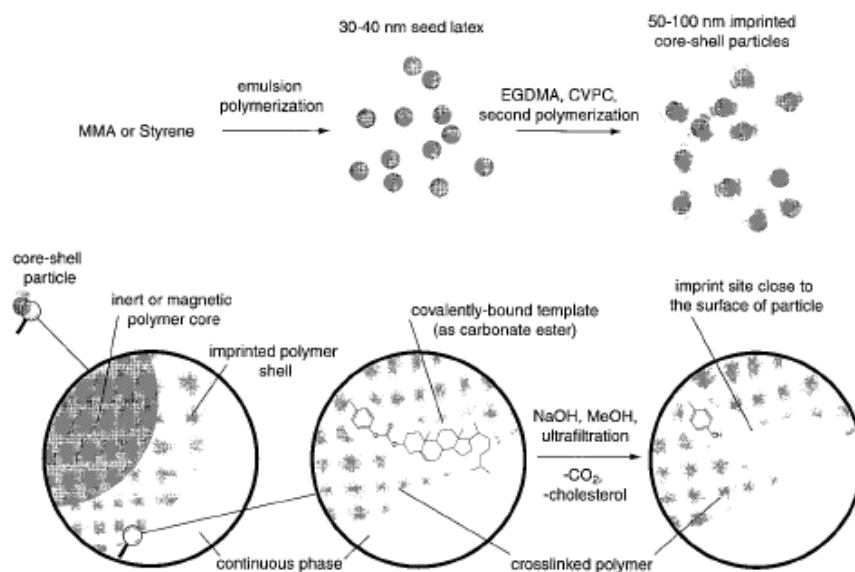


Figure 1.13: Synthesis of imprinted core-shell nanoparticles by emulsion polymerization (Perez et al., 2000)

Perez et al (2000) reported the synthesis of cholesterol imprinted core-shell nanoparticles by two-stage emulsion polymerization using covalent imprinting. The core comprised of methyl methacrylate or styrene whereas the shell was made up of ethylene glycol dimethacrylate. Cholesterol was imprinted in the core by using the carbonate ester sacrificial spacer methodology (Vulfson et al., 1997). After removal of cholesterol from the shell by hydrolysis, the imprinted nanoparticles showed the higher specific binding compared to the imprinted polymers obtained by bulk or suspension polymerization.

Emulsion or suspension polymerizations are kinetically controlled and lead to imprinted polymers, which lack homogeneity. Vaihinger et al., (2002) reported the use of mini emulsion polymerization a thermodynamically controlled polymerization methodology to obtain the imprinted polymers. The imprinted MAA-co-EGDMA microgel particles were obtained by mini-emulsion polymerization in presence of a chiral amino acid derivative. The molar ratio 2.5 to 1 of MAA to EGDMA showed the best enantioselectivity amongst all the compositions. The imprinted nanoparticles obtained by this methodology have high specific surface area and defined shape, which may allow their use in new affinity processes using fully synthetic receptors.

Thus the imprinted microgels or nanoparticles obtained by various methodologies have applications in drug delivery, chromatographic separation chiral separation, bio or chemical sensors as well as in medical devices etc (Ciardelli et al., 2004; Chronakis et al., 2006; Li et al., 2006).

1.4.2.2 Novel Functional Cross-linkers

As described earlier the synthesis of molecularly imprinted polymers by conventional non-covalent approach comprises first the formation of self-assembly complex between the functional monomers and the template and is followed by the copolymerization of complexed functional monomers and cross-linker to form the polymer network around the template molecule. After extraction of the template the resulting imprinted polymers contain the specific cavities, which are complementary in shape and functionality to the template molecule. In the covalent imprinting approach, increase in the cross-linking density of the imprinted matrix increases the specific recognition (Wulff et al., 1987). However in non-covalent imprinting the functional monomers and the template

molecules are bound by the non-covalent interactions and thus to increase in the concentration of template need to increase the concentration of functional monomer. This in turn decreases the amount of cross-linker and thus the recognition properties because of the random motion of loosely cross-linked polymer (Sellergren 1989). Thus optimum balance between the functional monomer and the cross-linkers is needed and is difficult to achieve.

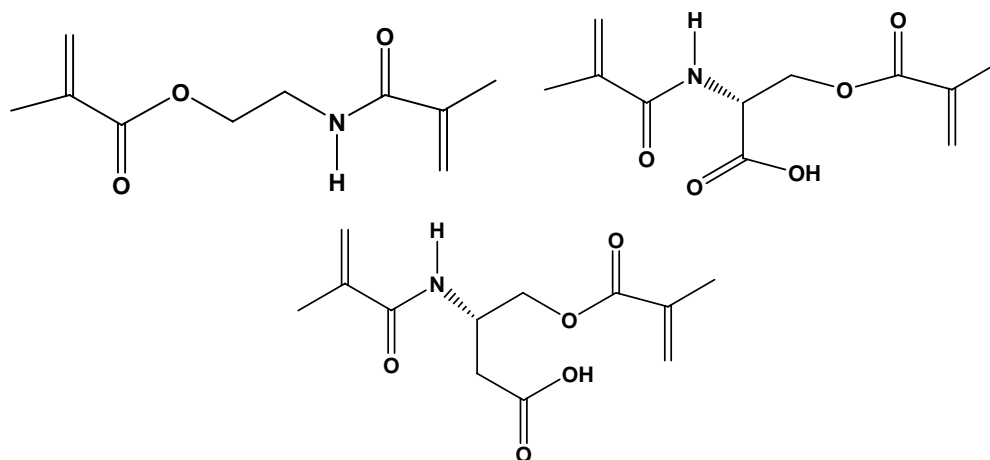


Figure 1.14: Novel cross-linkers for molecular imprinting
(From Sibrian-Vazquez and Spivak 2003, 2004)

In view of this new strategy to synthesize the functional cross-linkers i.e. the monomers comprising both the recognition as well as cross-linking functionality was developed (Sibrian-Vazquez and Spivak 2004 and 2003). These novel cross-linkers eliminated the need to limit the concentration of functional monomer, cross-linkers and template molecules as well as their relative ratio optimization during imprinting. Imprinted polymers obtained from these functional cross-linkers exhibited the improved the selectivity and thus better performance as compared to the conventional functional monomers used for molecular imprinting (Sibrian-Vazquez and Spivak, 2004).

1.4.2.3 Two Stage Approach / Processable Imprinting

Molecularly imprinted polymers are highly cross-linked materials and are therefore difficult to process (Southard et al., 2006). This limits their application in fabricating the chemical and biological sensors where the membranes or film formation is necessary

(Nickel et al., 2001; Das et al., 2003). Recent approaches to overcome this involve the synthesis of polymer and then its fabrication into imprinted polymer (Li et al., 2005, 2006, Southard et al., 2006).

Li et al., (2006) reported the synthesis of novel multi functional copolymers, poly (methacryloyl methacrylate-co-methacrylic acid) comprising both the recognition as well as cross-linkable functionality. These copolymers were interacted with the theophylline template using non-covalent and specific binding interactions i.e. hydrogen bonding. This polymer-template complex was then cross-linked using thermal or photo initiator, after film formation on a suitable substrate or in the bulk. Theophylline was extracted in a suitable solvent. The imprinted polymers exhibited the enhanced selectivity towards theophylline when compared with its structural analogues i.e. caffeine and theobromine. Thus this approach is useful and enables the fabrication of imprinted devices after film formation.

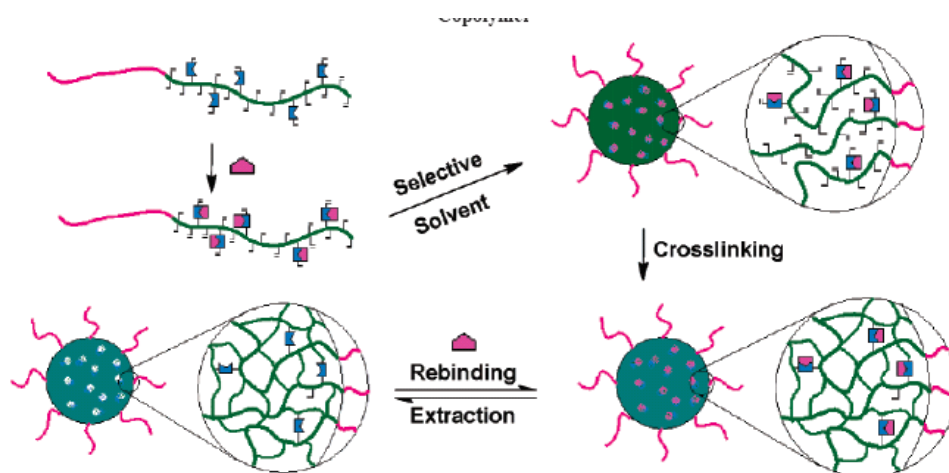


Figure 1.15: Preparation of imprinted nanospheres from the diblock copolymers

(From Li et al., 2006)

Li et al., (2006) extended their investigation further to obtain well-dispersed nanospheres using cross-linkable functional block copolymers. A diblock copolymer, poly [(tert-butyl methacrylate)-block-(2-hydroxyethyl methacrylate)], was synthesized by living free radical polymerization and further post functionalized with 2-acrylamido-6-carboxylbutylamidopyridine. Thus one block comprised both the interacting as well as cross-linking functionality. After interacting with the template molecules through

hydrogen bonding interactions these block copolymers self-assembled to form spherical micelle in block selective solvent. These micelles were then cross-linked to lock the desired structure. Imprinted nanospheres showed higher binding capacities and comparable selectivity to the materials obtained by conventional bulk imprinting. Also these nanospheres are easily dispersible in solvent, as they comprise a highly cross-linked, porous core and soluble corona layer. Thus the nanoscopic size, structure and properties make them potential candidate in designing the biosensors and other bio-applications.

Recently Southard et al., (2007) reported a novel approach to obtain processable imprinted star polymers containing intramolecularly cross-linked core. The soluble imprinted star polymers were obtained by the reversible addition fragmentation chain transfer polymerization (RAFT) followed by intramolecular cross-linking reaction by ring closing metathesis in presence of template molecules. These intramolecularly cross-linked imprinted polymers were soluble in common organic solvent and demonstrated to be useful at sub-ppb detection limit. Thus the soluble and processable molecular imprinting approach is a powerful step towards the design and development of bio and chemical sensors with improved performance.

1.4.2.4 Stimuli Responsive Imprinted Polymers

The binding sites in the imprinted polymers prepared by traditional molecular imprinting approach are rigid and are difficult to deform. The newer applications of imprinted polymers desire the flexible binding sites. Therefore various synthetic approaches are emerged to obtain the stimuli sensitive imprinted polymers.

Kanekiyo et al., (2003) explored the synthesis of pH sensitive imprinted polymers. The inclusion complex of acryloylamylose and the template bisphenol was co polymerized with ionizable monomers. The cross-linking density was tuned by varying the degree of acryloyl substitution on the amylose. The resulting imprinted polymers demonstrated pH dependent reversible binding characteristics.

Similarly, Alvarez-Lorenzo et al., (2000) reported the synthesis of thermo responsive imprinted polymers. These were the loosely cross-linked N-isopropyl acrylamide (NIPA) polymers in which the functional groups were dispersed. These polymers showed the rebinding of the metal ion as a function of temperature.

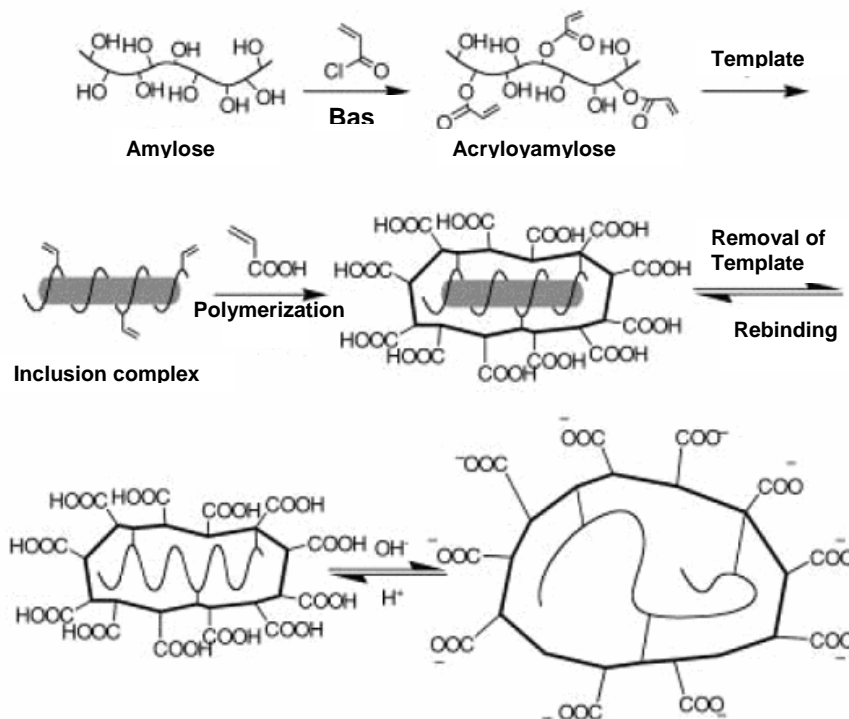


Figure 1.16: pH responsive imprinted polymers synthesis

(From Kanekiyo et al., 2003)

1.4.3 Imprinted Polymers for Drug Delivery

Molecularly imprinted polymers have been widely studied and used in analytical chemistry, separation science, as catalysts and as enzyme mimics etc (Komiyama et al., 2002, Haupt and Mosbach, 2000, Wulff 1995, Zimmerman and Lemcoff 2004). Applications of molecularly imprinted polymers for drug delivery are now being explored (Cunliffe et al., 2005). The cross-linked networks having high affinity towards drug templates could be used as drug reservoirs. In the conventional drug delivery system the drug has limited affinity to the polymer matrix and the diffusivity is high. Molecular imprinting approach is expected to sustain release over longer duration since the effective diffusivity is lowered because of the enhanced affinity between the drug and the functional monomer as result of imprinting (Cunliffe et al., 2005) (Figure 1.17).

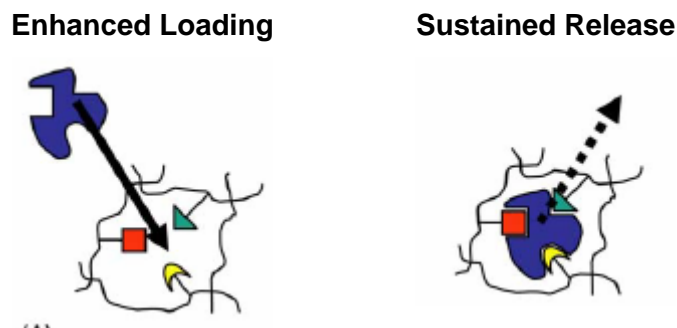


Figure 1.17: Molecularly imprinted polymers: drug loading and release
(van Nostrum 2005)

Norell et al., (1998) reported for the first time, the use of imprinted EGDMA-MAA polymer matrix for sustained release of theophylline. Theophylline has a narrow therapeutic window (30 to 100 μM) and concentrations higher than 110 μM are toxic. The release kinetics of theophylline was studied in phosphate buffer (pH 7) by varying the loading of theophylline from 0.1 to 50 mg theophylline per g of dry polymer. The authors observed that the polymers containing higher load of theophylline released it faster compared to the polymers containing lower theophylline loading. This was attributed to the heterogeneity of binding sites in imprinted polymers.

Recently Ciardelli et al., (2004) reported theophylline release from cross-linked poly (methyl methacrylate-co-methacrylic acid) nanospheres. The nanospheres were obtained by simultaneous precipitation and cross-linking polymerization using MAA as a functional monomer, MMA as a non-functional monomer and trimethylolpropane trimethacrylate (TMPTMA) as a cross-linker in dilute acetonitrile solution. These nanospheres showed sustained release of theophylline depending on the composition of nanospheres i.e. the concentration of functional monomer (MAA) and non-functional monomer (MMA). The imprinted nanospheres containing the nonfunctional monomer, MMA i.e. poly (MMA) released the substantial amount (about 50 %) of theophylline in first 3h. As the percentage of MAA increased from zero to 25 % to 50 % poly (MMA-co-MAA) (75:25 and 50:50) in the polymeric nanospheres, only 40 % theophylline release was observed in 3h. This was attributed to the presence of recognition functionality in the nanospheres, which binds the theophylline and sustained the release. Further increase in the MAA concentration i.e. in poly (MMA-co-MAA) (25:75) increased the release rate of theophylline and upto 60 % was released within first 4h.

The author concluded that the two factors regulated the release of theophylline from the imprinted nanospheres i. concentration of MAA and ii. the particles size of the nanospheres. Thus varying the percentage of functional and non-functional monomers during imprinting can modulate the release rate of theophylline.

Hiratani and coworkers (2004, 2005) evaluated imprinted soft contact lenses for improved loading and sustained release of Timolol. The authors studied various parameters influencing the release of Timolol from the imprinted lenses. To study the influence of nature of backbone monomers on loading and release four types of Timolol imprinted soft contact lenses were prepared by UV polymerization of N, N-diethylacrylamide (DEAA), 2-hydroxyethylmethacrylate (HEMA), 1-(tristrimethylsilyloxypropyl)-methacrylate (SiMA) and N, N-dimethylacrylamide (DMAA) (50:50 v/v), or methylmethacrylate (MMA) and DMAA (50:50 v/v) solutions, to which functional monomer, methacrylic acid (MAA, 100 mm), cross-linker, ethyleneglycol dimethacrylate (EGDMA, 140 mm), and timolol maleate (25 mm) were previously added. The calculated Timolol overall affinity (SK) ranked as HEMA > SiMA–DMAA > MMA–DMAA > DEAA. The release of Timolol was studied in 0.9 % NaCl solution. The imprinted lenses made up of MMA–DMAA and SiMA–DMAA showed higher Timolol release rate, the entire dose was released within 3h. In contrast, the imprinted lens made of HEMA showed the sustained release, wherein entire dose was released in 9h. The author attributed this to increase in hydrophilic nature in MMA-DMAA and SiMA-DMAA as compared to the lens made up of HEMA. Thus the increased swelling of the MMA-DMAA and SiMA-DMAA matrix resulted in decrease in the affinity of the Timolol. The authors further demonstrated the influence of interactions between Timolol and backbone monomer on its loading on soft contact lenses. The hydroxyl group of HEMA has strong ability to form the hydrogen bonding interactions with the amino, ether and hydroxyl groups of Timolol. But they observed that the presence of only MAA or HEMA in soft contact lenses do not significantly load the drug. The presence of HEMA and MAA created the microenvironment and thus in enhanced the drug loading. Thus the nature of backbone monomers, their composition as well as their interactions with the other monomers and drug molecule are important in regulating the drug release.

Suedee et al., (2002) reported the sustained delivery of the pharmacologically active S-propranolol from a racemic mixture using imprinted polymers. The effect of swelling of polymer matrix along with the type of functional monomers used on the loading and release profile of S-propranolol from the imprinted matrix was studied. Swelling of polymer matrix changed the shape of the specific cavities and thus caused the burst release of the drug. Thus controlling the swelling of imprinted matrix is a critical factor to be considered during the screening of the monomers for the synthesis of molecularly imprinted polymers for sustained drug delivery. Figure 1.18 illustrates the enantioselective release from the imprinted polymer. In this the imprinted enantiomer (+) is retained in the MIP, whereas the non-imprinted enantiomer (-) does not fit properly in the binding site and will be released.

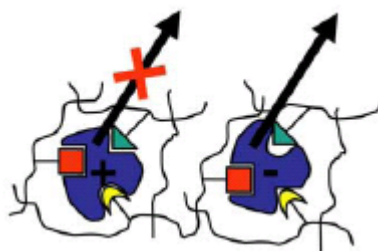


Figure 1.18: Enantioselective release

(From van Nostrum 2005)

Sreenivasan (1999) reported the template responsive release from the imprinted polymers. In this 2-hydroxyethyl methacrylate polymers were imprinted with hydrocortisone. After extracting hydrocortisone the imprinted and non-imprinted polymers were subjected to testosterone loading. The hydrocortisone-imprinted polymers absorbed considerable amount of testosterone because of its structural resemblance with print molecule and the presence of specific cavity. The testosterone loaded imprinted polymers were evaluated for its release in distilled water in absence of and presence of hydrocortisone. The release of testosterone from the imprinted polymers in deionize water was very slow. In contrast the rapid release of testosterone was observed in presence of print hydrocortisone. Since the imprinted polymers comprise the specific cavities and have high affinity for hydrocortisone, it causes the

rapid displacement of testosterone and thus its fast release. The Figure 1.19 illustrates the mechanism for template responsive release. In this the testosterone having low affinity is replaced by the imprinted hydrocortisone that has higher affinity for binding site. This approach could be useful for the release of steroids and peptides.

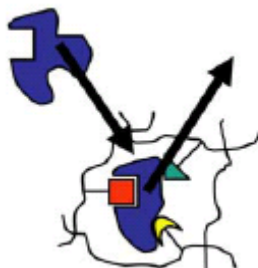
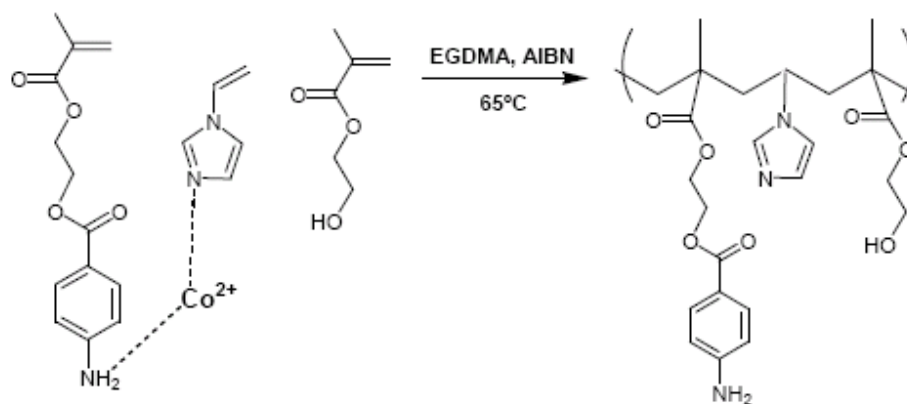


Figure 1.19: Template responsive drug release
(From van Nostrum 2005)

Karmalkar et al., (1997) reported the hydrolytically induced drug delivery from the imprinted polymers, in which the rate of hydrolysis of drug-polymer linkage modulated the drug release. The rate of hydrolysis of the drug-polymer linkage i.e. ester or amide bonds under mild conditions of pH was enhanced by incorporating the imidazole groups (nucleophilic catalyst) near the drug linkage using the molecular imprinting approach. The hydrogels, designed for the release of p-amino benzoic acid, were prepared by polymerizing 2-hydroxyethyl methacrylate (HEMA), N-vinyl imidazole (NVIIm) and 2-methacryloylethyl p-amino benzoate (PAP). In this NVIm and PAP were mixed with Co^{2+} ions to form a co-ordination complex between them before polymerization (Scheme 1.3). Polymerization of this complex and followed by subsequent removal of metal ion would lead to polymers having labile bonds and imidazole located in adjacent position to the PAP co-monomer.

The control hydrogels were also prepared without the co-ordination complex formation. The release of p-amino benzoic acid from the imprinted and non-imprinted hydrogels was studied in ethanol-phosphate buffer pH 8. The results indicated that the release from the imprinted hydrogels was considerably easier (first order release) when compared to the non-imprinted polymers



Scheme 1.3: Synthesis of hydrogel for p-amino benzoic acid release by hydrolytic cleavage (From Karmalkar et al., 1997)

Although molecular imprinting appears a promising approach for sustained drug delivery it has some limitations. The conventional imprinting approach involves the cross-linking of functional monomer-template assembly in presence or absence of porogenic solvents (Ye et al., 2001). This monolith is then ground and sieved to achieve the appropriate particle size distribution. The particles are generally irregularly shaped grinding destroys some of the cavities. The imprinted polymer matrix prepared by this method is highly cross-linked and there are possibilities of presence of entrapped monomers due to gel effect and need to be leached off so that the unreacted monomers do not leach during release under physiological conditions. In case of enantioselective release the optimal selectivity *viz* the complete retention of imprinted enantiomer and release of non-imprinted enantiomer has not been achieved yet. Also pure enantiomer is required as a template for the imprinting, which decreased the practical benefits of the imprinted polymers.

To overcome this drawback a number of new synthetic approaches to imprinting such as emulsion (Perez et al., 2001 and 2004, Carter et al., 2003), suspension (Flores et al., 2000, Ansell and Mosbach 1997, Ansell and Mosbach 1998), dispersion (Selligren, 1994) and precipitation (Ye and Mosbach, 2001, Wang et al., 2003, Li et al., 2003, Zhang et al 2004, Puoci et al 2004) polymerization have been explored. These approaches also improve the morphology and binding properties of the imprinted polymers. While these methodologies provide good control over particle size and

morphology, some inherent limitations are not yet overcome. Imprinted particles made by emulsion or suspension polymerization contain residues from emulsifiers, surfactants, swelling agents, stabilizers and porogens etc. The precipitation polymerization requires high dilution, optimal monomer to solvent ratio as well as careful choice of functional monomers to cross-linkers ratio in order to minimize the particle aggregation. Also in this case, the functional monomer complexed with the template molecule will not effectively co polymerize with the cross-linker and in dilute solutions the cross-linker will react inter and intramolecularly because of high dilution (Serra et al., 2006 and Elliott et al., 2004). Thus there is a need to develop a promising simple methodology to yield the imprinted polymer matrix with enhanced purity, controlled particle size and higher binding capacity.

In summary, the review of literature reveals the need to develop a single step method for the synthesis of sequentially cross-linkable polymers. We demonstrate how this can be achieved by polymerizing inclusion complexes comprising the multivinyl monomers and the cyclodextrin. The approach has then been extended to synthesis of copolymers containing functional monomers. These have been imprinted non-covalently with drugs and intra chain crosslinked to yield nanoparticles, which release the drug over extended time periods.

Chapter 2

Objectives & Scope of Work

The literature review presented in the first chapter has highlighted the use of cyclodextrin (CD) in synthetic organic and polymer chemistry. In organic chemistry CD has been used to control the reactivity of included guest molecule. In polymer science CD has been utilized mainly to solubilize the hydrophobic monomers in water and mediate their polymerization in aqueous media. The literature review also emphasized the urgency to develop latent cross-linkable polymers and summarized the synthetic efforts made in past. The present research work has been undertaken with a view to demonstrate that CD can be used to control the reactivity of multivinyl monomers during free radical polymerization and yield soluble polymers bearing pendant unsaturations i.e. latent cross-linkable polymers.

The objectives of the present research work are summarized below:

I. Synthesize and characterize the supramolecular inclusion complexes (ICs) comprising multivinyl monomers and CD. This involves,

- i. Standardization of methodology to obtain the true ICs free from uncomplexed CD as well as multivinyl monomers.
- ii. Selection of solvent to remove the uncomplexed multivinyl monomers as to enable isolation of IC.
- iii. Structural evaluation of ICs by instrumental techniques such as FTIR, NMR, XRD, and TGA.
- iv. Computational analysis of ICs that includes conformational analysis and docking calculations to identify stable conformation of multivinyl monomer included in CD cavity.

II. Inclusion complex mediated polymerization of multivinyl monomers. This involves,

- i. Solvent selection for the polymerization of IC in which the complex is stable and does not dissociate under polymerization conditions.
- ii. Copolymerization of ICs with various co-monomers and study co-monomer reactivity ratios using standard methods.
- iii. Structural characterization and evaluation of properties synthesized polymers by instrumental techniques such as FTIR, NMR, GPC, Intrinsic viscosity, MALLS and DSC.

III. Explore applications of synthesized polymers in various fields such as synthesis of functional nanoparticles, in molecular imprinting and sustained drug release. This involves,

- i. Synthesis of functional copolymers of MMA and MAA with EGDMA and TMPTMA.
- ii. Theophylline - imprinted nanoparticles synthesis by combining the principles of intramolecular cross-linking and molecular imprinting.
- iii. Evaluation of rebinding properties, binding capacity and selectivity of imprinted nanoparticles over non-imprinted as well as the molecularly imprinted polymers reported in literature.
- iv. Evaluation of release profile of Theophylline from imprinted and non-imprinted nanoparticles.

Thus the broad objective of the present research plan is to apply the principles of supramolecular CD host - guest chemistry to control the reactivity of multivinyl monomers in free radical polymerization to yield solvent soluble polymers bearing pendant vinyl unsaturations. Another objective is to explore applications of these polymers in sustained drug delivery exploiting molecular imprinting approach.

The scope of the present research investigation is defined more precisely as follows:

- i. Synthesis and characterization of ICs comprising hydrophobic divinyl and trivinyl monomers and CD and its derivatives.
- ii. Inclusion complex mediated homo and copolymerization of divinyl and trivinyl monomers.
- iii. Structural characterization and property evaluation of polymers by instrumental techniques such as FTIR, NMR, GPC, IV, MALLS, DSC, and XRD.
- iv. Comparison of copolymerization behavior of divinyl and trivinyl monomers and their IC. Evaluation of co-monomer reactivity ratios for methyl methacrylate with divinyl and trivinyl monomers before and after inclusion in CD and structurally similar monovinyl monomers.

- v. Synthesis of functional nanoparticles from the copolymers by combining the principles of molecular imprinting and intra chain cross-linking and the use of these imprinted functional nanoparticles in sustained drug delivery.

Chapter 3

Supramolecular Inclusion Complexes: Synthesis

Reproduced with permission from,

J. Am. Chem. Soc. **2006**, 128(24), 7752-7753,
© **2006 American Chemical Society**

And

Macromolecules **2007**, 40(6), 1824-1830,
© **2007 American Chemical Society**

3.1 Introduction

Cyclodextrins (CDs) and their derivatives are attracting attention of researchers because of their unique ability to form inclusion complexes (ICs) (Szejtli, 1998). CDs form IC with hydrophobic molecules and modify solubility and reactivity of included guest molecules without altering their chemical structure (Ritter and Tabatabai, 2002). The ICs are stabilized by hydrophobic and hydrogen bonding interactions between CD cavity and the guest molecule included.

In synthetic organic chemistry, the ability of CD to form IC has been exploited to control selectivity in reactions (Takahashi 1998). Breslow and Campbell reported selective chlorination of anisole at 'p' position using CD complexation. Other reactions investigated include oxidation, reduction, hydrolysis, addition as well as photochemical reactions (Takahashi 1998).

In polymer chemistry, CD ICs are being used for variety of applications. The ICs comprising hydrophobic monomer and CD have been used to enhance solubility of monomers in aqueous media during polymerization (Ritter and Tabatabai 2002). Chen et al., (2006) explored the use of CD in the condensation polymerization of 1-(2-aminoethyl) piperazine-CD IC and divinylsulfone to yield linear polymers, which otherwise yields hyperbranched structures. Sarvothaman and Ritter (2004) reported ICs comprising diacrylate and dimethacrylate and CD to obtain supramolecular architectures such as interlocked polyrotaxanes.

In view of the potential applications of latent cross-linkable polymers in emerging fields such as microelectronics, molecular imprinting, optical waveguides, photolithography, this research investigation was undertaken to explore the use of CD to control the reactivity of multivinyl monomers during free radical polymerization.

This chapter deals with the synthesis and characterization of ICs comprising multivinyl monomers and CD to be used in free radical polymerization. The structure of ICs was investigated by instrumental techniques such as ^1H NMR, ^{13}C CP/MAS, FTIR, XRD as well as computational analysis.

3.2 Experimental

3.2.1 Materials

β -CD (SD Fine chemicals), α -CD (Aldrich), γ -CD (Aldrich), DM- β -CD (Wacker), trimethylolpropane (TMP), 2-hydroxyethyl methacrylate (HEMA), ethylene glycol dimethacrylate (EGDMA), ethylene glycol diacrylate (EGDA), trimethylolpropane trimethacrylate (TMPTMA), trimethylolpropane triacrylate (TMPTA) (all from Aldrich chemicals) were used as received. Triethyl amine (TEA), thionyl chloride (SOCl₂) and 4-vinyl benzoic acid (VBA) and solvents N, N dimethyl formamide (DMF), dichloromethane (DCM), tetrahydrofuran (THF), pet ether and ethyl acetate (EA) (all from Merck chemicals).

3.2.2 Measurements

Fourier Transform Infrared Spectroscopy (FTIR)

The FTIR spectral studies were carried out using Shimadzu 8300 FTIR spectrometer. The powder samples of CD and complexes were milled with Nujol and placed between potassium bromide discs. The spectra were recorded over the frequency range 4000 - 400 cm⁻¹, with resolution range of 4 cm⁻¹.

Nuclear Magnetic Resonance Spectroscopy (NMR)

¹H NMR and ¹³C NMR measurements were carried out on DRX 500. The solid state ¹³C CP/MAS NMR spectra of ICs were obtained at 125.76 MHz at a sample-spinning rate of 8 kHz.

Wide Angle X-ray Diffraction (XRD)

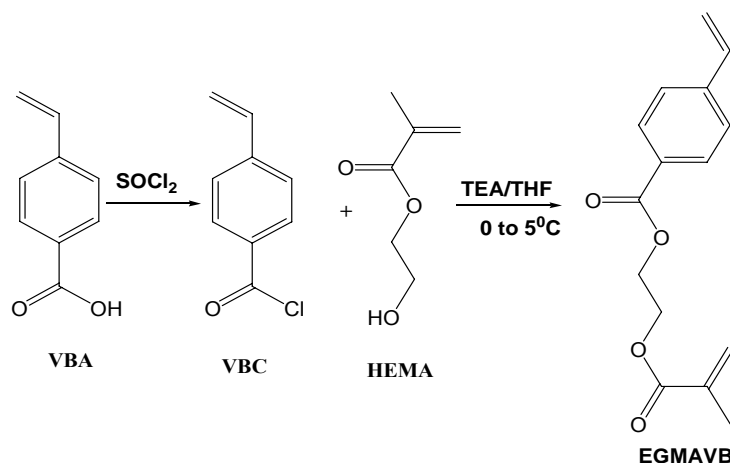
Powder X-ray diffraction (XRD) patterns of ICs were recorded on a Rigaku Dmax 2500 diffractometer with Cu K_α (1.541 Å) radiation (40 kV, 100 mA). Powder samples such as CD and ICs were mounted on a sample holder and scanned with a step size of 0.05° in the range 2θ = 5 to 40°.

3.2.3 Monomers Synthesis

3.2.3.1 Ethylene Glycol Methacrylate 4-Vinyl Benzoate (EGMAVB)

The synthesis involved,

- I. Preparation of 4-vinyl benzoyl chloride,
- II. Reaction of 4-vinyl benzoyl chloride and HEMA.



Scheme 3.1: EGMAVB monomer synthesis

Step I. Preparation of 4-Vinylbenzoyl Chloride

1.60 g 4-VBA (0.0108 mol) was used for the reaction. 2 drops of DMF were added as a catalyst. 0.9 mL (0.0123 mol) of SOCl₂ was added drop wise to the reaction mixture at 0 to 5°C. After the addition of SOCl₂ was completed, the reaction mixture was stirred for 24 h at room temperature. Excess SOCl₂ was vacuum distilled to obtain 4-vinyl benzoyl chloride. The product was characterized by ¹H NMR.

Step II. Reaction of 4-Vinylbenzoyl Chloride and HEMA

1.07 g (0.0083 mol) of HEMA and 0.84 g (0.0083 mol) TEA were dissolved in 10 mL of THF. To this solution 1.49 g p-vinyl benzoyl chloride diluted with 5 mL of THF was added in drop wise manner at 0 to 5 °C. Reaction mixture was stirred for 24 h. Yellowish white precipitate of TEA salt was filtered and THF solution was concentrated on rota-vapor. EA was added to the concentrated solution to ensure complete precipitation of TEA salt. EA layer was concentrated and crude monomer was purified by column chromatography and characterized by NMR for purity.

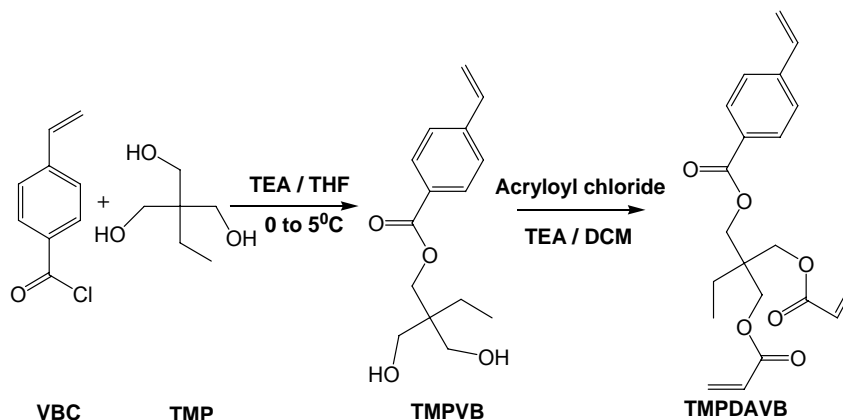
¹H NMR (500 MHz, CDCl₃) δ: 1.85 (3H, -CH₃ of EGMAVB), 4.47 (4H, -OCH₂CH₂O- of EGMAVB), 5.68 and 6.04 (2H, vinyl protons of EGMAVB i.e. aliphatic part), 6.88-6.74, 5.95, 5.46 (3H, vinyl protons of EGMAVB i.e. aromatic part), 7.60, 7.64 (2H, of EGMAVB aromatic part), 7.89, 7.93 (2H of EGMAVB aromatic).

3.2.3.2 Trimethylolpropane Diacrylate 4-Vinyl Benzoate (TMPDAVB)

The synthesis involved,

I. Reaction of 4-vinylbenzoyl chloride and TMP.

II. Reaction of trimethylolpropane 4-vinyl benzoate (TMPVB) and acryloyl chloride



Scheme 3.2: TMPDAVB monomer synthesis

Step I. Reaction of 4-Vinylbenzoyl Chloride and TMP

7.16 g (0.0533 mol) of TMP and 5.39 g (0.0533 mol) TEA were dissolved in 25 mL of THF. To this solution 8.89 g (0.0533 mol) 4-vinyl benzoyl chloride diluted with 15 mL THF was added in a drop wise manner at 0 to 5 °C. Reaction mixture was stirred for 24 h. Yellowish white precipitate of TEA salt was formed. Pure TMPVB was obtained by following the same purification procedure described earlier for the purification of EGMAVB.

Step II. Reaction of TMPVB and Acryloyl Chloride

5.02 g (0.019 mol) of TMPVB and 1.92 g (0.019 mol) TEA were dissolved in 30 mL of THF. To this solution 1.72 g (0.019 mol) acryloyl chloride diluted with 15 mL THF was added in a drop wise manner at 0 to 5 °C. Reaction mixture was stirred for 24 h. Yellowish white precipitate of TEA salt was formed. Pure TMPDAVB was obtained by following the purification procedure described for the purification EGMAVB. The monomer was characterized by ^1H NMR.

^1H NMR, 500 MHz, DMSO d_6 : 0.91 (3H, $\text{CH}_2\text{-CH}_3$ of TMPDAVB), 1.55 (2H, $\text{CH}_2\text{-CH}_3$ of TMPDAVB), 4.22 to 4.29 (6H, OCH_2 of TMPDAVB), 5.92 to 6.38 (6H, vinyl

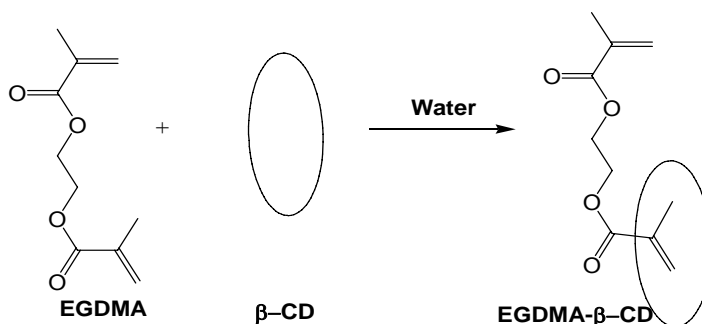
protons of aliphatic part of TMPDAVB), 5.47, 5.41 and 6.75 to 6.90 (3H, vinyl protons of aromatic part), 7.95-7.60 (4H, aromatic proton of TMPDAVB).

3.2.4 Inclusion Complex: Preparation

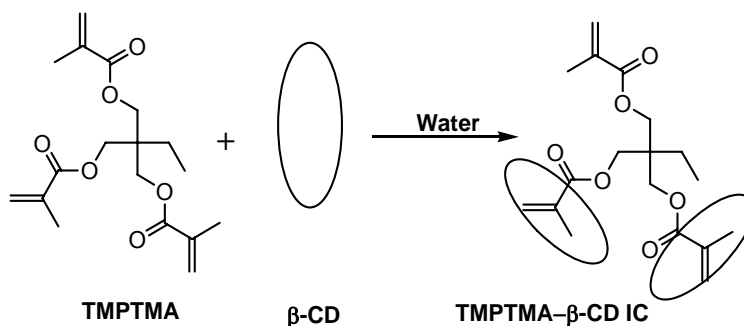
3.2.4.1 Precipitation Method

To the aqueous solution of CD, the multivinyl monomer was added in stoichiometric amount and the mixture was stirred at room temperature. The complex precipitated out from the mixture. The precipitated complex was filtered, washed with water and pet ether to remove uncomplexed CD and multivinyl monomer respectively. The stoichiometry of the ICs was determined using ^1H NMR. EGDMA, EGMAVB, TMPTMA, TMPTA, and TMPDAVB were used for complexation.

The ICs of EGDMA, TMPTMA, TMPTA and β -CD were also prepared by varying the molar ratio of multivinyl monomer to β -CD to study the effect of feed composition on the stoichiometry of ICs.



Scheme 3.3 : EGDMA- β -CD IC preparation



Scheme 3.4: TMPTMA- β -CD IC preparation

EGDMA- β -CD IC

11.35 g (0.01mol) β -CD was dissolved in 615 ml water. To this 1.99 g (0.01mol) EGDMA was added and stirred for 24 h at room temperature. The complex slowly precipitated out. It was filtered and washed with distilled water followed by petroleum ether to remove uncomplexed β -CD and EGDMA respectively.

3.2.4.2 Solvent Evaporation Method

In this method both DM- β -CD and EGDMA were dissolved in chloroform and the mixture was stirred for 4 days at room temperature. The IC was isolated by evaporating the solvent at room temperature. The dried complex was washed with petroleum ether to remove adsorbed i.e. uncomplexed EGDMA. Yield: 96%. The stoichiometry of the IC was determined using ^1H NMR.

3.3 Results and Discussion

3.3.1 Inclusion Complex: Preparation

The ICs comprising native CD and hydrophobic multivinyl monomers were obtained by precipitation method (Hedges 1998) and ICs comprising DM- β -CD were obtained by solvent evaporation method.

In precipitation method the hydrophobic monomer was added to the aqueous CD solution. The solution slowly became turbid indicating the formation of stable, crystalline IC between the CD and added monomer (Sarvothaman and Ritter 2004). The precipitated complexes were filtered and thoroughly washed with distilled water and petroleum ether to remove uncomplexed CD and multivinyl monomers. Presence of uncomplexed CD would create difficulties in evaluating the stoichiometry of IC and the presence of uncomplexed multivinyl monomers would lead to cross-linking reactions during polymerization.

All the ICs were characterized by NMR, FTIR and XRD for their stoichiometry, nature of interactions between CD and multivinyl monomer and structure of formed IC respectively.

3.3.2 Inclusion Complex: Characterization

3.3.2.1 NMR of ICs

NMR spectroscopy is extensively used to characterize the stoichiometry of ICs and evaluate the interactions between the CD and guest molecule included (Sarvothaman

and Ritter, 2004, Schneider et al., 1998). In the present study all the ICs were characterized in DMSO; the solvent in which the CD ICs rapidly undergoes the dethreading (Zhao and Beckham, 2003). Therefore the NMR spectrum of the ICs in DMSO appeared identical to the spectrum of a physical mixture of the two components. This de-complexation of multivinyl monomers from β -CD was also confirmed by the polymerization of the ICs in DMSO, which led to cross-linked product as expected (discussed in chapter 4). While the shifts due to formation of ICs are not expected to be seen, the integration of the peaks helps establish the stoichiometry of IC.

The stoichiometry of IC of EGDMA- β -CD IC was established by integrating the peak at 4.34 δ , which corresponded to four protons of EGDMA (-OCH₂-CH₂O-) and the peak at 4.48 δ corresponded to seven protons of β -CD (-CH₂OH) and the peak at 4.82 δ corresponded to seven protons of β -CD (C₁-H). The integration showed 1:1 stoichiometry of EGDMA- β -CD complex (Figure 3.1). Similar examination of all ICs showed that the divinyl monomers always formed 1:1 IC with CD.

The stoichiometry of TMPTMA- β -CD IC was established by integrating the peak at δ 4.16, which corresponded to six protons of TMPTMA (OCH₂), and the peaks at δ 4.49 and 4.82, which corresponded to seven protons of β -CD for (CH₂-OH) and (C₁-H) respectively. The integration showed 1:2 stoichiometry of TMPTMA- β -CD complex. Similar characterization for TMPTA and TMPDAVB showed the formation of 1:1 and 1:2 ICs with β -CD respectively (Figures 3.4 to 3.6).

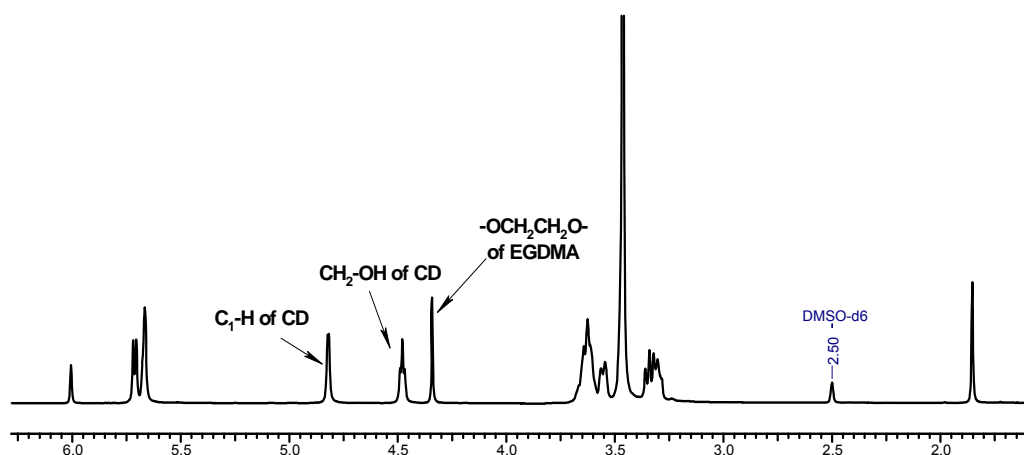


Figure 3.1: ¹H NMR of EGDMA- β -CD (1:1) IC

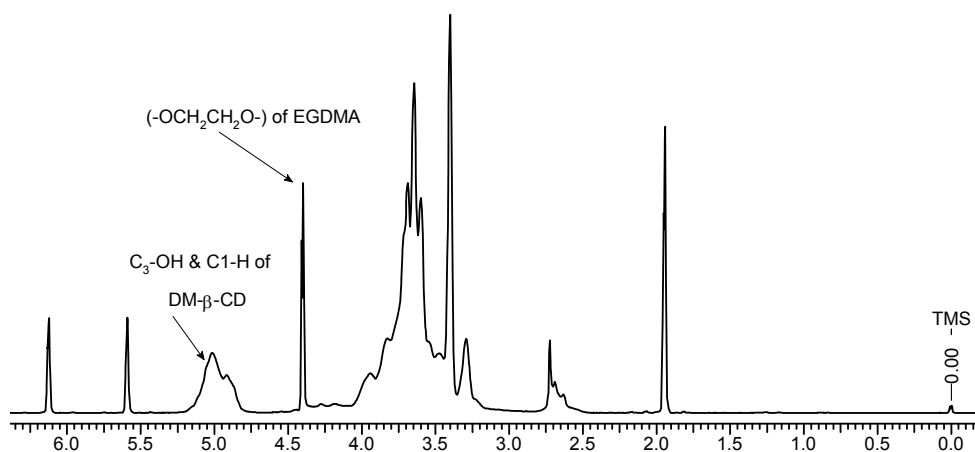


Figure 3.2: ^1H NMR of EGDMA-DM- β -CD (1:1) IC

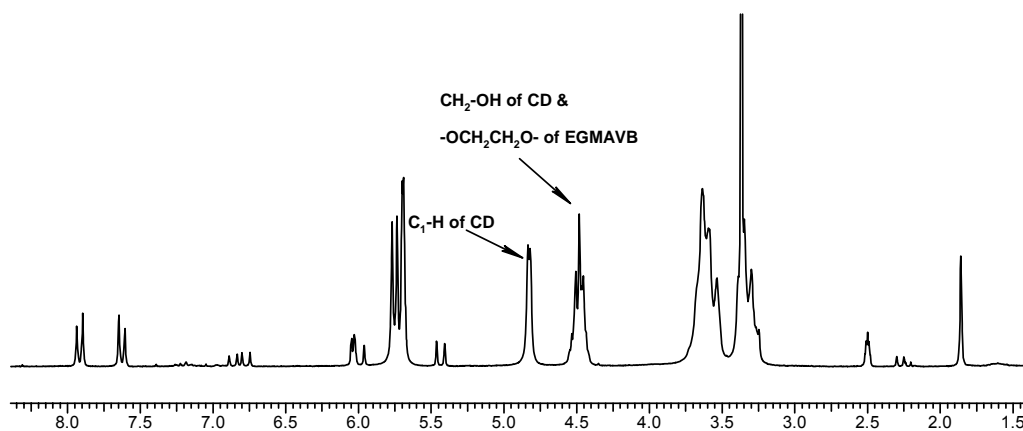


Figure 3.3: ^1H NMR of EGMAVB- β -CD (1:1) IC

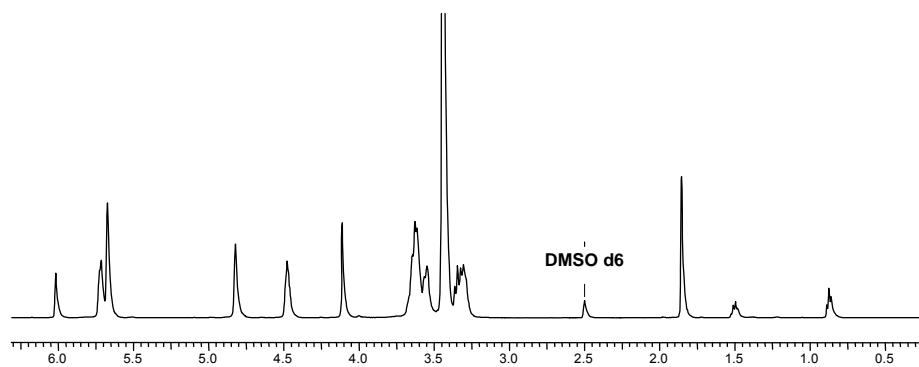


Figure 3.4: ^1H NMR of TMPTMA- β -CD (1:2) IC

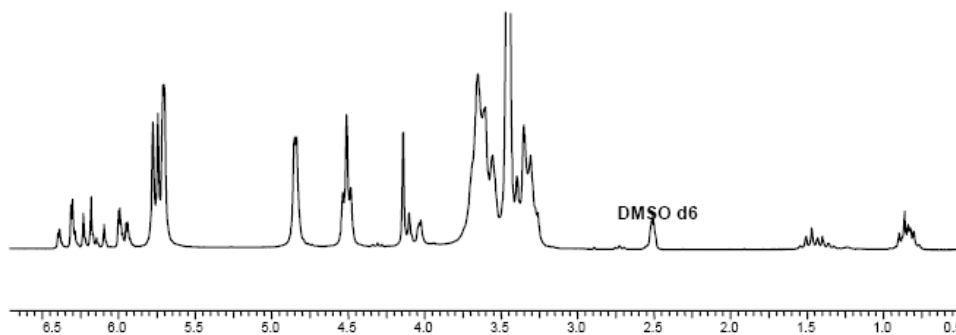


Figure 3.5: ^1H NMR of TMPTA- β -CD (1:1) IC

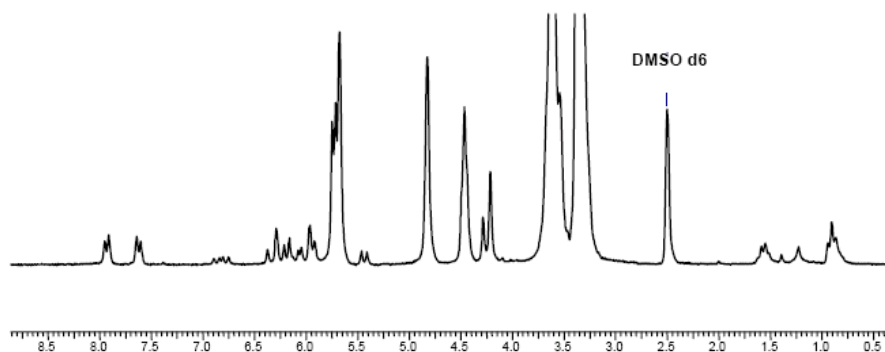


Figure 3.6: ^1H NMR of TMPDAVB- β -CD (1:2) IC

^1H NMR (500 MHz, DMSO d6) δ :

EGDMA- β -CD IC: 1.85 (6H, 2- CH_3 groups of EGDMA), 4.34 (4H, $-\text{OCH}_2\text{CH}_2\text{O}-$ of EGDMA), 5.67 and 6.01 (4H, vinyl protons of EGDMA), 5.72 ($\text{C}_2\text{-OH}$ of β -CD), 5.71 ($\text{C}_3\text{-OH}$ of β -CD), 4.48 ($\text{C}_6\text{-OH}$ of β -CD), 4.82, ($\text{C}_1\text{-H}$ of β -CD), 3.30 ($\text{C}_2\text{-H}$ of β -CD), 3.34 ($\text{C}_4\text{-H}$ of β -CD), 3.55 ($\text{C}_5\text{-H}$ of β -CD), 3.61 ($\text{C}_3\text{-H}$ of β -CD), 3.64 (C_6 , H_a and H_b of β -CD).

EGDMA-DM- β -CD IC: 1.94 (6H, 2- CH_3 groups of EGDMA), 4.40 (4H, $-\text{OCH}_2\text{CH}_2\text{O}-$ of EGDMA), 5.59 and 6.12 (4H, vinyl protons of EGDMA), 4.91-5.01 (14 H, $\text{C}_1\text{-H}$ and $\text{C}_3\text{-OH}$ of DM- β -CD), 3.59 to 3.68 ($\text{C}_6\text{-H}$, $\text{C}_2\text{-H}$, $\text{C}_4\text{-H}$, $\text{C}_3\text{-H}$ and $\text{C}_2\text{-H}$ of DM- β -CD), 3.29 (8- CH_3 of DM- β -CD), 3.40 (7- CH_3 of DM- β -CD).

EGMAVB- β -CD IC: 1.85 (3H, $-\text{CH}_3$ of EGMAVB), 4.47 (4H, $-\text{OCH}_2\text{CH}_2\text{O}-$ of EGMAVB and 7H $\text{C}_6\text{-OH}$ of CD), 5.68 and 6.04 (2H, vinyl protons of EGMAVB i.e. aliphatic), 6.88 - 6.74, 5.95, 5.46 (3H, vinyl protons of EGMAVB i.e. aromatic part), 7.60, 7.64 (2H, of EGMAVB aromatic), 7.89, 7.93 (2H of EGMAVB aromatic).

TMPTMA- β -CD IC: 0.87 (3H, $\text{CH}_2\text{-CH}_3$ of TMPTMA), 1.52 (2H, $\text{CH}_2\text{-CH}_3$ of TMPTMA), 1.85 (9H, CH_3 adjacent to vinyl group of TMPTMA), 4.11 (6H, OCH_2 of TMPTMA), 5.67 and 6.01 (6H, vinyl protons of TMPTMA).

TMPTA- β -CD IC: 0.85 (3H, $\text{CH}_2\text{-CH}_3$ of TMPTA), 1.46 (2H, $\text{CH}_2\text{-CH}_3$ of TMPTA), 4.0 to 4.12 (6H, OCH_2 of TMPTA), 5.92 to 6.38 (9H, vinyl protons of TMPTA).

TMPDAVB- β -CD IC: 0.91 (3H, $\text{CH}_2\text{-CH}_3$ of TMPDAVB), 1.55 (2H, $\text{CH}_2\text{-CH}_3$ of TMPDAVB), 4.22 to 4.29 (6H, OCH_2 of TMPDAVB), 5.92 to 6.38 (6H, vinyl protons of aliphatic part of TMPDAVB), 5.47, 5.41 and 6.75 to 6.90 (3H, vinyl protons of aromatic part), 7.95-7.60 (4H, aromatic proton of TMPDAVB).

The results in Table 3.1 further indicate that EGDMA and TMPTA molecules always yielded 1:1 IC while TMPTMA yielded 1:2 IC irrespective of the feed composition. The results showed that the stoichiometry was independent of feed composition.

Table 3.1: Stoichiometry of ICs

a. EGDMA- β -CD IC

Ratio in feed	Ratio in complex by ^1H NMR	
EGDMA: β -CD	4.82 δ	4.49 δ
1:0.3	1:1.25	1:1.21
1:0.5	1:1.25	1:1.30
1:1	1:1.00	1:1.00
1:2	1:1.01	1:1.09
1:3	1:0.97	1:1.03

b. TMPTMA- β -CD IC

Ratio in feed	Ratio in complex by ^1H NMR	
TMPTMA: β -CD	4.82 δ	4.49 δ
1:1	1:2.20	1:2.20
1:2	1:2.04	1:2.01
1:3	1:2.11	1:2.13
1:4	1:2.07	1:2.06

c. TMPTA- β -CD IC

Ratio in feed TMPTA: β -CD	Ratio in complex by ^1H NMR	
	4.82 δ	4.49 δ
1:1	1: 1.13	1:1.15
1:2	1: 1.16	1:1.19
1:3	1: 1.10	1:1.10

Solid-State ^{13}C CP / MAS NMR

Solid-state NMR spectra of ICs confirm inclusion of guest in the CD cavity (Gidley and Bociek 1988; Harada et al 1993). ^{13}C CP / MAS solid-state NMR spectra of β -CD and EGDMA- β -CD (1:1) IC are shown in Figure 3.7.

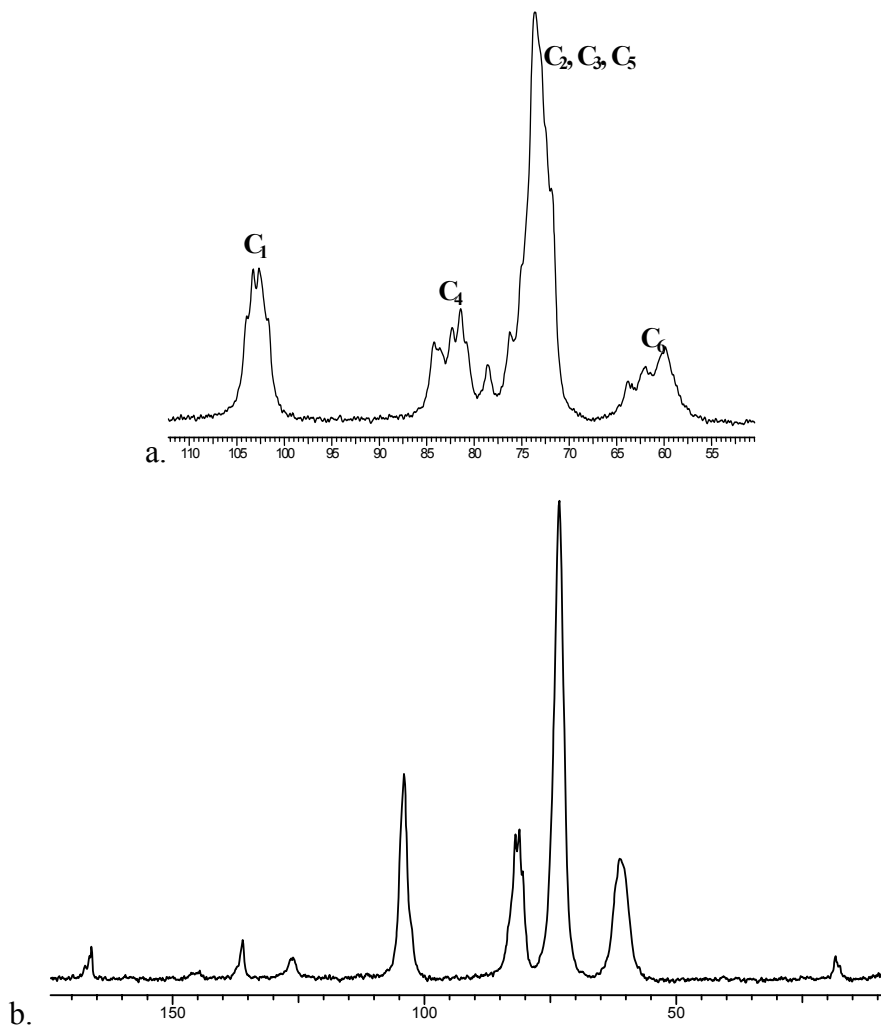


Figure 3.7: Solid state CP/MAS ^{13}C NMR of a. β -CD, b. EGDMA- β -CD (1:1) IC

The spectra of EGDMA- β -CD IC (Figure 3.7 b) displayed well-resolved, single peaks for each carbon of all glucose units. Also the peaks at ~ 78.59 and ~ 101 ppm, corresponding to C₁ and C₄, adjacent to conformationally strained glycosidic linkage, disappeared. These results confirmed symmetrical conformation of glycosidic linkage due to the inclusion of vinyl group of EGDMA within the β -CD cavity (Harada et al 1993). Similar results were obtained for TMPTMA- β -CD and TMPTA- β -CD ICs (Figure 3.8).

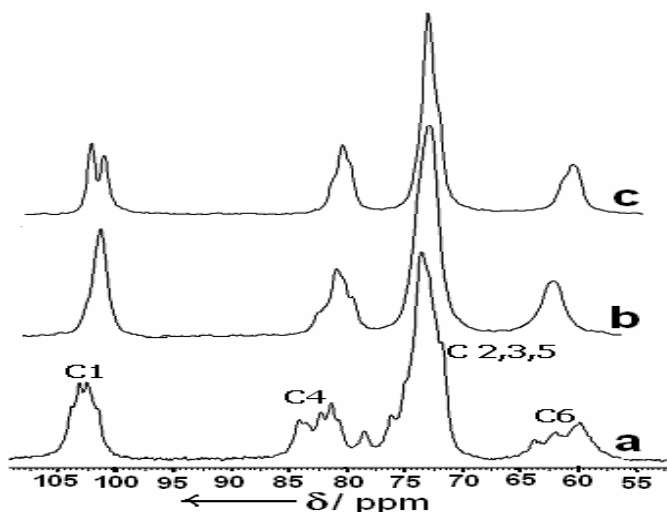


Figure 3.8: Solid state CP / MAS ^{13}C NMR spectra of a. β -CD, b. TMPTMA- β -CD (1:2) IC, c. TMPTA- β -CD (1:1) IC

3.3.2.2 FTIR of ICs

FTIR spectroscopy is useful to evaluate the interactions between the guest molecules and CD after IC formation (Jeromin and Ritter 1999). The FTIR signals and shift in the peak positions for ICs and their comparison with un-complexed compounds are summarized in Table 3.2.

The comparison between the FTIR spectra of free and complexed molecules showed the relative shift in ester carbonyl of multivinyl monomers and the O-H band of β -CD (Figure 3.9). The FTIR spectrum of EGDMA- β -CD IC showed shift from 1720 to 1726 cm^{-1} in ester carbonyl stretching vibrations (Jeromin and Ritter 1999). The O-H stretching band of β -CD at 3370 cm^{-1} shifted to 3323 cm^{-1} and narrowed as a result of replacement of intramolecular hydrogen bonding in β -CD by intermolecular hydrogen

bonding between the EGDMA molecule and β -CD (Rao 1967) (Figure 3.9a). Similar results were obtained for TMPTMA- β -CD IC (Table 3.2).

Table 3.2: FTIR of ICs

Inclusion Complex	>C=O (Monomer)	O-H (β -CD)
EGDMA- β -CD	1726 (-6)	3323 (+47)
EGMAVB- β -CD	1722 (-6)	3328 (+42)
EGDMA-DM- β -CD	1718 (+2)	3419 (-10)
TMPTMA- β -CD	1727 (-5)	3311 (+59)
TMPTA- β -CD	1732 (0), 1708 (+24)	3329 (+41)
TMPDAVB- β -CD	1733 (+5, -2)	3330 (+40)

Differences with respect to the uncomplexed compounds in cm^{-1}

In contrast, the FTIR spectrum of TMPTA- β -CD IC showed splitting of broad peak at 1732 cm^{-1} into two peaks in the ester carbonyl region, one at 1708 cm^{-1} and other at 1732 cm^{-1} (Figure 3.9b). This was attributed to the inclusion of acrylate groups in CD cavity. The spectrum also showed the presence of two peaks at 1640 and 1616 cm^{-1} for the double bonds, which indicated the presence of hydrogen bonded interactions in these acrylate groups. Thus the differences in the complexation behavior with β -CD may be attributed to the formation of intramolecular hydrogen bonds in TMPTA and lack of it in TMPTMA. To confirm this hypothesis, a new trivinyl monomer, *viz.* TMPDAVB was synthesized and complexed with CD. This monomer indeed formed 1:2 IC with CD as shown by ^1H NMR (Figure 3.6) and also displayed a shift in the ester carbonyl of monomer and O-H of β -CD. This was attributed to the disruption of hydrogen bonding interactions between two acrylate units so that each acrylate group occupied the separate CD cavity.

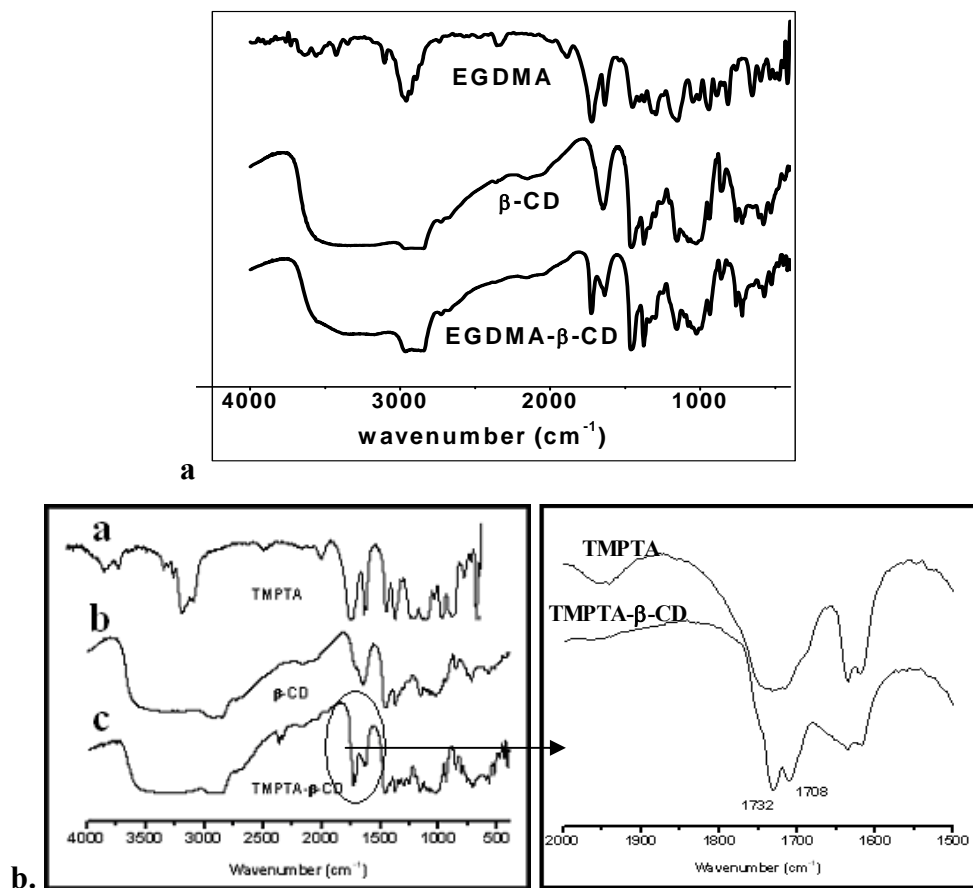


Figure 3.9: FTIR spectra of a. EGDMA- β -CD IC, b. TMPTA- β -CD IC

3.3.2.3 X-ray Powder Diffraction of ICs

XRD is extensively used to characterize the structure of CD based ICs (Saenger 1980, Szejtli and Osa 1996). All multivinyl monomers used herein are liquid and do not cause X-ray diffraction. Therefore in these cases X-ray diffractograms are even more useful in establishing the binding modes of complexation and structure of the IC (Szejtli and Osa 1996). The XRD patterns of EGDMA- β -CD and EGMAVB- β -CD are isomorphous with the cage type structure of β -CD (Figure 3.10). The shifts in peak position and emergence of new peaks seen in Figure 3.10 further support the formation of ICs rather than the physical mixture. The X-ray characterization of TMPTMA- β -CD, TMPTA- β -CD and TMPDAVB- β -CD complexes displayed similar results.

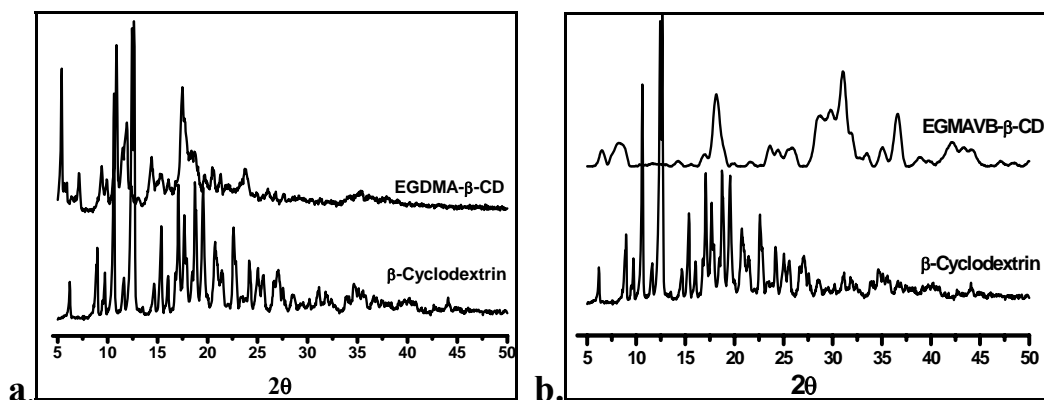


Figure 3.10: X-ray diffractogram of a. EGDMA- β -CD IC b. EGMAVB- β -CD IC

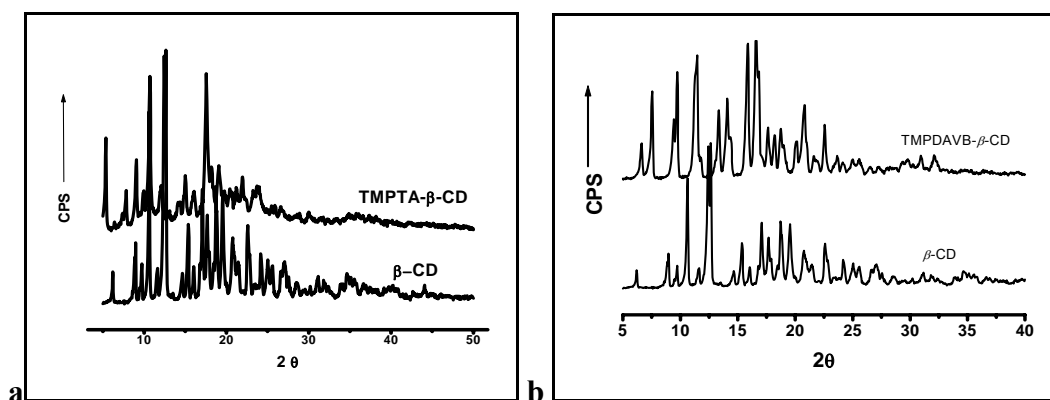


Figure 3.11: X-ray diffractogram of a. TMPTA- β -CD IC, b. TMPDAVB- β -CD IC

3.3.3 Molecular Modeling Calculations of ICs

3.3.3.1 Divinyl Monomers

Computational analysis of ICs is helpful in predicting the most stable conformation of multivinyl monomer after inclusion in CD cavity. The conformational analyses of EGDMA and EGMAVB, their complexation with β -CD, and thermodynamics of oligomerization, were analyzed by computational studies. The force field and density functional theory, B3LYP/6-31G, calculations showed the stability of the bent conformation over linear one by 3-5 kJ/mol. The complexation of the ligands with β -CD was analyzed by docking, quantum chemical and molecular dynamics simulations using Autodock 3.0.5 (Morris et al., 1998), Gaussian 03 (Frisch et al., 2004), and AMBER 8.0 (Case et al., 2004) programs, respectively. The lowest energy complex, obtained from the Autodock calculation, was taken as initial structure for MD

simulations. TIP3P water models were used as solvent and equilibration was performed for 500ps and MD simulation was carried for 2ns. The MD simulations of EGMAVB complexation with β -CD revealed that the conformation wherein the styrene end is outside the cavity is stable (Figure 3.12).

Computations were also carried out to ascertain if the monomers could bind to second β -CD. Docking studies and the subsequent binding energies evaluated at B3LYP/6-31G level of theory revealed that the complexation of the ligand with the first β -CD has substantial stabilization of the order of 50-100 kJ/mol, while the addition of second β -CD does not provide substantial stabilization. Therefore all the divinyl monomers always formed 1:1 IC with CD cavity.

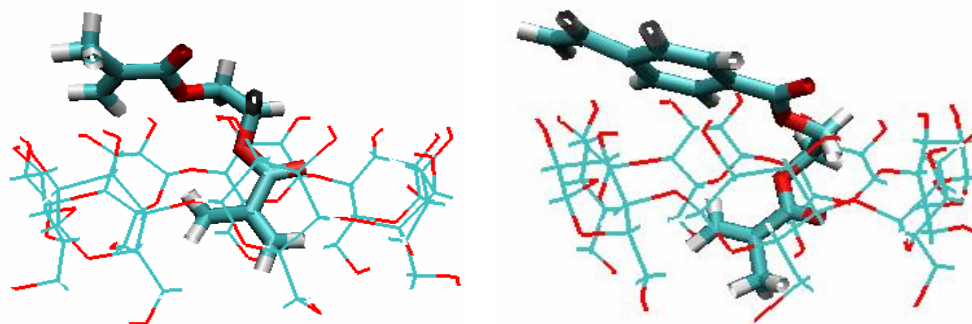


Figure 3.12: Conformational studies on a. EGDMA- β -CD and b. EGMAVB- β -CD

3.3.3.2 Trivinyl Monomers

The conformational analysis of TMPTMA and TMPTA, and their ICs with β -CD, was undertaken using computational techniques. Conformational analysis has been carried out on all the ligands and various minima on the potential energy have been identified. Both force field and density functional theory, B3LYP/6-31G, calculations indicate that in case of TMPTA the bent conformation is more stable than linear one by 5-7 kJ/mol, where both conformations form intra-molecular hydrogen bond between C-H---O=C group (Figure 3.13). The hydrogen bond distances are 3.31Å, 3.57Å, and bond angles are 133.7°, 110.2° in bent and stretched conformations respectively. However, in case of TMPTMA, the hydrogen-bonded structure cannot be formed. As a result, stretched conformation is more stable than bent conformation by 8-10 kJ/mol.

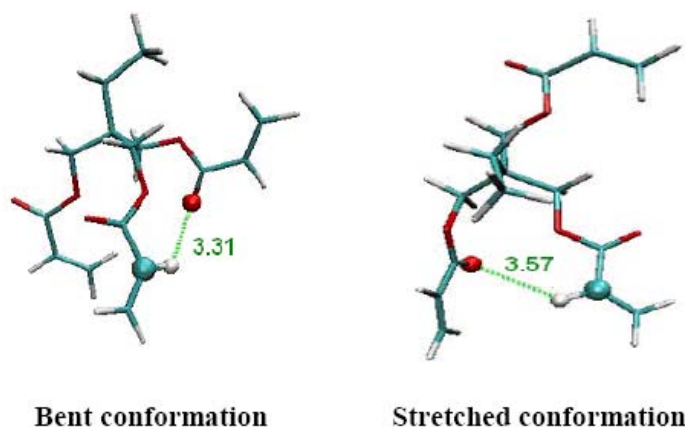


Figure 3.13: Hydrogen bonding in bent and stretched conformation of TMPTA

Thus the differences in the complexation behavior with β -CD have been traced to the formation of hydrogen bond in TMPTA and lack of it in TMPTMA. The lowest energy complex, obtained from the Autodock calculation, was taken as the initial structure for MD simulations. TIP3P water models were used as solvent and carried for 10 ns and first 2 ns were considered for equilibration. The lowest energy conformations of TMPTMA and TMPTA clearly indicate that, two β -CDs constitute the IC in the former but only one in the later. Thus, the MD simulations clearly account for the observed stoichiometry of the ICs.

Computations were also carried out to ascertain the energetics of the sequential addition of β -CDs for TMPTMA and TMPTA. Docking studies and the subsequent binding energies evaluated at B3LYP/6-31G level of theory revealed that the complexation of the ligand TMPTA with the first β -CD results in substantial stabilization of the order of 27-30 kJ/mol, while the addition of a second β -CD does not provide additional substantial stabilization. In case of TMPTMA the addition of a second β -CD provides additional substantial stabilization of the order of 46-50 kJ/mol. Thus, the formation of 1:1 complex in case of TMPTA and 1:2 complex in case of TMPTMA is controlled by hydrogen bonding.

To ascertain if the disruption of hydrogen bonding in TMPTA results in the formation of 1:2 IC, conformational analysis of the trivinyl monomer TMPDAVB and its β -CD IC was undertaken. The results show that TMPDAVB indeed forms 1:2 IC with β -CD

wherein the two acryloyl groups rather than the 4-vinyl benzoyl group, are preferentially included in the two β -CD cavities (Figure 3.14).

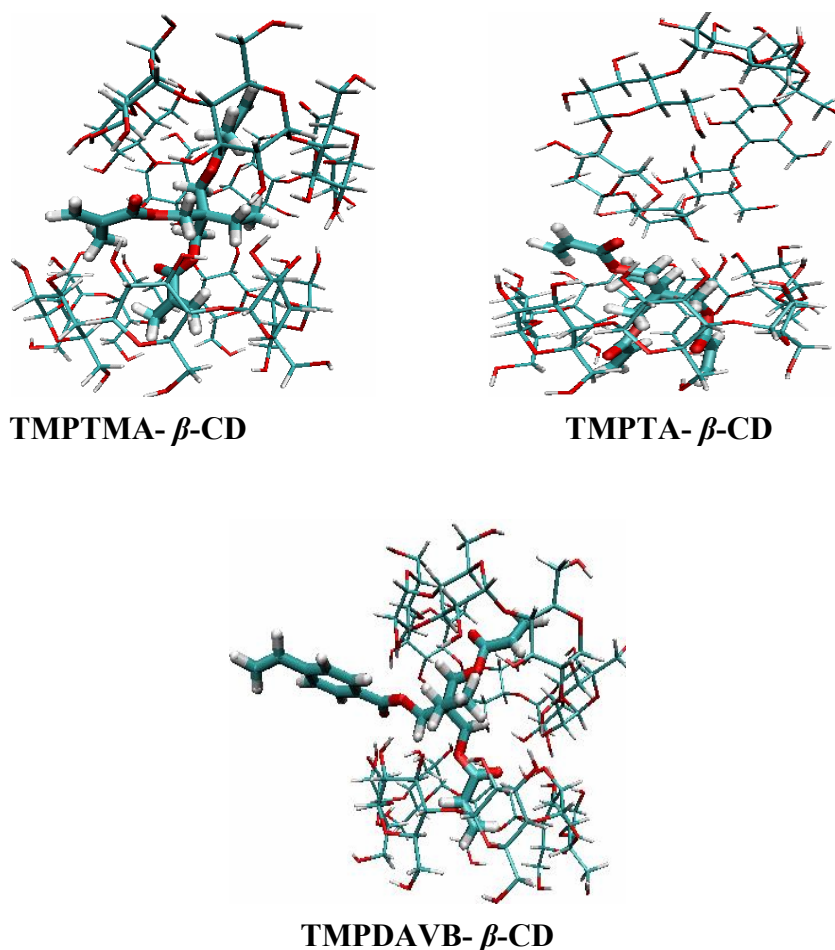


Figure 3.14: MD simulations of TMPTMA, TMPTMA, and TMPDAVB conformations

3.4 Conclusions

Divinyl and trivinyl monomers form stable IC with CD. The stoichiometry of IC depends on the structural arrangement of multivinyl monomers before and after formation of IC. Divinyl monomers always formed 1:1 IC complex with CD because of the stability of bent conformation over the linear conformation of included divinyl monomer. Trivinyl monomers formed 1:1 or 1:2 IC depending on the presence or absence of intramolecular hydrogen bonding interactions within the molecule. All the ICs can be exploited for the selective polymerization of vinyl group not included in the CD cavity.

Chapter 4

Supramolecular Inclusion Complex: Homopolymerization

Reproduced with permission from,

J. Am. Chem. Soc. **2006**, 128(24), 7752-7753,

© **2006 American Chemical Society**

And

Macromolecules **2007**, 40(6), 1824-1830,

© **2007 American Chemical Society**

4.1 Introduction

The latent cross-linkable polymers are increasingly being explored because of their applications in electronics, optoelectronics, molecular imprinting, microlithography, and nanotechnology (Koo et al., 2002, Li et al., 2005, 2006, Southard et al., 2007, Nagelsdiek et al., 2004, Mecerreyes et al 2001). These are the soluble, linear polymers comprising unsaturated groups in polymer structure and will undergo cross-linking reactions on thermal treatment or UV irradiation.

The synthetic approaches explored so far to develop polymers containing latent crosslinking sites include 1) polymerization of divinyl monomers in presence of large amount of chain transfer agent, (Sato et al., 2004), polymerization of divinyl monomers by specialized polymerization techniques such as 2) transition metal mediated polymerization, 3) group transfer radical polymerization (Guan 2002, Isaure et al., 2004), 4) polymerization of divinyl monomer containing the vinyl groups differing in reactivity (Nagelsdiek et al., 2004), 5) synthesis of linear polymers bearing pendant hydroxyl functionality and its subsequent conjugation with vinyl monomers (Koo et al., 2002 and Li et al 2005, 2006) etc. These approaches have their own limitations. For instance use of high concentration of initiator yields hyperbranched structures, specialized polymerization techniques demand stringent reactions conditions e.g. dry solvent, highly pure reagents, limitations on the choice of multivinyl monomers, as well as functional monomers for pendant group modification. These clearly indicate the need for a single step method, which can lead to latent cross-linkable polymers.

We have found that the divinyl and trivinyl monomers form inclusion complexes (IC) with cyclodextrin (CD) in such a way that only one of the vinyl groups is accessible for polymerization. The selective polymerization of this vinyl group leads to soluble polymers containing pendant vinyl unsaturations. These pendant vinyl groups can subsequently undergo inter or intramolecular crosslinking to yield insoluble cross-linked polymers or nanoparticles.

Thus this chapter deals with the IC mediated homopolymerization of divinyl and trivinyl monomers viz. ethylene glycol dimethacrylate (EGDMA), ethylene glycol methacrylate 4-vinyl benzoate (EGMAVB), trimethylolpropane triacrylate (TMPTA), trimethylolpropane trimethacrylate (TMPTMA), and trimethylolpropane diacrylate 4-

vinyl benzoate (TMPDAVB) and characterization of these homopolymers by instrumental techniques such as NMR, FTIR, GPC, IV, MALLS, DSC and TGA etc.

4.2 Experimental

4.2.1 Materials

Inclusion complexes viz EGDMA- β -CD, EGDMA-DM- β -CD, EGMAVB- β -CD, TMPTMA- β -CD, TMPTA- β -CD, TMPVBDA- β -CD were prepared as described in chapter 3.

4.2.2 Measurements

Fourier Transform Infrared Spectroscopy (FTIR)

Soluble polymers were characterized by FTIR in CHCl_3 . The cross-linked polymers were characterized in diffuse reflectance mode (DRS) of FTIR. The spectra were recorded over the frequency range $4000 - 400 \text{ cm}^{-1}$, with resolution range of 4 cm^{-1} .

Nuclear Magnetic Resonance Spectroscopy (NMR)

^1H NMR and ^{13}C NMR measurements were carried out on DRX 500. CDCl_3 or CDCl_3 and $\text{DMSO-}d_6$ mixtures were used as solvents.

Gel Permeation Chromatography (GPC)

Molecular weights of poly (EGDMA) and poly (TMPTMA) were measured by GPC using two polystyrene-DVB cross-linked gel columns $1 \times 60 \text{ cm } 100 \text{ \AA}$ and $1 \times 60 \text{ cm } 100 \text{ \AA}$ from PSS GmbH using THF as eluent at a flow rate of 1 mL min^{-1} . The columns were calibrated with poly (methyl methacrylate) standards.

Multi-angle Laser Light Scattering (MALLS)

The molecular weights of poly (EGDMA) and poly (TMPTMA) were also determined in THF by light scattering with a Malvern instrument in vertically polarized light ($\lambda = 488 \text{ nm}$) using five concentrations ($C_{\text{max}} = 1.8 \times 10^{-3} \text{ g/ml}$ for poly (EGDMA) and $1.91 \times 10^{-3} \text{ g/ml}$ for poly (TMPTMA)). For static light scattering, light scattered from all solutions was detected at scattering angles ranging between 30° and 130° in 10° increments. Scattering from pure THF solution at all angles was taken to account for scattering from the solvent. Data was analyzed using THF refraction index $n = 1.404$. The refractive index increment (dn/dc) was determined in THF at 25°C using a Brice-Phoenix differential refractometer. The measured dn/dc for poly (EGDMA) is 0.089 mLg^{-1} and for poly (TMPTMA) is 0.11 mLg^{-1} .

Intrinsic Viscosity (IV)

The intrinsic viscosity of polymer solutions in THF was measured at 25 °C using an Ubbelohde capillary viscometer

Differential Scanning Calorimetry (DSC)

DSC measurements were performed under nitrogen (N₂) at a flow rate of 50 mL min⁻¹ on TA Instruments, model Q-10. Polymer sample (3 to 5 mg) was heated from -50 to 150 °C at 10 °C min⁻¹ and scanned to calculate the glass transition temperature (*T_g*) of the polymer in subsequent heating cycles.

4.2.3 Inclusion Complex: Homopolymerization

4.2.3.1 EGDMA-β-CD IC (Polymerization in DMF)

1 g (7.5×10^{-4} mol) of EGDMA-β-CD IC was dissolved in 6.5 mL of DMF. 10 mg (6.10×10^{-5} mol) of AIBN was used as an initiator and N₂ was purged for 15 min. The polymerization was carried out for 15 h at 65 °C. The polymer was precipitated in cold distilled water. The crude polymer was dissolved in THF, re-precipitated in petroleum ether, filtered and dried at room temperature. The polymer was soluble in common organic solvent such as THF, CHCl₃, DCM, MEK, DMSO and DMF etc.

Similarly, the polymerization of the inclusion complexes of EGMAVB, TMPTMA, TMPTA and TMPDAVB was carried out in DMF (Scheme 4.1 and 4.2).

Poly (EGDMA) and poly (TMPTMA) of various molecular weights were also prepared by varying initiator concentration in the range 5 to 15 mol % of monomer and characterized for intrinsic viscosity in THF at 25 °C.

4.2.3.2 EGDMA-β-CD IC (Polymerization in DMSO)

1 g (7.5×10^{-4} mol) of EGDMA-β-CD IC was dissolved in 8 mL of DMSO. 10 mg (6.10×10^{-5} mol) of AIBN was used as an initiator and N₂ was purged for 15 min. The polymerization was carried out for 15 h at 65 °C. The gel formation was observed in solution. The precipitated product was insoluble in all solvents.

4.2.3.3 EGDMA-DM-β-CD IC (Polymerization in Chloroform)

1 g (6.54×10^{-4} mol) of EGDMA-DM-β-CD complex was dissolved in 5 mL of CHCl₃. 10 mg (6.10×10^{-5} mol) of AIBN was used as initiator and N₂ was purged for 15 min. Reaction mixture was refluxed at 60 °C for 24 h. The polymer was precipitated in methanol. The crude polymer was dissolved in THF, re-precipitated in petroleum ether,

filtered and dried. The polymer was soluble in THF, CHCl_3 , DCM, MEK, DMSO and DMF etc.

4.2.3.4 EGDMA-DM- β -CD IC (Polymerization in Water)

1 g (6.54×10^{-4} mol) of EGDMA-DM- β -CD complex was dissolved in 7 mL of water. 10 mg (3.7×10^{-5} mol) of $\text{K}_2\text{S}_2\text{O}_8$ was used as initiator. Polymerization was carried out at 65 °C for 24 h. The polymer precipitated in the polymerization medium. The precipitated polymer was filtered washed with water and petroleum ether to remove DM- β -CD and unreacted monomers respectively. The polymer was insoluble in all solvents.

4.2.3.5 Polymerization of EGMAVB Monomer

0.5 g (1.92×10^{-3} mol) of EGMAVB monomer was dissolved in 6 mL of DMF. 10 mg (6.10×10^{-5} mol) of AIBN was used as an initiator; N_2 was purged for 15 min. The polymerization was carried out for less than 1h at 65 °C. The polymer was precipitated in distilled water and purified by dissolving it in THF and re-precipitating in petroleum ether.

4.2.3.6 Comparative Experiments

i. 0.2 g (1.0×10^{-3} mol) of EGDMA was dissolved in 9 mL of DMF. 10 mg (6.10×10^{-5} mol) of AIBN was used as an initiator and N_2 was purged for 15 min. The polymerization was carried out for 15 h at 65 °C. The gel formation was immediately observed in polymerization solution. The mass was poured in distilled water to precipitate the polymer completely and dried. The precipitate was insoluble in all solvents, which indicated that the polymer was cross-linked during polymerization.

ii. 0.2 g (1.0×10^{-3} mol) of EGDMA and 1.145 g β -CD were dissolved in 9 mL of DMF. 10 mg (6.10×10^{-5} mol) of AIBN was used as an initiator and N_2 was purged for 15 min. The polymerization was carried out for 15 h at 65 °C. Gel formation was observed. The mass was poured in distilled water to precipitate the polymer completely and dried. The precipitate was insoluble in all solvents indicating that the polymer cross-linked during polymerization.

4.2.4 Second Stage Polymerization

4.2.4.1 Intermolecular Cross-linking

i. Photo Cross-linking: 80 mg of poly (EGDMA) and 3 mg of photo initiator (1-hydroxy cyclohexyl phenyl ketone) were dissolved in 5 mL of CHCl_3 . To prepare a film, solvent was evaporated at room temperature. UV curing was carried out for 15 min. at room temperature. The UV cured films were insoluble in excess of CHCl_3 .

ii. Thermal Cross-linking: 100 mg of poly (EGDMA) and 5 mg of AIBN were dissolved in 5 mL of DMF. The polymer solution was heated at 65 °C in water bath. The gel formation was observed indicating that the polymer was crosslinked.

4.2.4.2 Intramolecular Cross-linking

Intramolecular cross-linking of poly (EGDMA) ($M_n = 11,465$, Intrinsic viscosity $[\eta] = 0.053 \text{ dL/g}$) was carried out at three different concentrations viz. 0.80 mg/mL ($C^*/235$), 0.22 mg/mL ($C^*/857$), and 0.11 mg/mL ($C^*/1715$) where ($C^* = 1/[\eta]$, denotes critical overlap concentration).

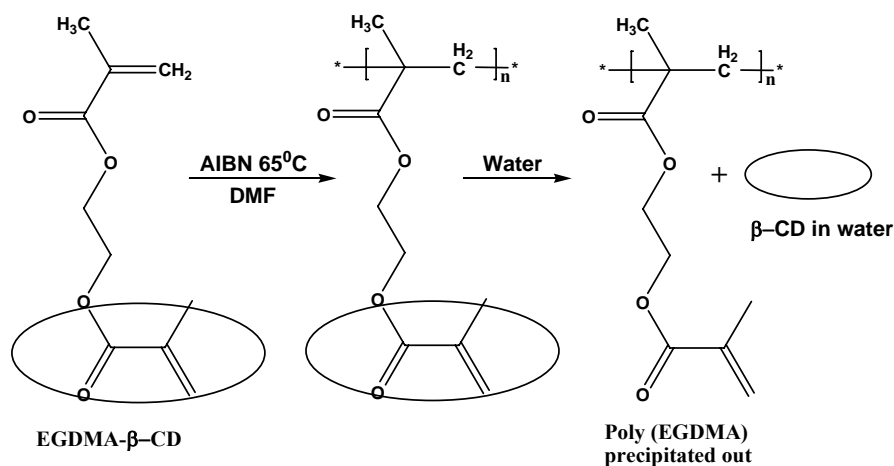
For the intramolecular cross-linking reaction, 50 mg of poly (EGDMA) was dissolved in 450 mL of DMF. 20 mg of AIBN was added to the dissolved polymer solution. N_2 was purged for 30 min. and the reaction mixture was heated at 65 °C in oil bath for 20 h with magnetic stirring. The reaction mixture remained transparent throughout the reaction time. The polymer solution was concentrated on rotary evaporator. The concentrated polymer solution was poured in water to precipitate the polymer. The precipitated polymer was filtered and dried at room temperature.

4.3 Results and Discussion

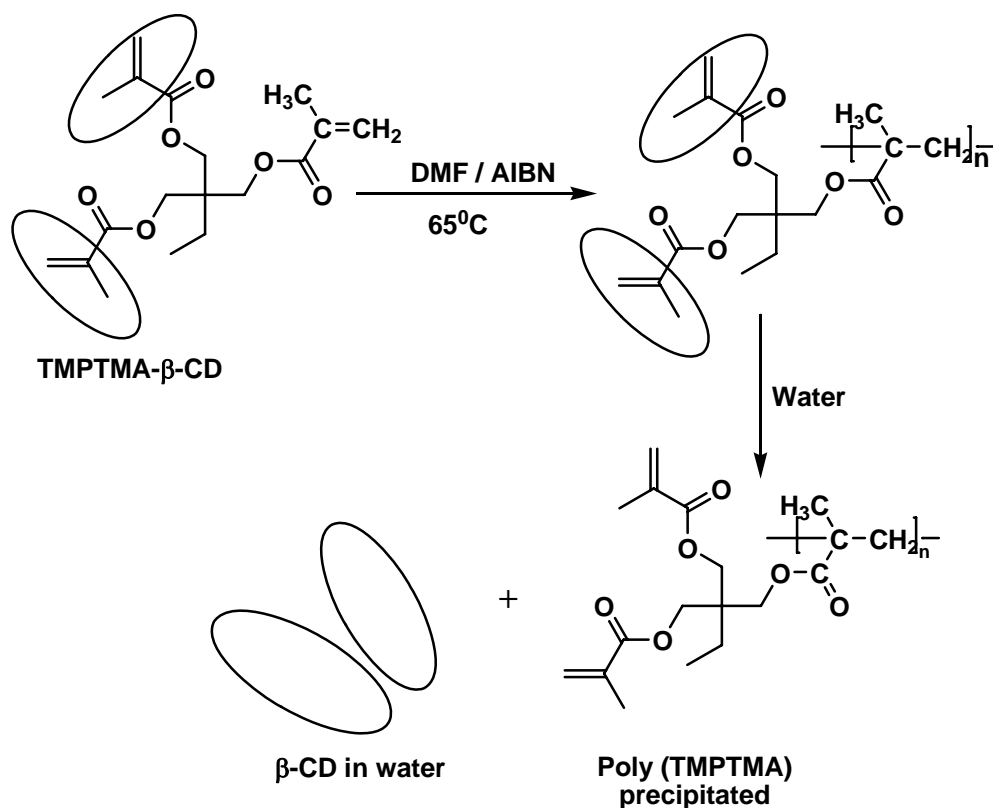
4.3.1 Inclusion Complex: Homopolymerization

Free radical polymerization of di and trivinyl monomers leads to cross-linked products in early stages of polymerization. In contrast, IC mediated polymerization of di or trivinyl monomers yields soluble polymers. The formation of IC between CD and the multivinyl monomer in well defined stoichiometric proportions and the purification of formed IC to free it from the uncomplexed multivinyl monomer prior to polymerization are essential prerequisites to obtain the soluble polymers. This was evident from gel formation in the polymerization of EGDMA in absence as well as in mere presence of

β -CD. The solvent plays important role during polymerization of CD complexed multivinyl monomers.



Scheme 4.1: Polymerization of EGDMA- β -CD IC



Scheme 4.2: Polymerization of TMPTMA- β -CD IC

Free radical polymerization of β -CD complexed di and trivinyl monomers in DMF yielded soluble polymers, whereas polymerization in DMSO resulted in the cross-linked

products. This indicated the stability of multivinyl monomer- β -CD ICs in DMF and its de-complexation in DMSO (Maciejewski et al., 1979, Zhao and Beckham, 2003). The EGDMA-DM- β -CD IC was soluble and stable in CHCl_3 as evident from the formation of soluble polymer. However, the polymerization of EGDMA-DM- β -CD IC in water yielded cross-linked products. Since poly (EGDMA) is insoluble in water, DM- β -CD slips off as polymerization proceeds, which exposes the included unsaturated groups to the growing radical chain (Sarvothaman and Ritter 2004).

The homo polymers obtained were soluble in common organic solvents such as THF, CHCl_3 , DCM, MEK, DMF and DMSO. The structure and properties of these polymers were evaluated by instrumental techniques such as FTIR, NMR, GPC, IV measurements, DSC, TGA and XRD.

4.3.2 Homopolymers: Characterization

4.3.2.1 FTIR of Homopolymers

Divinyl Monomers

FTIR spectra of poly (EGDMA) and poly (EGMAVB) showed the peaks at 1674 cm^{-1} and 1672 cm^{-1} respectively attributed to the presence of vinyl double bonds in the polymer structure (Figure 4.1) (Li et al 2005, 2006 and Koo et al., 2004). These vinyl groups were protected against the radical attack during polymerization because of their inclusion in CD cavity (Hedges 1998). FTIR spectra also showed the absence of any peaks at $3370 - 3300\text{ cm}^{-1}$ due to O-H symmetric and antisymmetric stretching vibrations of O-H groups of CD. This indicated de-complexation of CD from the polymer in water during its precipitation and thus absence of rotaxane type structure (Storsberg et al., 2000, Sarvothaman and Ritter, 2004).

Trivinyl Monomers

FTIR spectra of polymers of trivinyl monomers, poly (TMPTMA), poly (TMPTA) and poly (TMPDAVB) also displayed the presence of vinyl unsaturations at 1633 cm^{-1} , 1636 cm^{-1} , and 1673 cm^{-1} respectively and absence of rotaxane type structure (Figure 4.2b, 4.3b and 4.4). The IC mediated polymers of trivinyl monomers were also evaluated for their structure during polymerization by FTIR (Table 4.1).

Table 4.1: FTIR of IC, Polymer

Compound	>C=O (Trivinyl Monomer)	O-H (β-CD)
TMPTMA- β -CD	1727 (-5)	3311 (+59)
Poly (TMPTMA) (In presence of β -CD)	1729 (-7)	3338 (+32)
Poly (TMPTMA) (After removal of β -CD)	1720 (+2)	-
TMPTA- β -CD	1732 (0), 1708 (+ 24)	3329 (+ 41)
Poly (TMPTA) (In presence of β -CD)	1738 (-6)	3345 (+ 25)
Poly (TMPTA) (After removal of β -CD)	1716 (+16), 1732 (0), 1741 (-9)	-
TMPDAVB- β -CD	1733 (+5, -2)	3330 (+ 40)
Poly (TMPDAVB) (In presence of β -CD)	1731 (+5, 0)	3351 (+19)
Poly (TMPDAVB) (After removal of β -CD)	1728 (+10, +5)	-

Comparison with the uncomplexed compounds (differences in cm^{-1})

FTIR spectrum of poly (TMPTMA) before removal of CD showed the formation of polypseudorotaxane structure. The O-H band in TMPTMA- β -CD complex shifted from 3370 cm^{-1} to 3338 cm^{-1} in poly (TMPTMA- β -CD) i.e. before the removal of β -CD from the polymer. This indicated the presence of intermolecular hydrogen bonding between polymer and β -CD even after polymerization of included TMPTMA. Also the ester carbonyl peak at 1727 cm^{-1} in TMPTMA- β -CD shifted to 1729 cm^{-1} in poly (TMPTMA- β -CD) and further to 1720 cm^{-1} after removal of β -CD. Thus FTIR showed the existence of intermolecular hydrogen bonding interactions between β -CD and polymer even after polymerization of included TMPTMA monomers and confirms the presence of CD in the polymer before de-complexation in water (Figure 4.2 b). Thus, inclusion of the

methacryloyl group in the β -CD cavity during polymerization suppresses cyclization and cross-linking reactions during polymerization and yield soluble polymers having pendant vinyl unsaturations.

Similar results were obtained for polymerization of TMPTA- β -CD (1:1) IC and TMPDAVB- β -CD (1:2) IC (Table 4.1 Figures 4.3 and 4.4).

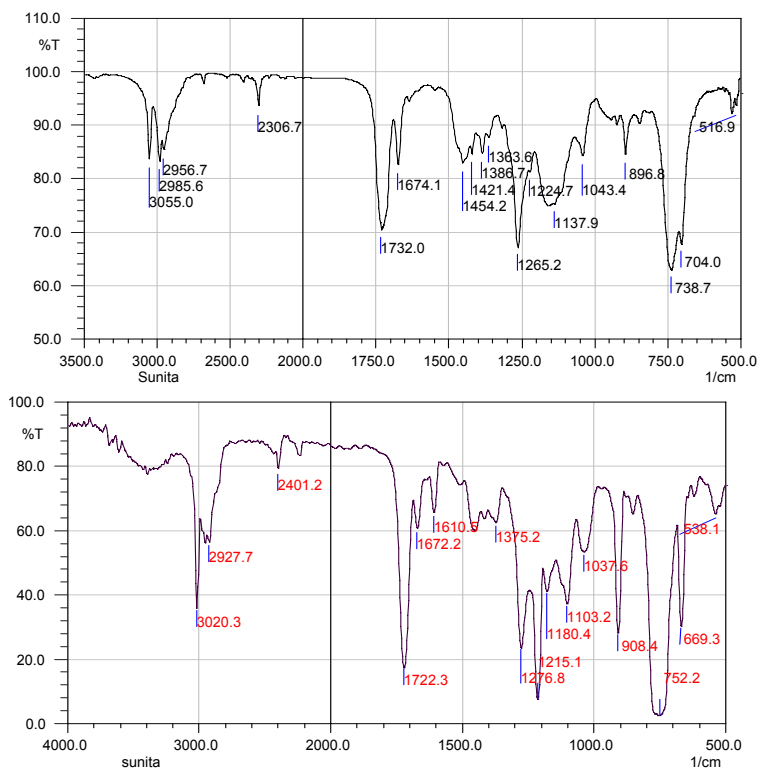


Figure 4.1: FTIR spectra a. poly (EGDMA) b. poly (EGMAVB)

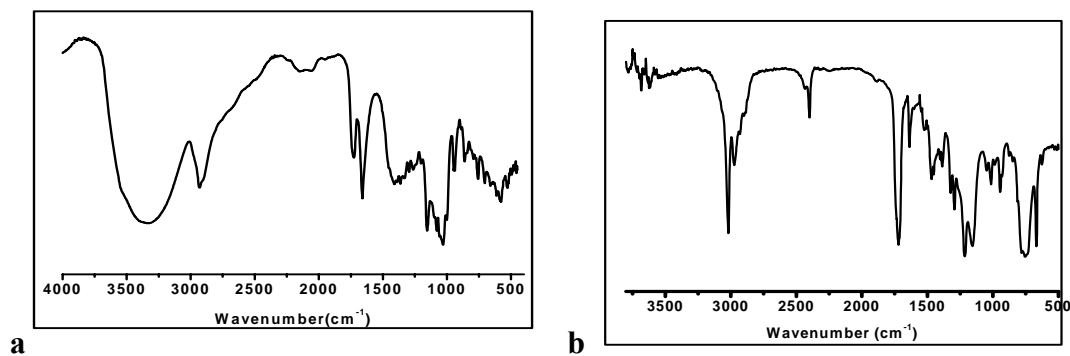


Figure 4.2: FTIR spectra of poly (TMPTMA) a. in presence of β -CD
b. after removal of β -CD

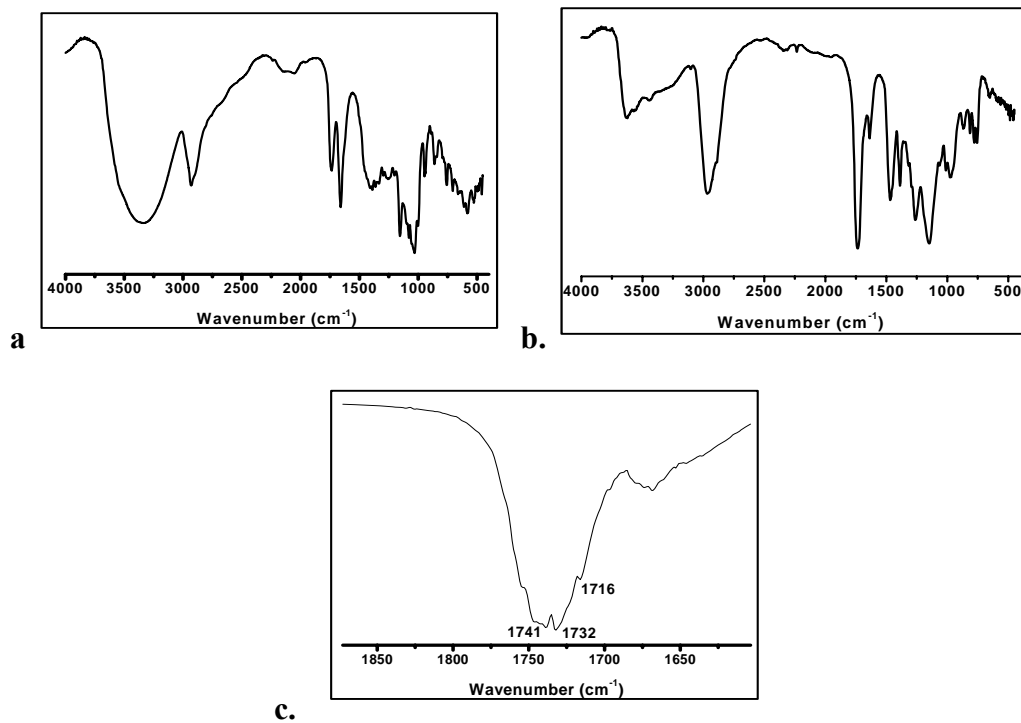


Figure 4.3: FTIR spectra of poly (TMPTA) a. in presence b. after removal of β -CD
c. expanded ester carbonyl region of poly (TMPTA)

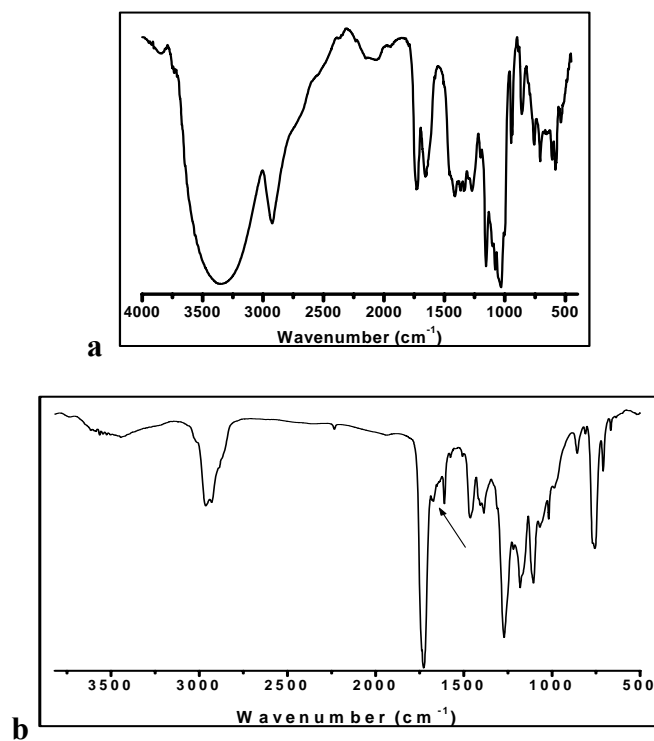


Figure 4.4: FTIR spectra poly (TMPDAVB) a. in presence of β -CD;
b. after removal of β -CD

4.3.2.2 NMR of Homopolymers

Poly (EGDMA), ^1H NMR

In the ^1H NMR (Figure 4.5) of poly (EGDMA), the peaks at 6.05 δ and 5.53 δ revealed the presence of vinyl unsaturation in polymer. Two different peak positions were obtained for the methyl group, 0.80 – 1.40 δ and 1.87 δ attributed to the methyl group adjacent to the reacted and unreacted vinyl unsaturation respectively. The integration showed the 1:1 ratio of unreacted vinyl group to reacted one. This 1:1 ratio was further confirmed by integrating the peaks at 4.33 δ corresponding to (-OCH₂CH₂O-) group of EGDMA and the peak at 6.05 δ or 5.53 δ corresponding to vinyl unsaturation. Furthermore no peak was observed at 6.22 δ apart from the peak due to terminal vinyl unsaturation at 5.53 δ and 6.05 δ indicated the absence of hyperbranched structure (Guan 2002). Thus ^1H NMR indicated the participation of one of the vinyl unsaturation during IC mediated free radical polymerization of EGDMA.

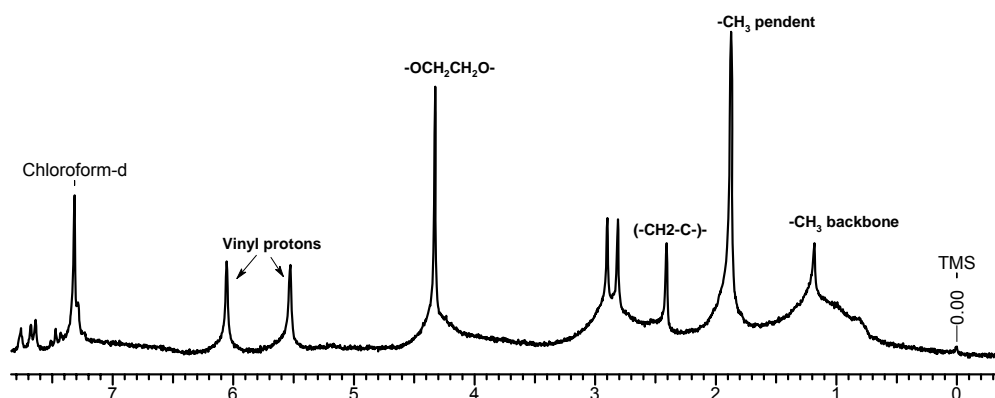


Figure 4.5: ^1H NMR of poly (EGDMA)

^1H NMR (CDCl_3): δ 0.80-1.40 (3H, backbone CH₃), 1.87 (3H, terminal CH₃), 2.41 (2H, backbone CH₂, This peak may vary between 2.05 to 2.5 depending on the molecular weight of the polymer), 4.33 (4H, -OCH₂CH₂O-, broadening of this peak will take place in high molecular weight polymers), 5.53 (1H, $\text{CH}_a\text{H}_b=\text{C}$), 6.05 (1H, $\text{CH}_a\text{H}_b=\text{C}$), the peaks at 2.90, 2.81 and 7.64 are due to residual DMF in polymer.

^{13}C NMR

Figure 4.6 shows the ^{13}C NMR spectrum of poly (EGDMA). In the spectrum two distinct peak positions corresponding to terminal methacrylate and backbone carbons are observed. The peaks attributed to polymer backbone which are relatively broad as

compared to the terminal or pendant groups revealed the strain in polymer backbone. The peaks at 135.75 δ and 125.89 δ indicated the presence of unreacted unsaturation i.e. vinyl group in polymer. The peak at 166.81 δ and 176.52 δ indicated the presence of two types of ester carbonyls *viz.* in the pendant methacrylate and the one adjacent to polymer backbone. The expansion of the spectrum in (O-CH₂CH₂-O) region shows splitting and different peak positions corresponding to the (O-CH₂) carbon adjacent to polymer backbone and (O-CH₂) carbon adjacent to terminal methacrylate group, in contrast to the single broad peak observed for (O-CH₂CH₂-O) carbon in fully cross-linked EGDMA copolymer. This supports the participation of only one of the double bonds of EGDMA and no cyclization reaction during its IC mediated polymerization (Figure 4.7) (Mathias et al., 1999).

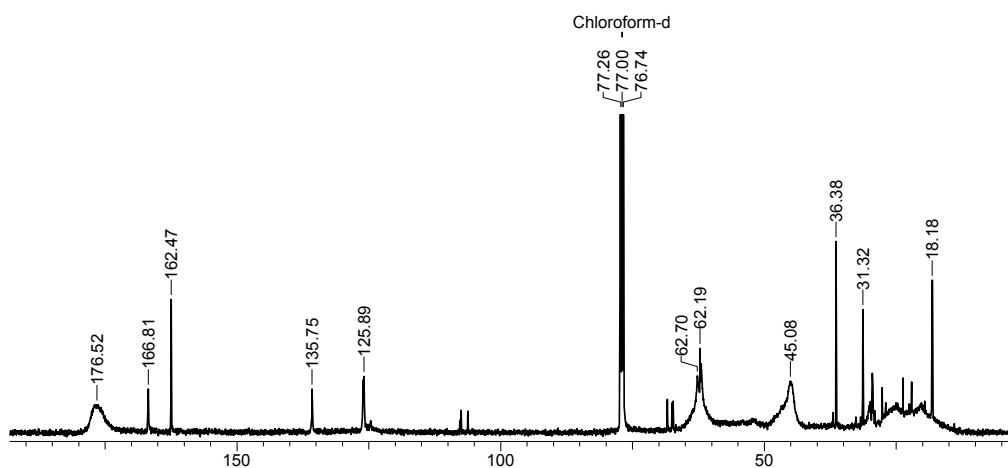


Figure 4.6: ¹³C NMR of poly (EGDMA)

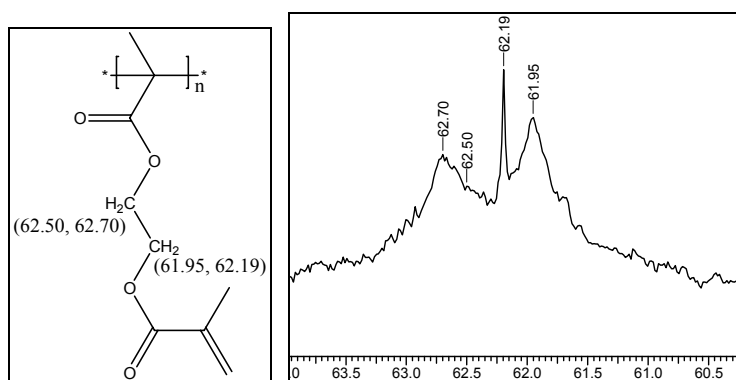


Figure 4.7: ¹³C NMR spectrum, expanded in (-OCH₂-CH₂O-) region

^{13}C NMR (CDCl_3) δ : 18.18 (terminal CH_3), 29.30 broad (backbone CH_3), 45.08 (backbone CH_2), 62.95 and 62.70 ($-\text{OCH}_2\text{CH}_2\text{O}-$), 125.89 (terminal $\text{CH}_2=\text{C}-$), 135.75 (terminal $\text{CH}_2=\text{C}-$), 166.81 (terminal ester carbonyl), 176.52 (internal ester carbonyl), the peak at 162.21, 36.38, 31.32 are due to residual DMF.

Poly (EGMAVB)

EGMAVB an unsymmetrical divinyl monomer formed 1:1 IC with CD and a soluble polymer on polymerization. The ^1H NMR spectrum of poly (EGMAVB) revealed the presence of methacrylate double bond protons (δ 5.59 and 6.15) and total absence of styrene double bond protons (δ 6.69-6.83 (m), 5.92, 5.83 (d) and 5.42, 5.37 (d)) (Figure 4.8). This indicated the participation of exclusively styrenic double bonds, during polymerization.

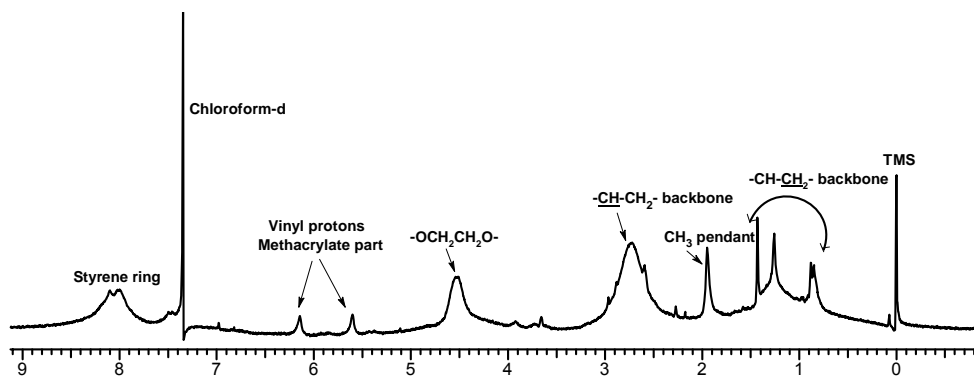


Figure 4.8: ^1H NMR of poly (EGMAVB) by polymerization of EGMAVB- β -CD IC

^1H NMR (CDCl_3) δ : 0.85-1.43 (2H, backbone CH_2), 1.95 (3H, terminal CH_3), 2.73 (1H, backbone CH), 4.50 (4H, $-\text{OCH}_2\text{CH}_2\text{O}-$), 5.59 (2H, $\text{CH}_a\text{H}_b=\text{C}$), 6.15 (2H, $\text{CH}_a\text{H}_b=\text{C}$), 8.10-7.99 (4H, of EGMAVB aromatic).

This could be attributed to the following,

- i. EGMAVB is an unsymmetrical monomer and in the free radical polymerization of divinyl monomers, the less reactive vinyl groups participate in polymerization only after the more reactive vinyl groups have undergone substantial conversion (Nagelsdiek et al., 2004).

ii. If the reactivity of both the double bonds of EGMAVB is equal, but only the styrene double bonds are able to react because of the selective inclusion of methacrylate double bonds in the CD cavity.

To distinguish between the two, neat EGMAVB was polymerized to lower conversions to yield a soluble polymer. In the ^1H NMR of poly (EGMAVB), the integration showed that 58 % of the styrenic double bond and 42 % of the methacrylate double bonds reacted (Figure 4.9a and 4.9b). This clearly indicated that the reactivity of both styrene and methacrylate double bonds of EGMAVB molecule was comparable. The exclusive participation of styrenic double bonds in polymerization could be attributed to the inclusion of methacrylate group in the CD cavity.

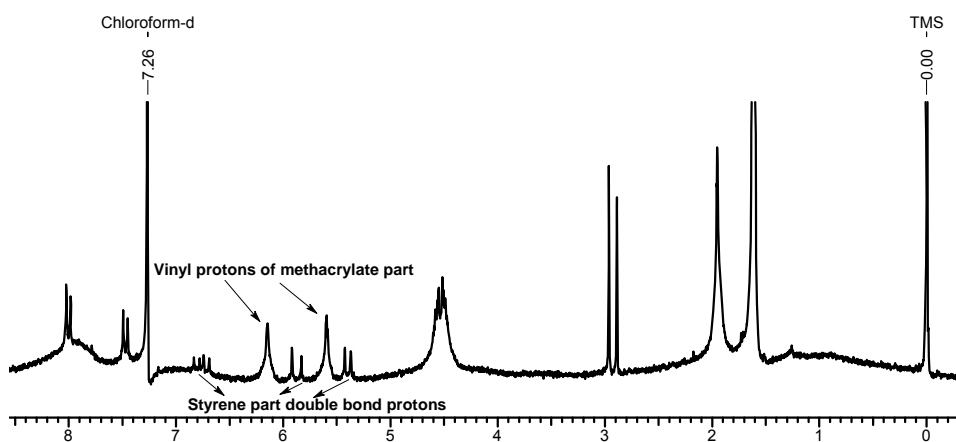


Figure 4.9a: ^1H NMR of poly (EGMAVB) by monomer polymerization

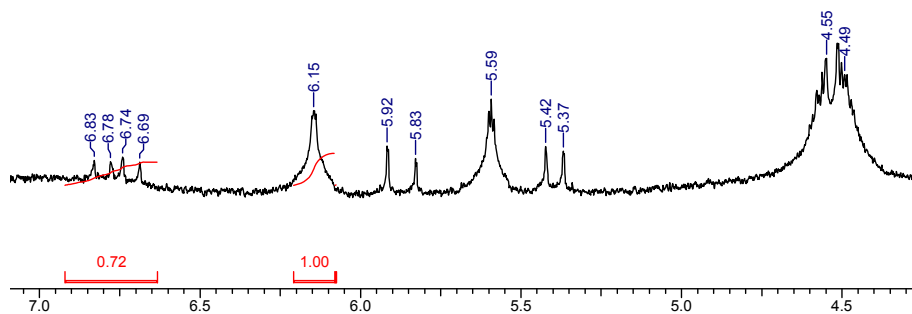


Figure 4.9b: Poly (EGMAVB): expanded spectrum

$^1\text{H NMR}$ (200 MHz, CDCl_3) δ : 4.49, 4.55 (4H, $-\text{OCH}_2\text{CH}_2\text{O}-$), 5.59 (2H, $\text{CH}_a\text{H}_b=\text{C}$ methacrylate part), 6.15 (2H, $\text{CH}_a\text{H}_b=\text{C}$ methacrylate part), 5.37, 5.42 (1H, $\text{Ar}-\text{CH}=\text{CH}_a\text{H}_b$), 5.83, 5.92 (1H, $\text{Ar}-\text{CH}=\text{CH}_a\text{H}_b$), 6.69-6.83 (1H, $\text{Ar}-\text{CH}=\text{CH}_2$).

Poly (TMPTMA)

$^1\text{H NMR}$ spectrum of poly (TMPTMA) revealed the presence of two vinyl unsaturations per repeat unit. This was anticipated from poly (EGDMA) and formation of 1:2 IC with CD (Figure 4.10).

Poly (TMPTMA) δ : 0.80 - 1.59 (3H, CH_2-CCH_3 , 2H, CH_2-CH_3 , 3H, CH_2-CCH_3 on polymer backbone), 1.70 (2H, CH_2-CCH_3 , backbone), 1.94 (6H, $\text{CH}_2=\text{CCH}_3$), 4.16 (4H, OCH_2 adjacent to unreacted vinyl unsaturation), 4.34 (2H, $-\text{OCH}_2$ adjacent to polymer backbone), 5.58 (2H, $\text{CH}_a\text{H}_b=\text{CH}$), 6.10 (2H, $\text{CH}_a\text{H}_b=\text{CH}$).

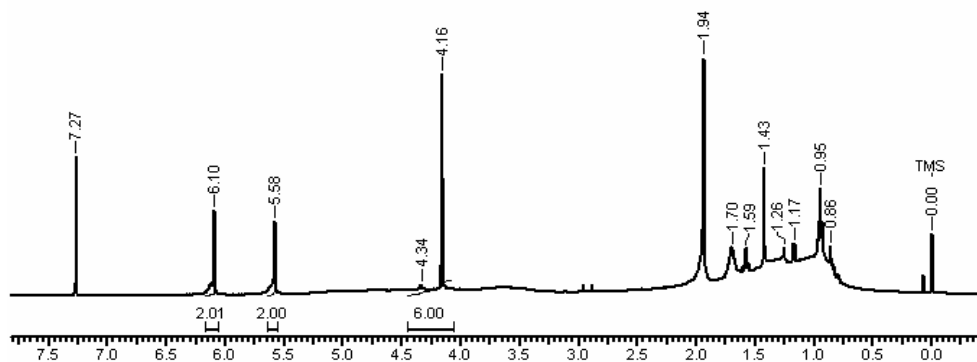


Figure 4.10: $^1\text{H NMR}$ of poly (TMPTMA)

Poly (TMPTA)

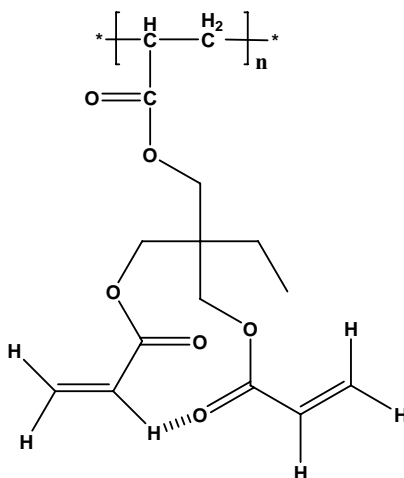


Figure 4.11: Structure of poly (TMPTA)

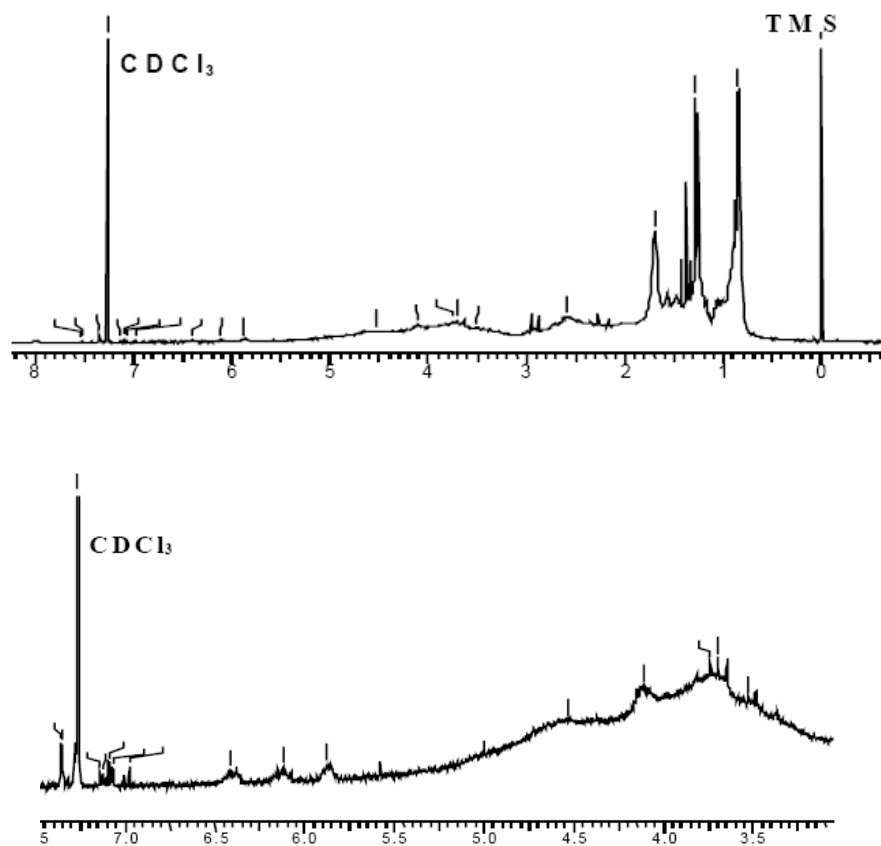


Figure 4.12: ^1H NMR of poly (TMPTA) a. whole spectrum
b. expanded region 3 to 7.60 δ

TMPTA formed 1:1 IC with β -CD in which two acrylate groups of TMPTA were included in single CD cavity because of intramolecular hydrogen bonding interactions present. ^1H NMR of poly (TMPTA) (Figure 4.12) showed a broad peak in the range 3 to 5 δ . This indicated that hydrogen bonding interactions between two acrylate groups of TMPTA persisted even after polymerization and formation of pseudo cyclic structure (Figure 4.11). This strained the system further and hence did not resolve the peaks. The presence of intramolecular hydrogen bonding was supported by the emergence of new peaks corresponding to hydrogen bonding along with free acrylate protons in the region δ 5.88 to 7.4. This was further confirmed by FTIR analysis of poly (TMPTA) after β -CD removal, wherein three peaks at 1716, 1732 and 1742 cm^{-1} attributable to the hydrogen bonded, non-hydrogen bonded and backbone ester carbonyl in poly (TMPTA)

(Figure 4.3c) were observed. The ratio of reacted double bonds to unreacted double bonds was calculated by integrating the peak at 2.59 δ for backbone protons and the peak at 3.52 – 4.58 δ for $-\text{CH}_2\text{O}-$ protons. The integration showed that the ratio was precisely 1:2 which further corroborated the inclusion of both acrylates in single CD cavity and their unavailability for polymerization reaction.

Poly (TMPTA) δ : 0.85 - 1.43 (3H, $\text{CH}_2-\underline{\text{CH}}_3$, 2H, $\underline{\text{CH}}_2-\text{CH}_3$), 1.70 (2H, $\text{CH}-\underline{\text{CH}}_2$ backbone), 2.59 (1H, $\underline{\text{C}}\text{H}-\text{CH}_2$ backbone), 3.52 – 4.58 (6H, OCH_2), 5.88 to 7.54 (6H, $\underline{\text{C}}\text{H}=\underline{\text{C}}\text{H}_2$).

Poly (TMPDAVB)

TMPDAVB formed 1:2 IC with β -CD which indicated the disruption of hydrogen bonding interaction between the two acrylate groups because of insertion of 4-vinyl benzoate group. ^1H NMR of poly (TMPDAVB) revealed the participation of styrenic double bond during polymerization as anticipated from EGMAVB- β -CD IC polymerization (Figure 4.13).

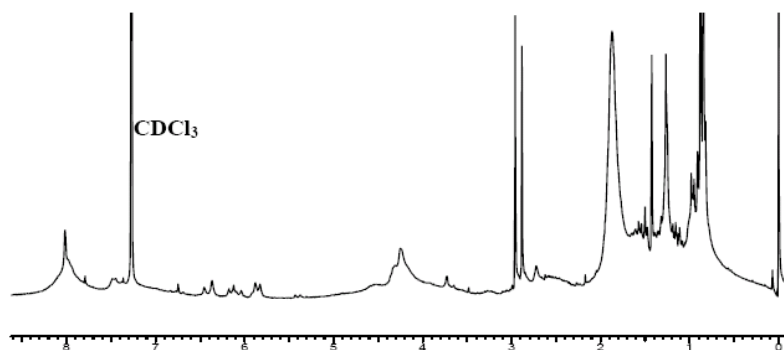


Figure 4.13: ^1H NMR of poly (TMPDAVB).

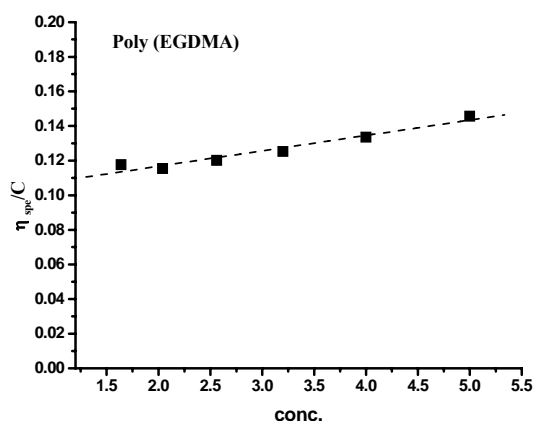
Poly (TMPDAVB) δ : 0.85 -1.43 (3H, $\text{CH}_2-\underline{\text{CH}}_3$, 2H, $\underline{\text{CH}}_2-\text{CH}_3$, and 2H, CH_2 backbone), 1.87 (1H, CH backbone) 4.25 to 4.31 (6H, OCH_2), 5.83 to 6.36 (6H, vinyl protons of acrylate double bonds), 7.49-7.45 (4H, aromatic protons), 8.02, 2.96, and 2.89 are due to DMF solvent impurity.

4.3.2.3 Intrinsic Viscosity of Homopolymers

The solution properties of the polymer reflect whether it is branched, hyperbranched, dendritic or linear. The dendritic, hyperbranched or branched polymers exhibit very low intrinsic viscosity and little dependence on molecular weights since the intermolecular

interactions are mostly limited to the surface layers of the spherical macromolecules and do not contribute to intermolecular entanglements (Sato et al., 2004). In contrast, linear polymers show a monotonic increase in intrinsic viscosity with the molecular weight (Guan 2002). The solution properties of poly (EGDMA) and poly (TMPTMA) were evaluated by measuring their intrinsic viscosity in THF.

Figure 4.14 illustrates the relationship between the reduced viscosity (η_{sp}/C) and polymer concentration. The reduced viscosity of poly (EGDMA), showed little dependence on polymer concentration. For poly (TMPTMA) the reduced viscosity appeared to be independent of polymer concentration.



a.

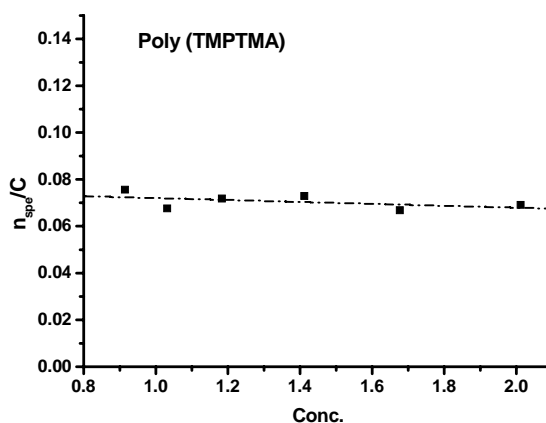


Figure 4.14: Relation between reduced viscosity and polymer concentration

a. Poly (EGDMA) b. Poly (TMPTMA)

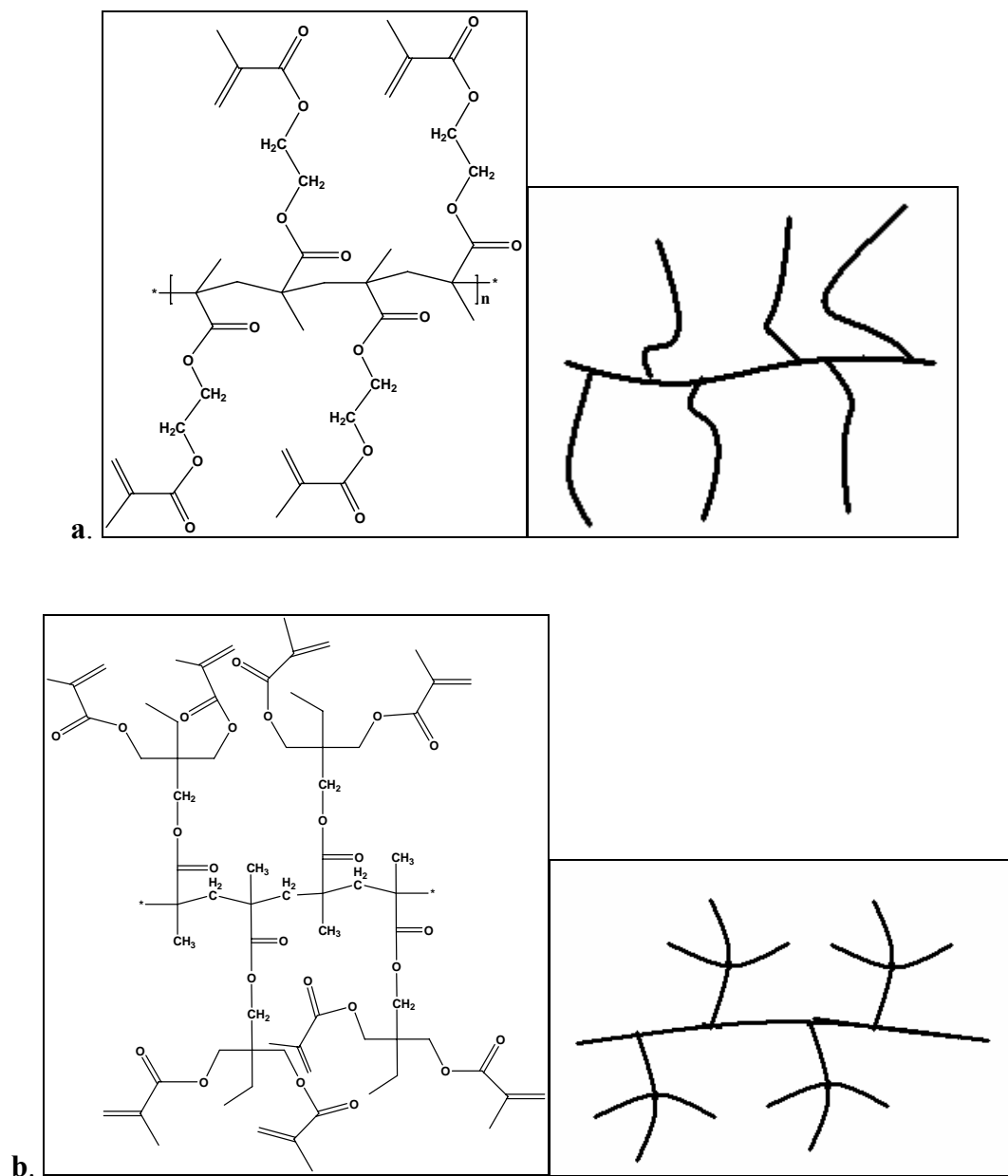


Figure 4.15: Structure of polymer a. poly (EGDMA) b. poly (TMPTMA)

This was due to the structure of polymers obtained by the IC mediated polymerization. Figure 4.15a and 4.15b shows the structure for poly (EGDMA) and poly (TMPTMA) respectively after CD de-complexation. In poly (EGDMA) the long pendant chains are distributed along the polymer backbone and the structure of the polymer appeared like a pseudo branch whereas in case poly (TMPTMA) the pendant chains appear more branched due to the inherent structure of TMPTMA monomer. This may be the reason

for very little dependence of reduced viscosity on polymer concentration in case of individual polymers.

Intrinsic viscosities of both poly (EGDMA) and poly (TMPTMA) exhibited linear dependence on molecular weights (Figure 4.16). This indicated the linear nature of the polymer and absence of any branching mechanisms during polymerization of complexed monomers. The Mark - Houwink - Sakurada exponent of poly (EGDMA) and poly (TMPTMA) are 0.29 and 0.39 respectively, while the corresponding value for hyperbranched poly (EGDMA) is 0.14 (Figure 4.17). The higher value of exponent compared to the hyperbranched polymers further confirmed the linear structure of IC mediated polymers of di and trivinyl monomers.

Poly (EGDMA)

Table 4.2: Molecular Weight and Intrinsic Viscosity of Poly (EGDMA)

M_w	M_n	M_w / M_n	$[\eta] \text{ dLg}^{-1}$
4,82,591	1,02,340	4.70	0.09895
2,12,564	54,600	3.80	0.08732
1,30,704	44,005	3.06	0.07948
1,12,075	34,869	2.97	0.07564
69,648	16,337	4.26	0.05910
52,871	11,465	4.50	0.05272

Initiator concentration was varied to obtain polymers of different molecular weights

Poly (TMPTMA)

Table 4.3: Molecular Weight and Intrinsic Viscosity of Poly (TMPTMA)

M_w	M_n	M_w / M_n	$[\eta] \text{ dLg}^{-1}$
6,00,150	2,31,300	2.59	0.1187
3,23,760	1,86,920	1.73	0.1096
5,18,870	1,30,450	3.97	0.0900
2,31,370	85,402	2.71	0.0836
1,43,410	66,478	2.16	0.0714

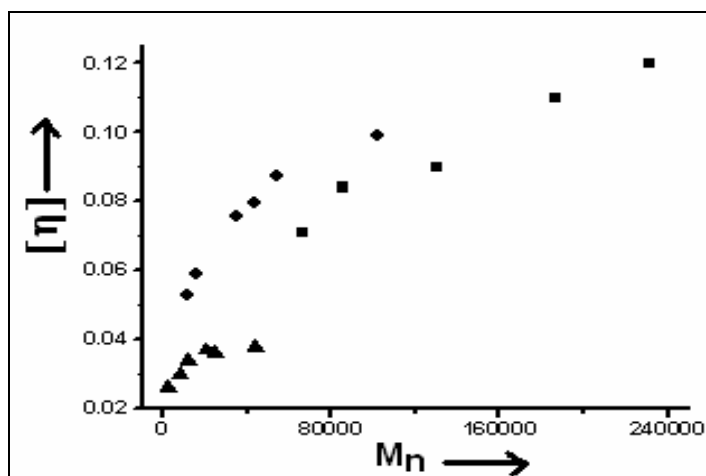


Figure 4.16: Intrinsic viscosity *versus* molecular weight plots for ■ poly (TMPTMA),
◆ linear poly (EGDMA) and ▲ hyperbranched poly (EGDMA)

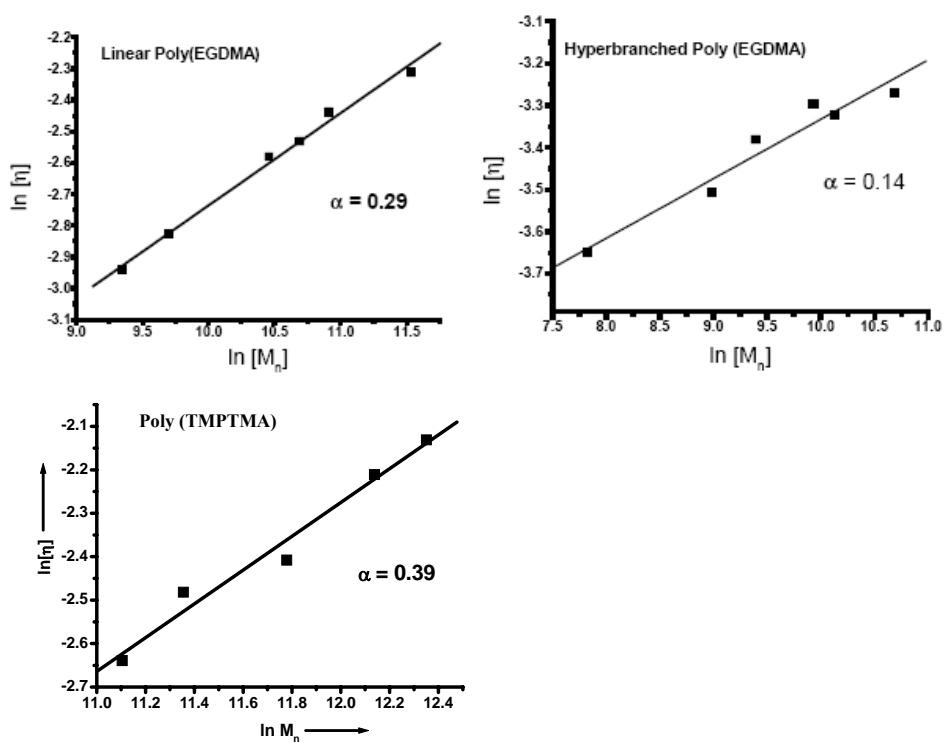


Figure 4.17: Mark-Houwink-Sakurada parameters of a. linear poly (EGDMA)
b. hyperbranched poly (EGDMA) c. poly (TMPTMA)

4.3.2.4 Molecular Weight of Homopolymers by MALLS and GPC

Poly (EGDMA) and poly (TMPTMA) were also characterized for their molecular weights by MALLS and the results are summarized in Table 4.4.

MALLS measurements at 25 °C in THF for poly (EGDMA) and poly (TMPTMA) show $M_w = 2.16 \times 10^5$ and 6.1×10^5 , which are comparable to M_w obtained by GPC *viz.* 2.46×10^5 and 2.7×10^5 respectively. In contrast, the values differ by an order of magnitude for the branched polymers. For instance, in the case of hyperbranched copolymers of EGDMA Sato et al., (2004) reported, $M_w = 7.68 \times 10^5$ by light scattering and 6.9×10^4 by GPC. The values of second virial coefficient 3.4×10^{-4} mol ml/g² and 1.3×10^{-4} mol ml/g² for poly (EGDMA) and poly (TMPTMA) of M_w 2.16×10^5 and 6.1×10^5 are comparable to the values of linear poly (methyl methacrylate) and poly (styrene), and far greater than that for the hyperbranched copolymers of EGDMA (Sato et al., 2004) *viz.* 7.2×10^{-6} mol ml/g² for M_w of 7.68×10^5 . All these results confirmed the linear structure of poly (EGDMA) and poly (TMPTMA) obtained by IC mediated polymerization.

Table 4.4: Properties of Poly (EGDMA) and Poly (TMPTMA)

Properties	Poly (EGDMA)	Poly (TMPTMA)	Poly (styrene) ^a
Mol. Wt. GPC (PMMA reference standard)	2.46×10^5	2.7×10^5	-
Mol. Wt. MALLS (Zimm plot)	2.16×10^5	6.1×10^5	2.9×10^5
Radius of gyration (R _g) (nm)	31.2	50.4	27.6
Second virial coefficient (A ₂) (mol ml/g ²)	3.5×10^{-4}	1.3×10^{-4}	4.4×10^{-4}

^a Sato et al., 2004.

4.3.3 Second Stage Polymerization

The pendant vinyl group of polymer can be reacted to undergo intermolecular or intramolecular cross-linking reactions. This approach of cross-linking of soluble polymers will find potential applications in optoelectronics, microlithography and molecular imprinting etc.

4.3.3.1 Intermolecular Cross-linking

TGA

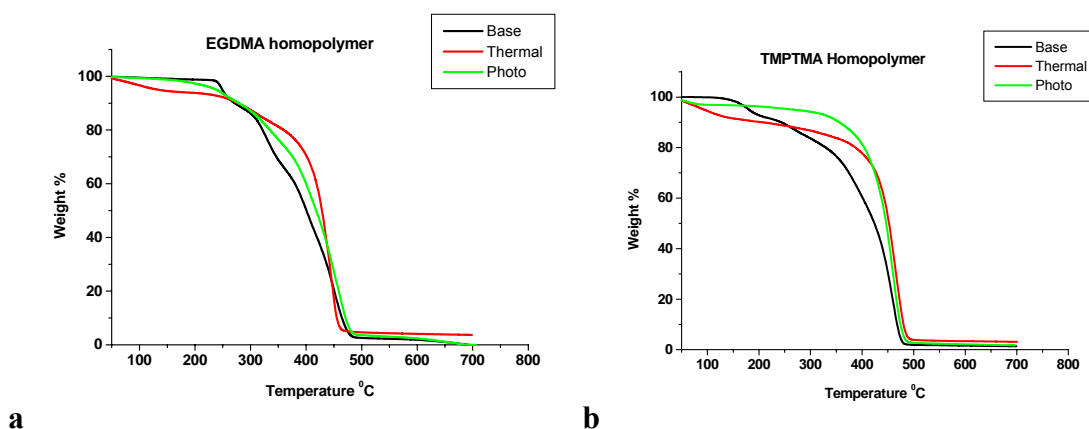


Figure 4.18: TGA scans before and after second stage polymerization
a. poly (EGDMA) b. poly (TMPTMA)

Table 4.5 Thermal Properties of Poly (EGDMA)

Polymer (EGDMA)	Degradation temp (°C)	
	T1 ^a	T2 ^b
Precursor polymer	321.64	400.68
Thermal X-link	359.87	428.58
Photo X-link	335.15	418.09

T1^a temp at 20 % wt loss, T1^b temp at 50% wt loss

The polymers cross-linked by thermal and photo cross-linking were characterized for their thermal stability by thermo gravimetric analysis. Figures 4.18a and b show the thermogram for degradation of poly (EGDMA) and poly (TMPTMA) respectively. The thermal decomposition temperature for poly (EGDMA) was increased from 321 °C to 359 °C and 335 °C respectively after thermal and photo cross-linking (Table 4.5). Poly

(TMPTMA) exhibited relatively higher thermal degradation temperature as compared to poly (EGDMA) which is only to be expected from the presence of two free double bonds per monomer unit in the former as compared to one in the later (Table 4.6).

Table 4.6 Thermal Properties of Poly (TMPTMA)

Polymer (TMPTMA)	Degradation temp (°C)	
	T1 ^a	T2 ^b
Precursor polymer	329.64	423.79
Thermal X-link	387.21	452.22
Photo X-link	404.24	446.65

T1^a temp at 20 % wt loss, T2^b temp at 50% wt loss

DSC

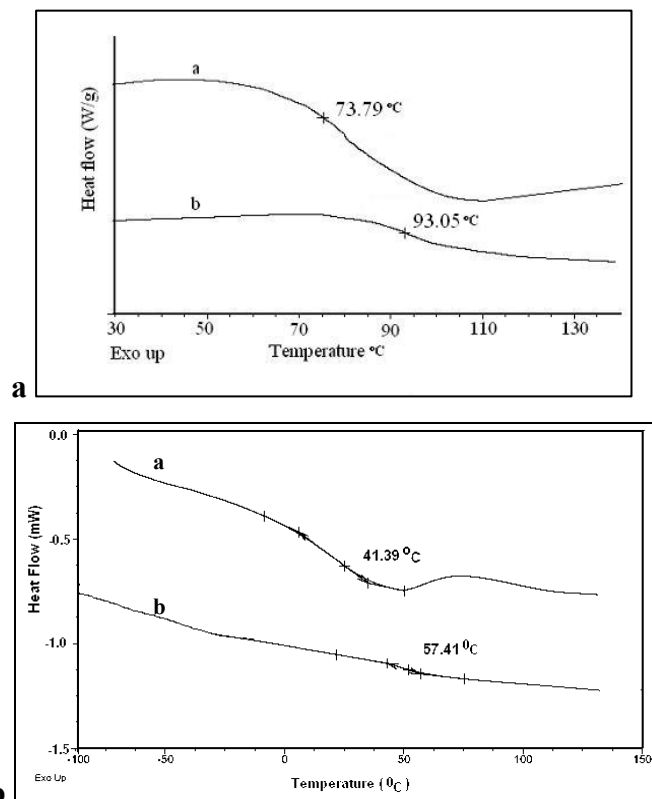


Figure 4.19: Thermograms of poly (EGDMA) and poly (TMPTMA)

(a) first and (b) second heating cycle

The DSC characterization of poly (EGDMA) showed the increase in T_g from 73.79 to 93.05 °C as a result of cross-linking. Poly (TMPTMA) showed increase in T_g from 41.39 °C to 57.41 °C and disappearance in subsequent heating cycles (Figure 4.19). This indicated the participation of pendant double bonds in crosslinking.

FTIR analysis

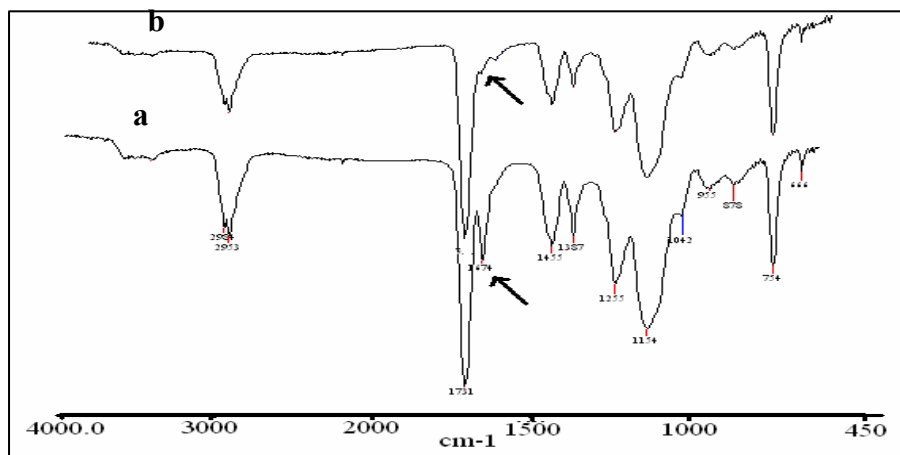


Figure 4.20: FTIR spectra of poly (EGDMA) a. before b. after cross-linking

The cross-linked products were also characterized by FTIR to estimate the extent of cross-linking. The FTIR analysis of poly (EGDMA) showed the disappearance of peak at 1674 cm^{-1} after second stage polymerization indicating the participation of double bonds in cross-linking reaction (Figure 4.20).

4.3.3.2 Intramolecular Cross-linking

Intramolecular cross-linking involved the reaction of pendant double bonds of linear polymer below critical overlap concentration. At this concentration each polymer chain was expected to be isolated and intramolecularly cross-linked to yield nanoparticles.

The intramolecular cross-linking reaction for poly (EGDMA) was carried out at three different concentrations *viz.* $C^*/235$, $C^*/857$, and $C^*/1715$. The particles size of the precursor polymer and the polymer after cross-linking was measured by dynamic light scattering measurements (Table 4.7).

Table 4.7: Particle Size of Nanoparticles by Light Scattering

Polymer	Particle Size (nm)
Base Poly (EGDMA)	78.0
X-link in 0.80 mgmL ⁻¹	89.2
X-link in 0.22 mgmL ⁻¹	73.8
X-link in 0.11 mgmL ⁻¹	38.0

The particle size of the polymer increased from 78 to 89 nm when crosslinking was carried out at in C*/235 but successively decreased to 73.8 and 38 nm with increasing dilution of polymer solution (C*/857 and C*/1715) during cross-linking. This indicated the presence of intermolecular cross-linking reactions along with the intramolecular reactions and further dilution needed to obtain the single chain cross-linked nanoparticles from poly (EGDMA). This approach to nanoparticles synthesis was used to obtain the molecularly imprinted nanoparticles with enhanced binding capacity and sustained release of the template molecules.

4.4 Conclusions

Inclusion complex mediated polymerization of di and trivinyl monomers yields soluble, linear polymers bearing pendant vinyl unsaturations depending on the number of vinyl groups previously included in CD cavity. The pendant unsaturation in the soluble homopolymers can be subsequently reacted inter or intramolecularly to yield cross-linked polymers or nanoparticles. The copolymerization of complexed di or trivinyl monomers will open up new areas of applications of these latent cross-linkable polymers.

Chapter 5
Supramolecular Inclusion Complex:
Copolymerization

5.1 Introduction

Inclusion complex mediated homopolymerization of di and trivinyl monomers leads to latent cross-linkable soluble polymers containing pendant vinyl unsaturation. The subsequent inter and intramolecular cross-linking reactions of pendant vinyl unsaturation yield insoluble, infusible products and nanoparticles respectively. The homopolymers will have limited applications because of the lack of functionalities in the polymer structure. Copolymerization allows the synthesis of polymers containing functional co-monomers and broadens the scope of applications. In view of the applications of latent cross-linkable, functional methacrylate copolymers in upcoming areas such as photolithography, nanotechnology, optoelectronics, molecular imprinting etc. we extended our investigation to copolymerize the multivinyl monomers with a variety of functional co-monomers.

The study of monomer reactivity ratios in copolymerization is useful to confirm the polymer structure and tailor the same (Odian 1991). These measurements also help understand the kinetic and mechanistic aspects of copolymerization (Ziaee and Nekoomanesh 1998). The multivinyl monomers yield cross-linked products in the free radical polymerization reactions because of the highly reactive pendant vinyl groups. In contrast, the multivinyl monomers after inclusion in CD cavity react with only one of its vinyl unsaturations and yield soluble copolymers. The determination of co-monomer reactivity ratio of complexed multivinyl monomers would be helpful to study their behavior during copolymerization.

In this study, monovinyl methacrylate monomers were copolymerized with β -CD complexes of multivinyl monomers. These copolymers were characterized for their structure and properties by instrumental techniques such as FTIR, NMR, GPC and intrinsic viscosity etc. Further, the co-monomer reactivity ratios were calculated for the copolymerization of multivinyl monomers after and before their inclusion in CD cavity. Amongst the various methods available to determine monomer reactivity ratios, Fineman-Ross (FR) and Kelen-Tudos (KT) methods were used.

5.2 Experimental

5.2.1 Materials

Inclusion complexes *viz* EGDMA- β -CD, EGMAVB- β -CD, TMPTMA- β -CD and EGIBMA- β -CD were prepared as described in chapter 3.

Isobutyric acid (IBA), benzoyl chloride (PhCOCl) and triethylamine (TEA) were purchased from SD Fine chemicals.

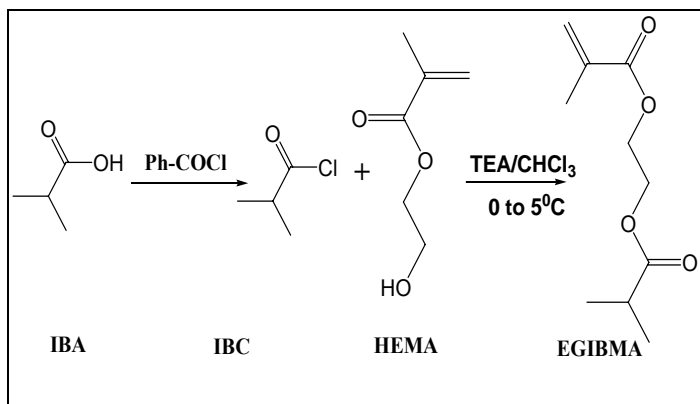
5.2.2 Measurements

FTIR, NMR, GPC, IV, and light scattering measurements were carried out to evaluate the structure and properties of the copolymers.

5.2.3. Monomers Synthesis

The monovinyl monomers, structurally identical to the multivinyl monomers were synthesized as described below.

5.2.3.1 Ethylene Glycol Isobutyrate Methacrylate (EGIBMA)



Scheme 5.1: EGIBMA monomer synthesis

13.7 g (0.10 mol) of HEMA and 15.5 mL (0.10 mol) of TEA were added in 200 mL of dry CHCl₃. To this, 10.5 mL (0.10 mol) solution of isobutyryl chloride (IBC) diluted with 40 mL dry CHCl₃ was added drop wise at 0 to 5 °C. The reaction mixture was stirred at room temperature for 24 h. The CHCl₃ layer was concentrated and the crude product was purified using column chromatography.

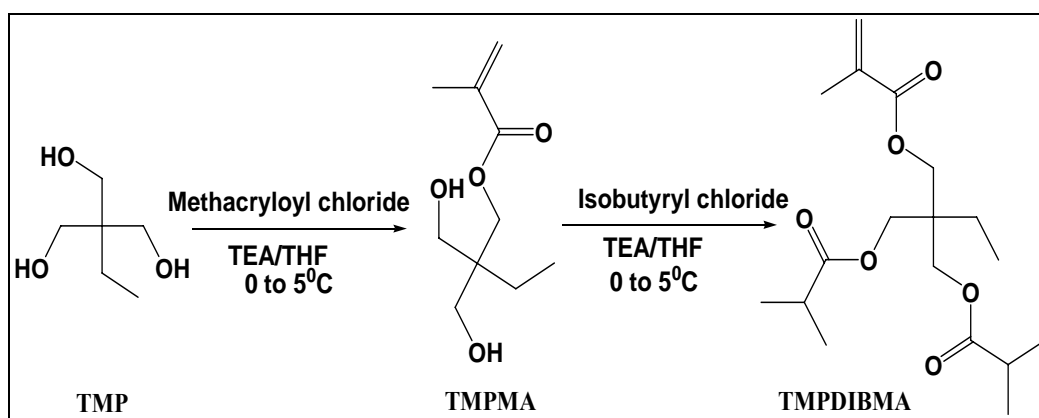
¹H NMR (CDCl₃) δ : 1.19(6H, HC-(CH₃)₂), 1.93(3H, -CH₃), 2.67 (H, -CH-(CH₃)₂), 4.36, 4.43 (4H, -OCH₂CH₂O-), 5.58 (1H, CHH=C-), 6.15 (1H, CHH=C-).

5.2.3.2 Trimethylolpropane Methacrylate (TMPMA)

36.04 g (0.27 mol) of TMP and 27.18 g (0.27 mol) of TEA were added in 20 mL of dry THF. To this 26 mL (0.27 mol) of methacryloyl chloride diluted with 20 mL THF was added drop by drop at 0 to 5°C. The reaction mixture was stirred at room temperature for 24 h. The TEA hydrochloride salt precipitated out from reaction mixture was separated by filtration. The filtrate was concentrated and the crude product was purified by column chromatography.

$^1\text{H NMR}$ ($\text{CDCl}_3 + \text{DMSO } d_6$) δ : 0.96 (3H, $-\text{CH}_2 - \underline{\text{CH}_3}$), 1.25 (2H, $-\underline{\text{CH}_2} - \text{CH}_3$), 1.93 (3H, $\underline{\text{CH}_3}$) 3.45 (4H, $-\text{CH}_2\text{OH}$), 4.07 (2H, $-\text{O}=\text{C}-\underline{\text{OCH}_2}$), 5.58 (1H, $\underline{\text{CHH}}=\text{C}-$), 6.15 (1H, $\text{CHH}=\text{C}-$).

5.2.3.3 Trimethylolpropane Diisobutyrate Methacrylate (TMPDIBMA)



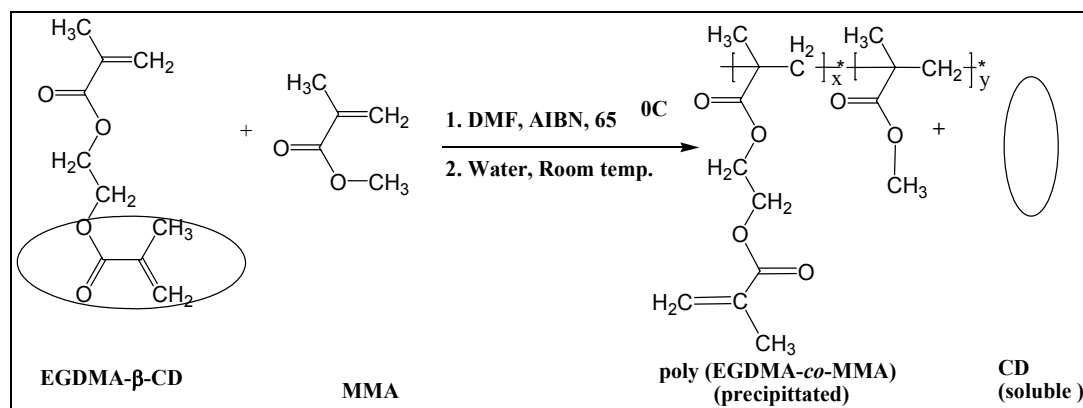
Scheme 5.2: TMPMA and TMPDIBMA monomers synthesis

40 g (0.20 mol) of TMPMA and 43.17 g (0.40 mol) of TEA were added in a 20 mL of dry THF. To this 42.14 g (0.40 mol) of isobutyryl chloride diluted with 20 mL of THF was added drop by drop at 0 to 5 °C. The reaction mixture was stirred at room temperature for 24 h. The TEA hydrochloride salt precipitated out from reaction mixture was separated by filtration. The filtrate was concentrated and the crude product was purified by column chromatography.

$^1\text{H NMR}$ CDCl_3 : 0.96 δ (3H, $\text{CH}_2-\underline{\text{CH}_3}$), 1.25 δ (2H, $\underline{\text{CH}_2}-\text{CH}_3$), 1.19 δ (12H, $2\text{CH}(\underline{\text{CH}_3})_2$), 1.93 δ (3H, $\underline{\text{CH}_3}$), 2.67 δ (2H, $2\underline{\text{CH}}(\text{CH}_3)_2$), 4.0 δ (4H, $2\underline{\text{CH}_2}$ adjacent to

isobutyrate group), 4.07 δ (2H, $\underline{\text{CH}}_2$ adjacent to vinyl group), 5.58 δ (1H, $\text{CHH}=\text{C}$ -), 6.15 δ (1H, $\text{CHH}=\text{C}$ -).

5.2.4 Inclusion Complex: Copolymerization



Scheme 5.3: Copolymerization of EGDMA- β -CD IC

Copolymerization of EGDMA- β -CD, EGMAVB- β -CD and TMPTMA- β -CD was carried out with various functional monomers. The typical copolymerization reaction was as follows,

Poly (EGDMA-co-MMA) (50:50)

15.84 g (1.18×10^{-2} mol) of EGDMA- β -CD complex was dissolved in 105 mL DMF. 1.18 g (1.18×10^{-2} mol) of MMA and 0.195 g (1.18×10^{-3} mol) of AIBN were added to the dissolved complex solution. N_2 was purged in reaction mixture for 15 min and polymerization was carried out at 65°C for 24 h. The polymer was precipitated in cold distilled water. The crude polymer was dissolved in THF, re-precipitated in petroleum ether, filtered and dried at room temperature. The polymer was soluble in common organic solvents such as THF, CHCl_3 , DCM, MEK, DMSO and DMF etc.

Poly (EGDMA-co-MMA) and poly (TMPTMA-co-MMA) of various molecular weights were prepared by varying initiator (1 to 7 mol %) and chain transfer agent (0 to 6 mol %) concentration.

5.2.5 Co-monomer Reactivity Ratio

Following systems were studied to evaluate the co-monomer reactivity ratios.

1. EGDMA-MMA
2. EGDMA- β -CD-MMA
3. EGIBMA-MMA
4. EGIBMA- β -CD-MMA
5. EGMAVB-MMA
6. EGMAVB- β -CD-MMA
7. TMPMA-MMA
8. TMPTMA-MMA
9. TMPDIBMA-MMA
10. TMPTMA- β -CD-MMA

Copolymerization reactions were carried out using different mole ratios of co-monomers (1:9 through 9:1) in presence of AIBN. The polymerization reactions were carried out at 65 °C and quenched at low conversions. The crude polymers were purified as described above. The conversions were measured gravimetrically. The compositions of the copolymers were determined using ^1H NMR. Finemann – Ross (FR) and Kelen – Tudos (KT) methods were used to calculate the monomer reactivity ratios.

5.2.6 Second Stage Polymerization

5.2.6.1 Intermolecular Cross-linking

i. Thermal Cross-linking

200 mg of poly (EGDMA-*co*-MMA) (50:50) was dissolved in 2 mL of DMF, 10 mg AIBN was added as thermal initiator. The polymer solution was heated at 65°C 15 h in order to ensure complete polymerization of pendant vinyl unsaturations. Gel formation was observed. Gel was separated by filtration. Addition of water to the filtrate showed no turbidity, indicating that the cross-linking was complete.

ii. Photo Cross-linking

200 mg of poly (TMPTMA-*co*-MMA) (50:50) and 10 mg 1-hydroxycyclohexyl phenyl ketone (photo initiator) were dissolved in 3 ml of DCM. UV irradiation was carried out for 10 min at room temperature. The UV irradiated polymer film was insoluble in

excess of DCM as well as in other organic solvents, which indicated that the cross-linking was complete.

Similarly, other copolymers were cross-linked thermally as well as photo chemically and evaluated for the extent of cross-linking. In all cases cross-linking was complete.

5.2.6.2 Intramolecular Cross-linking

Poly (EGDMA-*co*-MMA) and poly (TMPTMA-*co*-MMA) of varying co-monomer compositions as well as molecular weights were utilized for the intramolecular cross-linking reactions. Intramolecular cross-linking reaction of the copolymers was carried out as described in chapter 4 for the homopolymers. In the present study the effect of type and extent of cross-linker, molecular weight of precursor copolymer and polymer concentration during crosslinking on the particle size of nanoparticles was investigated.

5.3 Results and Discussion

5.3.1 Inclusion Complex: Copolymerization

Inclusion complex mediated copolymerization of multivinyl monomers with monovinyl monomers yields soluble polymers, as the vinyl group of multivinyl monomer included in the β -CD cavity does not react with growing polymer radicals. FTIR, NMR, IV and GPC measurements were used to characterize the resulting copolymers for their structure and properties evaluation.

5.3.2 Copolymers: Characterization

5.3.2.1 FTIR of Copolymers

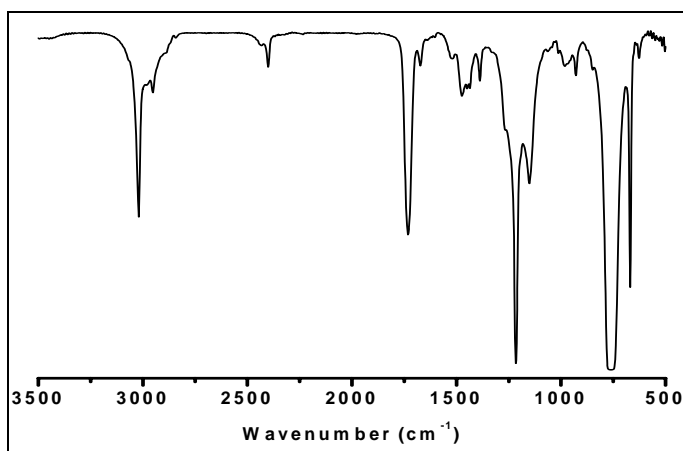


Figure 5.1: FTIR of poly (TMPTMA-*co*-MMA)

Figure 5.1 shows FTIR spectrum of poly (TMPTMA-*co*-MMA) (75:25). The peak at 1674 cm^{-1} was attributed to the presence of C=C bond in the copolymer. Also, the spectrum did not show any peaks in the region $3300\text{ to }3500\text{ cm}^{-1}$ which indicated total absence of CD and that of pseudorotaxane structure. Similar results were obtained for the other copolymers of multivinyl monomers.

5.3.2.2 NMR of Copolymers

NMR spectroscopy is useful to confirm the incorporation of the co-monomers as well as to calculate their molar composition in the polymer structure.

In the ^1H NMR spectrum of poly (EGDMA-*co*-MMA) peaks at $4.40 - 4.24\ \delta$ and the peak at $3.60\ \delta$ are attributed to the presence of (O-CH₂-CH₂-O) group of EGDMA and -OCH₃ group of MMA respectively, indicated the successful copolymerization of complexed EGDMA with MMA. Also, the peak at $5.59\ \delta$ and $6.13\ \delta$ confirms the presence of pendant vinyl unsaturation in polymer (Figure 5.2).

The ^1H NMR of poly (EGMAVB-*co*-MMA), the peak at $3.62\ \delta$ indicated the presence of -OCH₃ group of MMA. A broad signal at $4.52\ \delta$ and sharp signal at $4.40\ \delta$ were attributed to the presence -OCH₂ group of EGMAVB, adjacent to polymer backbone (adjacent to styrene) and pendant methacrylate group respectively. This indicated the participation of styrenic double bond during co polymerization of EGMAVB- β -CD IC. This was further confirmed by the presence of unsaturation from methacrylate at $5.59\ \delta$ and $6.13\ \delta$ and absence of styrene double bond signals at (δ $6.69\text{-}6.83$ (m), 5.92 , 5.83 (d) and 5.42 , 5.37 (d) in the polymer structure (Figure 5.3).

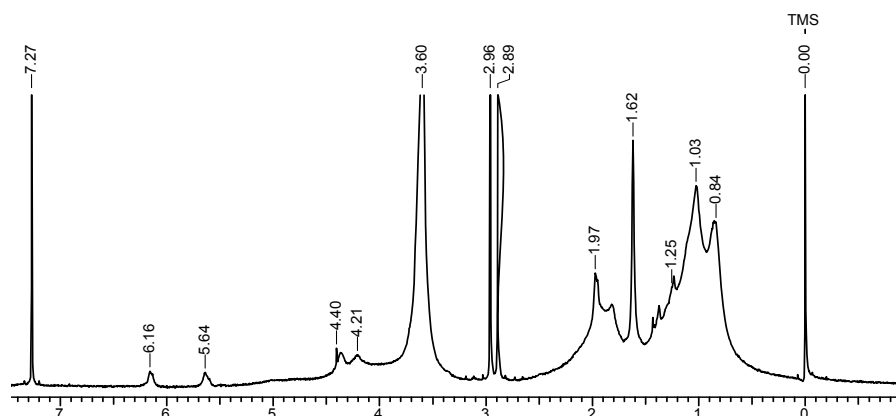


Figure 5.2: ^1H NMR of poly (EGDMA-*co*-MMA)

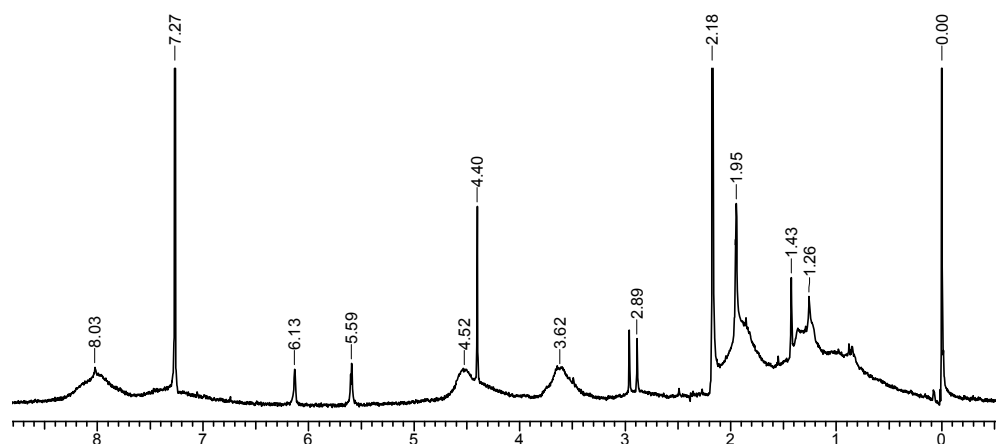


Figure 5.3: ^1H NMR of poly(EGMAVB-*co*-MMA)

Similarly, in the ^1H NMR spectrum of poly(TMPTMA-*co*-MMA) the peaks at 3.60 δ and 4.14 δ revealed the presence of MMA and TMPTMA in copolymer structure. The peaks at 5.57 δ and 6.08 δ indicated the presence of pendant unsaturation in the polymer structure (Figure 5.4).

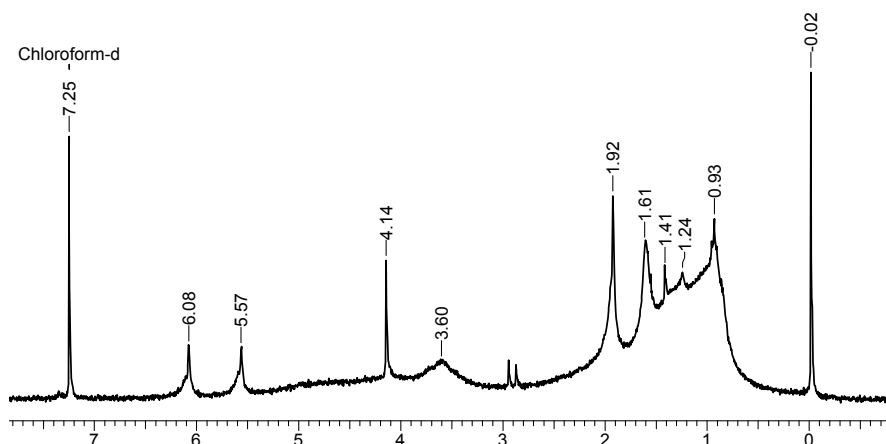


Figure 5.4: ^1H NMR of poly(TMPTMA-*co*-MMA)

5.3.2.3 Intrinsic Viscosity of Copolymers

Intrinsic viscosities of poly(EGDMA-*co*-MMA) (60:40) exhibited linear dependence on the molecular weight similar to the linear poly(EGDMA) obtained via inclusion complex mediated polymerization of EGDMA (Figure 5.5). This indicated the linear nature of the copolymer. The Mark - Houwink - Sakurada exponent of poly(EGDMA-*co*-MMA) is 0.21, which is higher than that for hyperbranched poly(EGDMA), 0.14

(Figure 5.6). This further confirmed the linear structure of IC mediated copolymers of EGDMA.

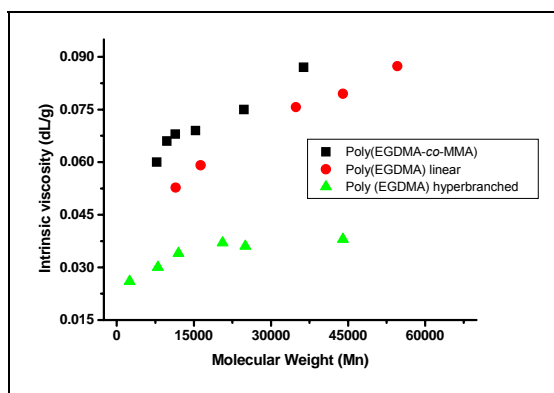


Figure 5.5: Intrinsic viscosity *versus* molecular weight plots for ■ poly (EGDMA-*co*-MMA) (60:40), ● linear poly (EGDMA) and ▲ hyperbranched poly (EGDMA)

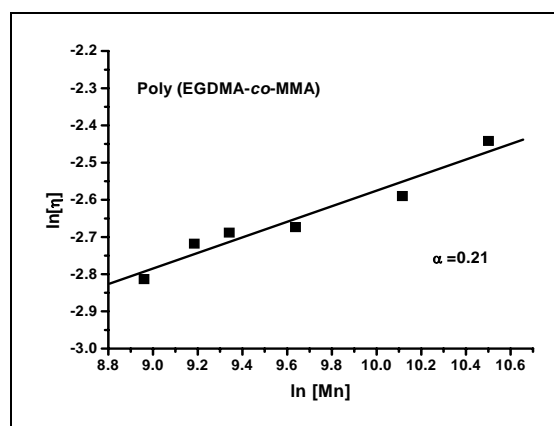


Figure 5.6: Mark-Houwink-Sakurada exponent for poly (EGDMA-*co*-MMA) (60:40)

5.3.3 Co-monomer Reactivity Ratio

The multivinyl monomers after formation of IC with the CD undergo selective polymerization with only one of its vinyl unsaturation and yield soluble homo and copolymers with pendant vinyl groups. The structure and performance of the copolymers depends upon the distribution of the co-monomers within the polymer (Odian 1991). The structure of copolymer is largely determined by the reactivity ratios of the two monomers r_1 and r_2 , which relate the preference of a monomer to reacting with itself or with the second monomer (Odian 1991). Thus, in order to understand the effect of complexation on co-monomer reactivity ratios of multivinyl monomers, the

reactivity ratios of MMA with EGDMA, EGMAVB and TMPTMA in the presence of and in absence of complexation were studied. Also to study the effect of structure of multivinyl monomer on co-monomer reactivity ratio, various monovinyl monomers, which resemble the structure of divinyl or trivinyl monomer, *viz.* EGIBMA, TMPMA and TMPIBMA were synthesized and their co-monomer reactivity ratios were estimated.

The copolymer composition was determined by ^1H NMR spectroscopy. The integrated characteristic signal of the incorporated MMA at δ 3.60 (OCH_3) was compared with the integrated signal of multivinyl monomer or structurally similar monovinyl monomers at δ 4 to 4.40 ($-\text{OCH}_2$). Fineman–Ross and Kelen-Tudos methods (Fineman et al., 1964, Kelen et al., 1975) were utilized to calculate the monomer reactivity ratio.

The Fineman–Ross equation is one of the earliest attempts to linearize the copolymer composition equation:

$$\mathbf{G} = \mathbf{H} \mathbf{r}_1 - \mathbf{r}_2 \quad (1)$$

Where:

$$\mathbf{G} = \mathbf{f}(\mathbf{F}-1) / \mathbf{F}$$

$$\mathbf{H} = \mathbf{f}^2 / \mathbf{F}$$

$$\mathbf{f} = \mathbf{f}_{\text{M1}} / \mathbf{f}_{\text{M2}} \quad \text{Mole ratio of monomers in feed}$$

$$\mathbf{F} = \mathbf{F}_{\text{m1}} / \mathbf{F}_{\text{m2}} \quad \text{Mole ratio of monomers in polymer}$$

The plot of G vs H values gives r_1 and r_2 from slope and intercept of the graph.

Kelen-Tudos introduced new parameters into the linearized copolymerization equation, such as η , ξ and α

$$\eta = (\mathbf{r}_1 + \mathbf{r}_2 / \alpha) \xi - \mathbf{r}_2 / \alpha \quad (2)$$

Where η and ξ are functions of the parameters G and H:

$$\eta = \mathbf{G} / (\alpha + \mathbf{H});$$

$$\xi = \mathbf{H} / (\alpha + \mathbf{H}); \text{ and}$$

$$\alpha = (\mathbf{H}_{\text{max}} \cdot \mathbf{H}_{\text{min}})^{1/2} \quad (\mathbf{H}_{\text{max}} \text{ and } \mathbf{H}_{\text{min}} \text{ are the highest and lowest values of H})$$

The intercepts at $\xi = 0$ and $\xi = 1$ of η versus ξ plot yield $-\mathbf{r}_2 / \alpha$ and r_1 , respectively.

The FR and KT parameters evaluated to arrive at the co-monomer reactivity ratios are summarized in Table 5.1. The plots to calculate r_{M1} and r_{M2} by FR and KT methods are presented in Figure 5.7.

Table 5.1 FR and KT Parameters to Calculate Co-monomer Reactivity Ratio
(f =feed, F =polymer, $G = f(F-1) / F$, $H = f^2 / F$, $\eta = G / (\alpha + H)$, $\xi = H / (\alpha + H)$)

EGDMA- MMA ($\alpha = 1.2707$)					
f	F	G	H	η	ξ
9.0000	6.2500	7.5600	12.9600	0.5312	0.9107
4.0000	2.1740	2.1600	7.3597	0.2502	0.8527
2.3333	1.7439	0.9953	3.1219	0.2265	0.7107
1.5000	1.3699	0.4050	1.6424	0.1390	0.5637
0.6666	1.2146	0.1177	0.3658	0.0719	0.2235
0.4285	0.6681	-0.2128	0.2748	-0.1376	0.1778
0.2500	0.5015	-0.2485	0.1246	-0.1780	0.0892

EGDMA-β-CD-MMA ($\alpha = 1.9465$)					
f	F	G	H	η	ξ
9.0000	5.0000	7.2000	16.2000	0.3967	0.8927
4.0000	2.3998	2.3331	6.6672	0.2708	0.7743
2.3333	1.8406	1.0656	4.1737	0.1741	0.6819
1.5000	1.3044	0.3500	1.7249	0.0953	0.4698
0.2500	0.2368	-0.8057	0.2639	-0.3645	0.1193

EGIBMA-MMA ($\alpha = 1.002$)					
f	F	G	H	η	ξ
4.0000	7.8959	3.4934	2.0263	1.1535	0.6691
2.3333	3.7727	1.7148	1.4430	0.7013	0.5901
1.5000	1.1001	0.1364	2.0450	0.0447	0.6711
1.0000	1.0298	0.0289	0.9710	0.0146	0.4921
0.6666	0.8404	-0.1265	0.5287	-0.0826	0.3453
0.4285	0.3699	-0.7299	0.4963	-0.4871	0.3312

EGIBMA-β-CD-MMA ($\alpha = 0.9810$)					
f	F	G	H	η	ξ
0.1583	0.1317	-1.0436	0.1902	-0.8903	0.1622
0.5978	0.3237	-1.2489	1.1040	-0.5987	0.5292
1.4257	1.2588	0.2931	1.6147	0.1128	0.6218
3.2154	3.7993	2.3690	2.7212	0.6397	0.7348
5.3792	5.7077	4.4367	5.0696	0.7331	0.8377

EGMAVB-MMA ($\alpha = 0.1429$)					
f	F	G	H	η	ξ
0.1111	0.2875	-0.2753	0.0429	-1.4808	0.2309
0.2500	0.5150	-0.2354	0.1213	-0.8907	0.4589
0.6667	1.6450	0.2614	0.2700	0.6329	0.6538
1.0000	2.0998	0.5237	0.4762	0.8458	0.7690

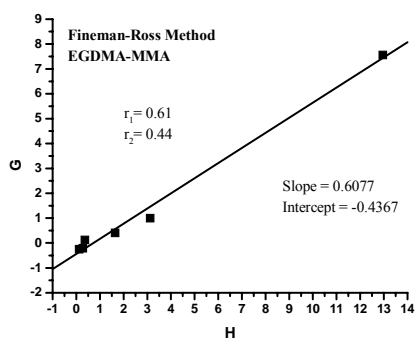
EGMAVB-β-CD-MMA ($\alpha = 0.5856$)					
f	F	G	H	η	ξ
0.1111	0.1124	-0.8772	0.1098	-1.2615	0.1579
0.2500	0.4499	-0.3056	0.1389	-0.4218	0.1917
0.4286	0.6225	-0.2599	0.2951	-0.2951	0.3350
1.0000	1.2675	0.2110	0.7889	0.1535	0.5739
1.5000	1.6278	0.5785	1.3822	0.2939	0.7024
4.0000	5.1236	3.2193	3.1228	0.8681	0.8420

TMPM - MMA ($\alpha = 0.4342$)					
f	F	G	H	η	ξ
0.1111	0.2900	-0.2720	0.0426	-0.5704	0.0893
0.2500	0.3064	-0.5659	0.2039	-0.8868	0.3195
0.4285	0.3862	-0.6810	0.4754	-0.7486	0.5226
0.6666	0.9741	-0.0177	0.4561	-0.0198	0.5122
1.0000	0.7977	-0.2536	1.2536	-0.1502	0.7427
1.5000	1.8071	0.6699	1.2450	0.3989	0.7414
4.0000	3.6142	2.8932	4.4269	0.5951	0.9106

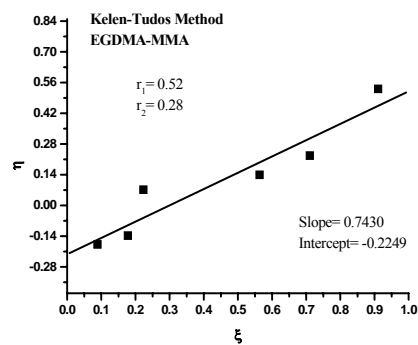
TMPTMA– MMA ($\alpha = 2.4162$)					
f	F	G	H	η	ξ
9.0000	6.1225	7.5300	13.2298	0.4812	0.8455
4.0000	2.6084	2.4664	6.1340	0.2884	0.7174
1.5000	1.4768	0.4842	1.5235	0.1229	0.3867
1.0000	0.6047	-0.6537	1.6537	-0.1606	0.4063
0.6666	0.5120	-0.6353	0.8678	-0.1934	0.2642
0.4285	0.3157	-0.9288	0.5816	-0.3098	0.1940
0.2500	0.1416	-1.5155	0.4413	-0.5303	0.1544

TMPIBMA-MMA ($\alpha = 1.2463$)					
f	F	G	H	η	ξ
4.0000	1.6232	1.5357	9.8570	0.1383	0.8877
1.5000	0.7898	-0.3992	2.8488	-0.0974	0.6956
1.0000	0.5219	-0.9160	1.9160	-0.2896	0.6058
0.6666	0.4166	-0.9334	1.0666	-0.4035	0.4611
0.4285	0.2548	-1.2532	0.7206	-0.6371	0.3663
0.1111	0.0783	-1.3078	0.1576	-0.9315	0.1122

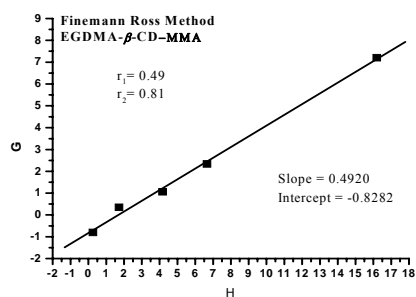
TMPTMA- β -CD-MMA ($\alpha = 1.0833$)					
f	F	G	H	η	ξ
0.1111	0.0796	-1.2846	0.1550	-1.0373	0.1251
0.2500	0.1082	-2.0605	0.5776	-1.2459	0.3477
0.4285	0.2216	-1.5051	0.8285	-0.7872	0.4336
0.6666	0.2566	-1.9312	1.7317	-0.6860	0.6151
1.0000	0.5483	-0.8238	1.8238	-0.2833	0.6273
4.0000	2.1132	2.1071	7.5714	0.2434	0.8748



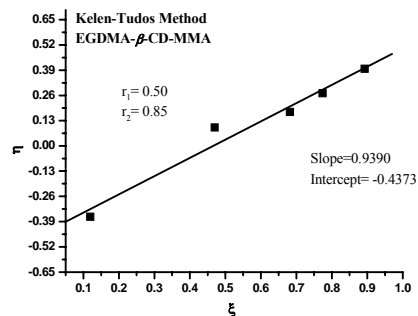
a



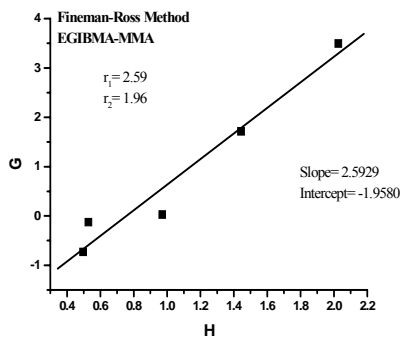
b



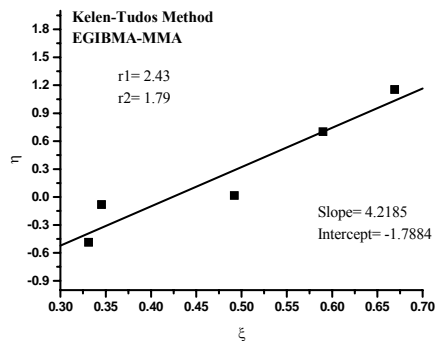
c



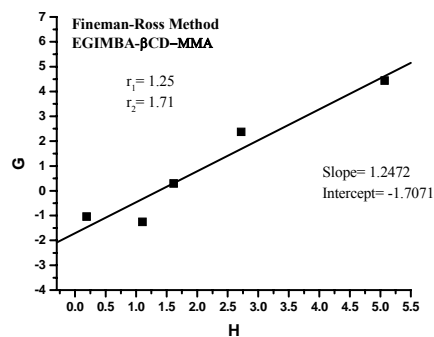
d



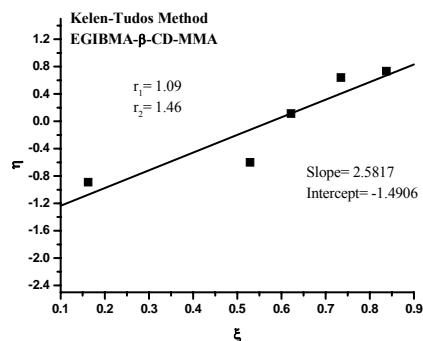
e



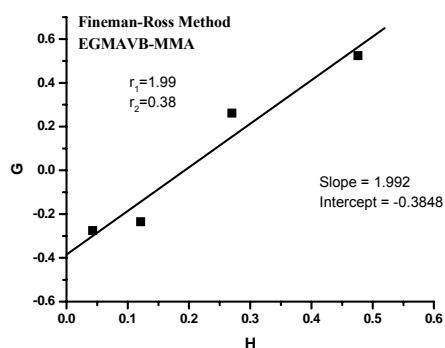
f



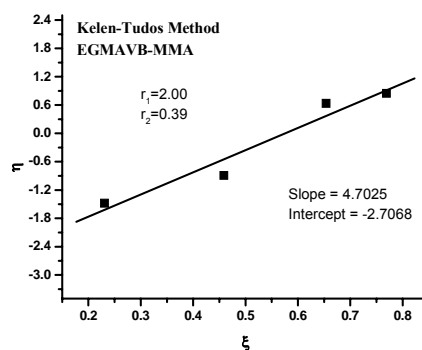
g



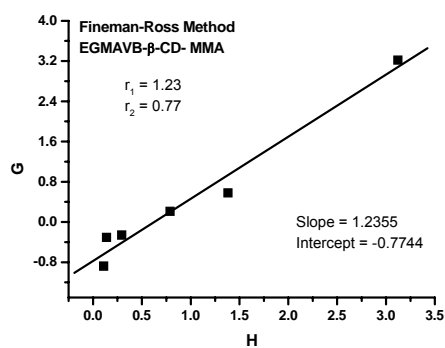
h



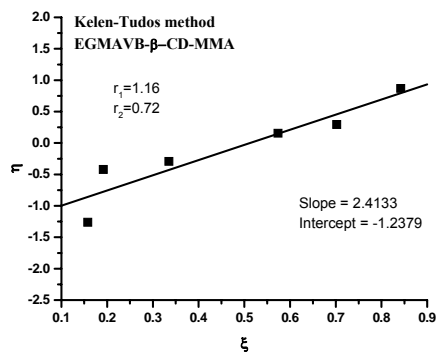
i



j



k



l

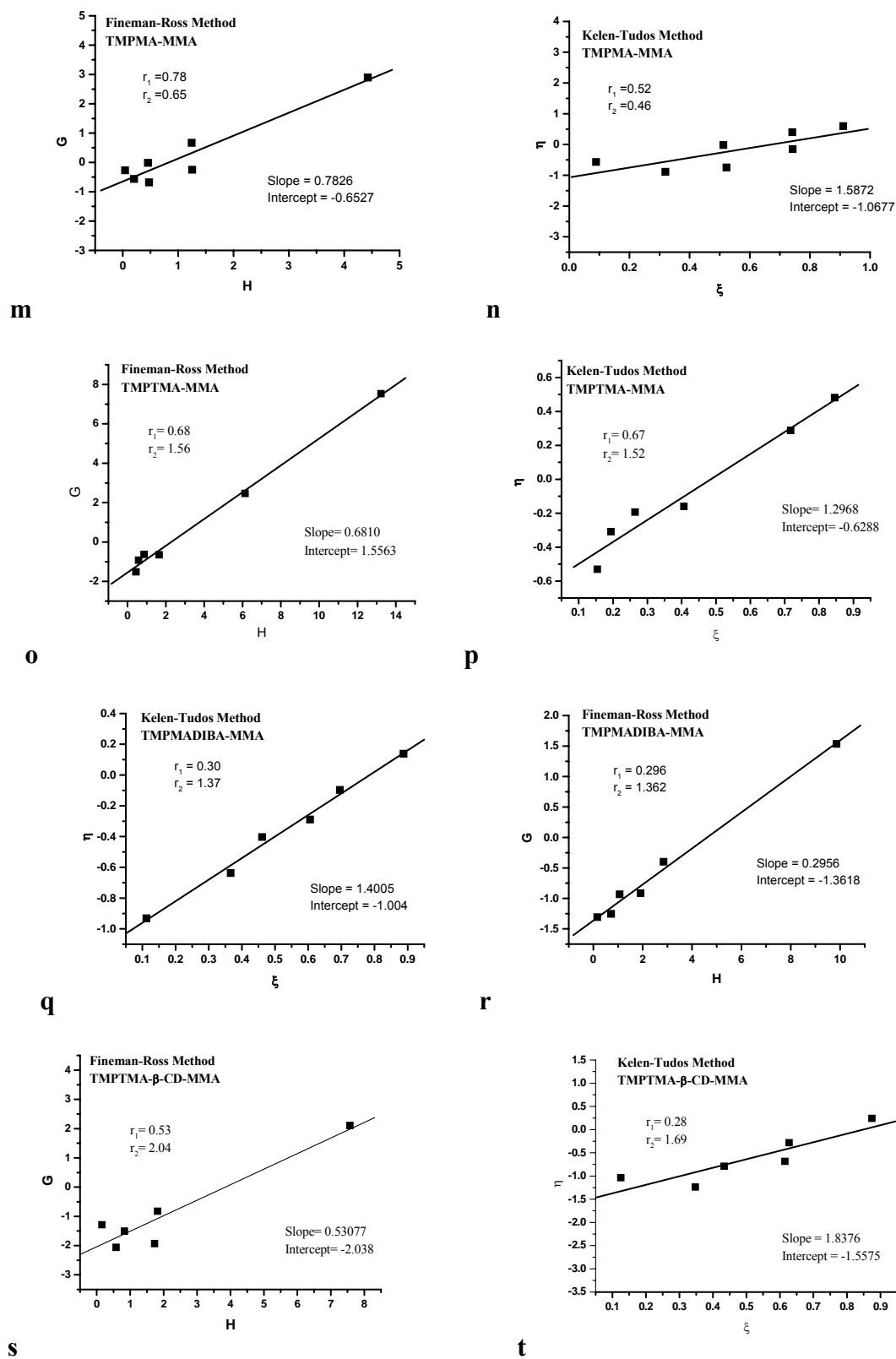


Figure 5.7: FR and KT plots to calculate co-monomer reactivity ratio

EGDMA and TMPTMA are the most commonly used multivinyl monomers to yield three-dimensional networks. During polymerization of these monomers the pendant vinyl unsaturations are formed when only one of the vinyl groups is reacted. The pendent vinyl groups are then reacted intermolecularly or intramolecularly or remain unreacted. In the IC mediated polymerization of di and trivinyl monomers the pendant vinyl groups included in CD cavity do not react with growing polymer radicals.

Table 5.2: Reactivity Ratios Evaluated by FR and KT Methods

Systems		FR	KT
EGDMA-MMA	EGDMA (r_1)	0.61	0.52
	MMA (r_2)	0.44	0.28
EGDMA- β -CD-MMA	EGDMA- β -CD (r_1)	0.49	0.50
	MMA (r_2)	0.83	0.85
EGIBMA-MMA	EGIBMA (r_1)	2.59	2.43
	MMA (r_2)	1.96	1.79
EGIBMA- β -CD-MMA	EGIBMA- β -CD (r_1)	1.25	1.09
	MMA (r_2)	1.71	1.46
EGMAVB-MMA	EGMAVB (r_1)	1.99	2.00
	MMA (r_2)	0.38	0.39
EGMAVB- β -CD-MMA	EGMAVB- β -CD (r_1)	1.23	1.16
	MMA (r_2)	0.77	0.72
TMPMA-MMA	TMPMA (r_1)	0.78	0.52
	MMA (r_2)	0.65	0.46
TMPTMA-MMA	TMPTMA (r_1)	0.68	0.67
	MMA (r_2)	1.56	1.52
TMPDIBMA-MMA	TMPMDIBA (r_1)	0.30	0.30
	MMA (r_2)	1.36	1.37
TMPTMA- β -CD-MMA	TMPTMA- β -CD (r_1)	0.53	0.28
	MMA (r_2)	2.04	1.69

In all the plots to calculate the monomer reactivity ratios the use of KT method, results in better distribution of the experimental points as compared to that by FR method. Our

analysis shows that in both cases *viz* FR and KT, the plots are linear which indicated that these polymerizations follow conventional copolymerization kinetics and the reactivity of polymer radical is determined only by the terminal monomer unit (Stergiou et al., 2003). The values of comonomer reactivity ratio in all the cases were reasonably close to each other, irrespective of the method used. Therefore in the following discussions only the values of KT method are used.

In the copolymerization of EGDMA–MMA, ($r_{\text{EGDMA}} = 0.52$, $r_{\text{MMA}} = 0.28$) the reactivity of EGDMA was approximately twice the reactivity of MMA. Mao et al., 1995 reported, the values of monomer reactivity ratios in the cross-linking copolymerization of MMA with EGDMA $r_{\text{EGDMA}} = 1.34$ and $r_{\text{MMA}} = 0.674$. In this case, the polymerization was carried out in bulk by γ irradiation and thus the high values of reactivity indicated the effect of solvent on co-monomer reactivity ratios (Bajaj et al., 2001). But the trend of reactivity remained same in both bulk as well as solution polymerization i.e. higher reactivity of EGDMA compared to that of MMA.

Formation of IC of EGDMA with β -CD reverses its reactivity during copolymerization with MMA ($r_{\text{EGDMA-}\beta\text{-CD}} = 0.50$, $r_{\text{MMA}} = 0.85$). As the methacrylate group included in CD cavity is now unavailable for polymerization, EGDMA should show the same reactivity as MMA. The results show decreased reactivity of EGDMA than MMA. This supported the hypothesis that the presence of CD associated with EGDMA during polymerization, results in a bulkier EGDMA and lowered its reactivity as compared to that of small MMA radical.

In order to compare the results of co-monomer reactivity ratio of EGDMA in presence and absence of β -CD and the effect of structure on monomer reactivity ratio, monomer EGIBMA structurally similar to EGDMA was synthesized. The results of comonomer reactivity ratio showed higher reactivity for EGIBMA than MMA during copolymerization ($r_{\text{EGIBMA}} = 2.43$, $r_{\text{MMA}} = 1.79$). High reactivity of EGIBMA was attributed to the presence of more electron releasing isobutyrate group. In contrast, the methacrylate group is less electron releasing or rather is electron withdrawing when present on EGDMA (Mathew-Krotz et al., 1997). The reactivity of EGIBMA was lowered when the IC with β -CD was formed. ($r_{\text{EGIBMA-}\beta\text{-CD}} = 1.09$, $r_{\text{MMA}} = 1.46$) which supported the increase in steric hindrance due to presence of β -CD.

Similar results were obtained in the copolymerization of EGMAVB with MMA in the presence and absence of IC. In absence of β -CD, double bonds in both methacrylate and styrene moieties in EGMAVB reacted. This was evident from the higher reactivity of EGMAVB compared to MMA in absence of IC ($r_{\text{EGMAVB}} = 2.00$, $r_{\text{MMA}} = 0.39$). After selective inclusion of methacrylate group in β -CD cavity, only styrenic double bonds in EGMAVB reacted during copolymerization. This resulted in decrease in its reactivity from 2.00 to 1.16.

TMPTMA, a trivinyl monomer, showed lower reactivity than MMA in absence of IC ($r_{\text{TMPTMA}} = 0.67$, $r_{\text{MMA}} = 1.52$). According to the classical gelation theory the cross-linked polymers from multivinyl monomers are formed in three steps. Initially only the linear macromolecules (primary molecules) with pendant functional groups are formed. With increasing conversion, branching occurs until finally cross-linking takes place (Flory 1953 and Stockmayer 1944). As the TMPTMA is bulky molecule as compared to MMA or EGDMA initially only the linear macromolecules (primary molecules) containing pendant functional groups are formed and more radicals of MMA will add to growing polymer chain. Thus the copolymer containing high incorporation of MMA would be obtained. But in both the cases i.e. EGDMA-MMA or TMPTMA-MMA the cross-linked products will be obtained on increasing conversion. Still the reactivity of TMPTMA obtained in absence of IC was higher compared to the monomer included into the CD cavity as discussed below.

The reactivity of TMPTMA was lowered in the presence of β -CD ($r_{\text{TMPTMA-}\beta\text{-CD}} = 0.28$, $r_{\text{MMA}} = 1.69$). TMPTMA formed 1:2 IC with CD. As a result, the two vinyl unsaturations included in the cavity did not react with the polymer radical. Also the presence of two more CD molecules on TMPTMA decreased its reactivity further from 0.67 to 0.28 due to increased steric hindrance.

To study the effect of structure on the co-monomer reactivity of TMPTMA included into β -CD cavity, structurally similar monomer TMPDIBMA was synthesized and co-monomer reactivity ratio ($r_{\text{TMPDIBMA}} = 0.30$, $r_{\text{MMA}} = 1.37$) was evaluated. Thus the comparable reactivity of TMPTMA- β -CD and TMPDIBMA supported the monovinyl behavior of TMPTMA after its inclusion in β -CD cavity.

To study the effect of steric hindrance on co-monomer reactivity ratio of TMPTMA, less bulky monovinyl monomer, TMPMA was synthesized and its comonomer reactivity ratio was evaluated ($r_{\text{TMPMA}} = 0.52$, $r_{\text{MMA}} = 0.46$). The results showed that the reactivity of TMPMA and MMA was comparable. Thus the introduction of isobutyl acrylate groups or the complexed methacrylate groups lowered its reactivity during copolymerization from 0.52 to 0.30 or 0.28 respectively. Higher value of TMPTMA ($r_{\text{TMPTMA}} 0.67$) in absence of inclusion complex indicated the participation of more than one vinyl groups during polymerization.

Thus, in all the above systems the incorporation of MMA units in copolymer increased with increase in the bulkiness of co-monomers. Also, the reactivity of monomers comprising multiple unsaturations altered after formation of IC with β -CD and the copolymers with unreacted pendant vinyl unsaturation were obtained.

5.3.4 Second Stage Polymerization

5.3.4.1 Intramolecular Cross-linking

Effect of Type and % of Multivinyl Monomer

Table 5.3: Copolymers with Varying Multivinyl monomer

Polymer	% of crosslinker	Particle size (nm)	
		Before	After X-link in 0.88 mg/mL
Poly (EGDMA-co-MMA)	31.64	47.2	105.3
Poly (EGDMA-co-MMA)	27.88	143.2	99.9
Poly (EGDMA-co-MMA)	24.61	187.5	62.9
Poly (TMPTMA-co-MMA)	29.00	42.0	65.7
Poly (TMPTMA-co-MMA)	9.10	124.2	91.6
Poly (TMPTMA-co-MMA)	7.55	129.4	115.9
Poly (TMPTMA-co-MMA)	3.00	398.2	108.7

The particle size data for the nanoparticles obtained from the copolymers varying in multivinyl monomer content is summarized in Table 5.3. Poly (EGDMA-co-MMA)

containing 32 % of EGDMA has particle size of 47 nm that increased to 105 nm on cross-linking. Similarly, poly (TMPTMA-*co*-MMA) comprising 29 % of TMPTMA, showed increase in particles size from 42 to 66 nm. This indicated the presence of intermolecular cross-linking reactions along with intramolecular cross-linking during synthesis. In contrast as the percentage of multivinyl monomer in the precursor copolymer decreased, the intramolecular cross-linking reactions predominated over the intermolecular cross-linking reactions. This was evident from the decrease in particle size of poly (EGDMA-*co*-MMA) from 187 nm to 63 nm and for poly (TMPTMA-*co*-MMA) from 398 nm to 108 nm after its intramolecular cross-linking.

Effect of Molecular Weight and Cross-linker Concentration

The particle size data for poly (EGDMA-*co*-MMA) prepared by varying molecular weight is summarized in Table 5.4.

Table 5.4: Copolymers with Varying Molecular Weights

Molecular weight (Mn)	Particle size (nm)		
	Before	X-link in 0.88 mg/mL	X-link in 0.22mg/mL
36354	85.5	119.2	34.8
11397	35.2	156.5	21.6
9753	21.0	103.2	36.9
7784	18.9	80.4	59.2

*Poly (EGDMA-*co*-MMA) (60:40 in feed) prepared using mercaptoethanol*

The particle size of the precursor polymer decreased from 85 to 20 nm with decrease in molecular weight of the precursor polymer from 36354 to 7784. The cross-linking of the pendant vinyl groups at polymer concentration 0.88 mg/mL concentration of polymer showed increase in particle size of the nanoparticles, whereas decrease in polymer concentration from 0.88 mg/mL to 0.22 mg/mL resulted in decrease in particle size but displayed the absence of any trend in particle size of nanoparticles. Thus the competition between intra and intermolecular cross-linking reactions during nanoparticles synthesis defines the particle size of the resulting nanoparticles. The

molecular weight of the precursor copolymer, the percentage of cross-linker and the cross-linking concentration are the external controls on the particle size of the nanoparticles.

5.4 Conclusions

This chapter described the extension of the methodology described in the previous chapter to obtain the latent cross-linkable soluble copolymers from the multivinyl monomers. The inclusion complex mediated copolymerization of multivinyl monomers follows the conventional copolymerization kinetics and the reactivity of polymer radical is determined only by the terminal monomer unit. This methodology can be easily extended to synthesize a wide range of copolymers comprising the reactive functionality and latent cross-linkable groups. The functional copolymers thus synthesized will find potential applications in coating, biosensors, microlithography, processable molecular imprinting and optical waveguides etc.

Chapter 6

**Molecularly Imprinted Nanoparticles for
Drug Delivery**

6.1 Introduction

Imprinted micro / nanoparticles are being extensively investigated in view of their applications in drug delivery systems, chromatographic separations, biomimetic sensors and catalysis (Norrel et al., 1998, Ciardelli et al., 2004, Cunliffe et al., 2005, Haupt and Mosbach 2000, Li et al., 2005, 2006). In most of these applications diffusion of the bioactive molecules, reactants / products plays critical role. Imprinting is expected to lead to enhanced interactions with the polymer support and influence product performance (Cunliffe et al., 2005).

Conventional non-covalent imprinting involves the formation of a self-assembled system comprising functional monomers and cross-linkers around the template molecule and cross-linking the same in the presence of porogens by thermal initiation or UV irradiation. The cross-linked polymers after extraction of the template exhibit enhanced rebinding capacity and selectivity for the template molecule. However, the processability of these materials is limited. This can be overcome by synthesizing soluble copolymers comprising both recognition and latent cross-link functionalities. New synthetic methodologies are being explored to design such polymers (Southard et al., 2007, Tunc et al., 2006, and Li et al., 2005). Li et al., (2005, 2006) reported the synthesis of functional copolymers containing carboxyl or amine functional groups by atom transfer radical polymerization of t-butyl methacrylate and 2-hydroxyethyl methacrylate and functionalization of the copolymer in the subsequent step. The resulting copolymers were then reacted with methacryloyl chloride to yield polymers containing a double bond. These random or block polymers could be cross-linked in concentrated solution or in a solvent selective to specific block in presence of template to yield imprinted polymer matrix or nanospheres. Clearly, there is a need to devise a simpler methodology for the synthesis of such polymers for molecular imprinting.

This chapter demonstrates how inclusion complex (IC) mediated selective polymerization of multivinyl monomers can be coupled with molecular imprinting and intramolecular cross-linking for sustained drug delivery. This involves the synthesis of functional copolymers *viz* poly (EGDMA-*co*-MAA) and poly (TMPTMA-*co*-MAA) comprising both the recognition as well as cross-linkable functionalities. The pendant vinyl groups of these copolymers are then cross-linked below critical overlap

concentration in presence of theophylline (THP) to yield nanoparticles. The resulting THP imprinted nanoparticles exhibited enhanced rebinding capacity and selectivity over caffeine (CAF). The imprinting lowered the effective diffusivity of THP and thus resulted in its sustained release from nanoparticles.

6.2 Experimental

6.2.1 Materials

EGDMA- β -CD and TMPTMA- β -CD ICs were prepared as described in chapter 3. The functional copolymers poly (EGDMA-*co*-MAA) and poly (TMPTMA-*co*-MAA) were synthesized as described in chapter 4. Theophylline (THP) and caffeine (CAF) were purchased from Aldrich and Merck respectively. Potassium dihydrogen phosphate (KH₂PO₄) and sodium hydroxide (NaOH) were purchased from Merck chemicals.

6.2.2 Measurements

Fourier Transform Infrared Spectroscopy (FTIR)

FT-IR spectra were recorded on Perkin-Elmer Spectrum One in diffuse reflectance spectrum mode (DRS). The spectra were recorded at frequencies from 4000 - 450 cm⁻¹ and resolution of 4 cm⁻¹.

Intrinsic Viscosity of Polymers

The intrinsic viscosity of polymer solutions in DMF was measured at 30 °C using Ubbelohde capillary viscometer.

Dynamic Light Scattering (DLS)

The particle size was measured by DLS on Malvern model 4700 at 25 °C in DMF with the laser operating at 488 nm (DMF viscosity 0.80 centipoise and refractive index 1.427). The scattered light intensity was measured at an angle of 90°.

UV-vis Spectrophotometer

UV-vis absorption spectra were recorded on Shimadzu UV-Visible spectrophotometer UV-1601PC model.

6.2.3 Functional Copolymers: Synthesis

A series of functional soluble copolymers were synthesized by free radical solution polymerization of IC, EGDMA- β -CD (1:1) or TMPTMA- β -CD (1:2) with MAA in DMF using AIBN as an initiator (Table 6.1).

Poly (EGDMA-*co*-MAA) (50:50)

25 g (1.875×10^{-2} mol) of EGDMA- β -CD (1:1) IC, 1.61 g MAA (1.875×10^{-2} mol), and 300 mg (1.875×10^{-3} mol, 5 mole % of total monomers) AIBN were dissolved in 175 mL of DMF and nitrogen was purged for 20 min. Polymerization was carried out for 16 h at 65°C. The polymer was precipitated in 0.1 N HCl. The precipitated polymer was filtered, washed with water to remove de-complexed β -CD. The crude polymer was dissolved in DMF and re-precipitated in diethyl ether. The polymer was filtered and dried at room temperature.

Similarly, the copolymers of EGDMA- β -CD and TMPTMA- β -CD of varying compositions were prepared by varying feed ratios of MAA and ICs. (Table 6.1)

¹H NMR (400 MHz, DMSO *d*₆)

Poly (EGDMA-*co*-MAA) (50:50) δ : 0.80-1.40 (6H, backbone CH₃), 1.87 (3H, terminal CH₃), 2.41 (4H, backbone CH₂), 4.33 (4H, -OCH₂CH₂O-), 5.53 (1H, CH_aH_b=C), 6.05 (1H, CH_aH_b=C), 12.3 (1H, COOH).

FT-IR (KBr, cm⁻¹) 1635 (C=C), 1728 (C=O), 3550 (-COOH).

Poly (TMPTMA-*co*-MAA) (30:70) δ : 0.80-1.59 (3H, CH₂-CH₃, 2H, CH₂-CH₃, 6H, CH₂-CCH₃ on polymer backbone), 1.70 (4H, CH₂-CCH₃, backbone), 1.94 (6H, CH₂=CCH₃), 4.16 (4H, OCH₂ adjacent to unreacted vinyl unsaturations), 4.34 (2H, -OCH₂ adjacent to polymer backbone), 5.58 (2H, CH_aH_b=CH), 6.10 (2H, CH_aH_b=CH) 12.4 (1H, -COOH).

FT-IR (KBr, cm⁻¹): 1648 (C=C), 1734 (C=O), 3556 (-COOH).

6.2.4 Functional Copolymers: THP Interaction Study (UV and FTIR)

UV-vis spectrophotometric analysis was performed to estimate the association constant of carboxyl groups as a part of copolymer and monomer with THP. A solution of THP (0.0275 mmol) in DMF was titrated with the carboxyl concentration in the range 0.24 to 4.0 mmol in poly (EGDMA-*co*-MAA) (50:50) and poly (TMPTMA-*co*-MAA) (30:70) as well as in the mixture of EGDMA and MAA (50:50) and TMPTMA and MAA (30:70). The change in absorbance (ΔA) of these solutions at 288 nm was determined. To confirm the presence of interactions between the carboxyl group of the functional copolymer and THP at the concentrations used for intramolecular cross-linking,

solution of THP in DMF (3.468×10^{-5} mol) was titrated with carboxyl group at concentration in the range 1.734×10^{-5} to 1.387×10^{-4} mol in the polymer. Thus the molar ratio between THP and carboxyl group of polymer was in the range 1:0.5 to 1:4). The change in absorption (ΔA) of these solutions at 275 nm was determined using THP as reference.

THP and functional copolymer were mixed together in DMF in molar ratio 1:1 to 1:4. The samples were characterized by FTIR in DRS mode after complete evaporation of DMF. The reference KBr was also mixed with the DMF and dried.

6.2.5 THP Imprinted Nanoparticles: Synthesis

Functional copolymers were first characterized for intrinsic viscosity $[\eta]$ in DMF to estimate critical overlap concentration ($C^* = 1/[\eta]$) (Table 6.1). The intramolecular cross-linking of latent cross-linkable functional copolymer was carried out in DMF at concentration $C^*/160$.

For the synthesis of THP-imprinted nanoparticles, 100 mg of functional copolymer $[\eta] = 0.19$ dl/g, containing 3.29×10^{-4} mol of acid, 59.3 mg THP (3.29×10^{-4} mol) and 40 mg (2.44×10^{-4} mol) AIBN were dissolved in 50 mL of DMF. THP bound copolymer solution was then added to DMF and stirred at 520 rpm at 65°C for 16 h in a jacketed reactor. After cooling to room temperature, the solution was concentrated to 5 mL and precipitated in water. The precipitated nanoparticles were filtered and dried at room temperature. THP was extracted from these nanoparticles by Soxhlet extraction in acetonitrile to obtain THP-imprinted nanoparticles (MIP). The non-imprinted (NIP) nanoparticles were prepared in the absence of THP.

FT-IR (KBr, cm^{-1}): Poly (EGDMA-*co*-MAA) nanoparticles, 1725 (C=O), 3521 (-COOH).

The imprinted nanoparticles comprising poly (EGDMA-*co*-MAA) (50:50), poly (EGDMA-*co*-MAA) (70:30) and poly (TMPTMA-*co*-MAA) (30:70) were prepared similarly by varying THP to carboxyl ratio from 1:2 to 1:4 to study the effect on the rebinding and release profile of THP.

6.2.6 THP Imprinted Nanoparticles: Rebinding

Rebinding on imprinted as well as non-imprinted nanoparticles was investigated in heterogeneous batch experiments using 7.32×10^{-5} mol THP in acetonitrile. THP

concentration in these solutions before and after rebinding experiments was estimated by UV-vis spectroscopy. A standard calibration equation for THP was established by measuring the intensity of the absorbance peak at 272 nm for concentrations in the range 1×10^{-4} to 8.67×10^{-6} mol.

In a typical experiment, the nanoparticles were repeatedly washed with acetonitrile and analyzed by UV-vis spectroscopy for the complete removal of residual THP as well as any UV active impurity. THP solution in acetonitrile was then added to these nanoparticles. After incubation time of 24 h the solution was centrifuged on Thermo Multi (RF) centrifuge machine. THP concentration in supernatant solution was estimated by UV-vis spectroscopy. The rebinding capacity of the imprinted and non-imprinted nanoparticles was calculated by comparing the THP concentration before and after absorption. Similarly, the rebinding experiments at varying THP concentration (8.429×10^{-5} to 2.53×10^{-6} mol) were carried to construct the binding isotherm.

6.2.7 THP Imprinted Nanoparticles: Selectivity

The selectivity of nanoparticles was evaluated by heterogeneous binding studies using 1.0×10^{-4} mol solution of CAF in acetonitrile. The standard calibration equation for CAF was established by monitoring absorbance at 274 nm for concentrations in the range 1.25×10^{-4} to 2.23×10^{-5} mol.

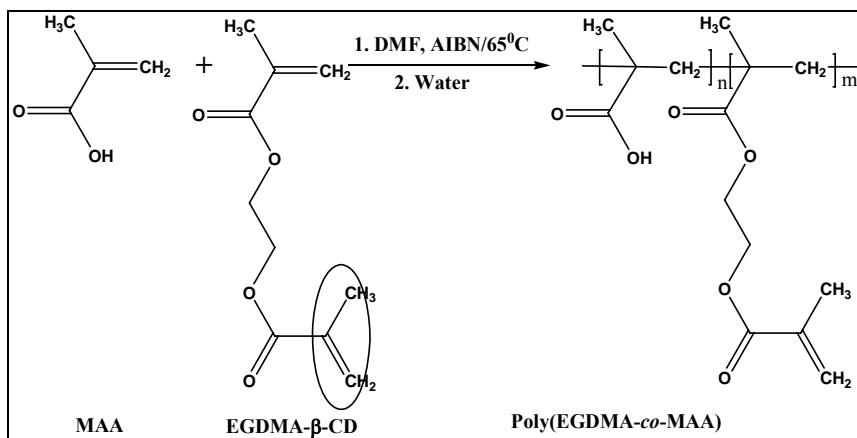
6.2.8 THP Imprinted Nanoparticles: Release

THP-imprinted and non-imprinted nanoparticles loaded with THP during rebinding experiments were dried and used for release study. In a typical experiment, 2 mg nanoparticles were suspended in a 1.5 mL phosphate buffer solution of pH 6.8 in a micro-centrifuge tube at 37 °C. After predetermined time intervals, 0.5 mL solution was withdrawn and replaced with 0.5 mL buffer. The samples withdrawn were analyzed for THP content by UV-vis spectrophotometer. The absorbance of control nanoparticles was subtracted from the absorbance obtained from the solution of THP-loaded nanoparticles to calculate the concentration of drug released. This procedure was repeated upto maximum release of drug from the nanoparticles.

6.3 Results and Discussion

6.3.1 Functional Copolymers: Synthesis

The procedure for copolymerization of IC with functional monomer is outlined in Scheme 1. The soluble copolymers containing multivinyl monomers, EGDMA or TMPTMA and MAA were synthesized using IC mediated selective polymerization methodology described in chapter 5 (Table 6.1).



Scheme 6.1: Synthesis of poly (EGDMA-co-MAA)

Table 6.1 Functional Co-polymers: Properties

Polymer	Composition ^a	Intrinsic viscosity (dL/g) ^b
Poly (EGDMA-co-MAA)	10.52: 89.48	0.2724
	30.93: 69.07	0.1005
	52.33: 47.67	0.1875
	66.00: 34.00	0.0956
	88.34: 11.66	0.2052
Poly (TMPTMA-co-MAA)	15.42: 84.58	0.1032
	35.19: 64.81	0.1245
	63.14: 36.86	0.2200

^aMolar ratio in polymer determined by acid value measurements in DMF,

^bMeasured in DMF at 30 °C using Ubbelohde capillary viscometer.

The effectiveness of molecular imprinting depends on the extent of interactions between the template molecule and functional monomers prior to cross-linking (Tunc et al., 2006). In this study MAA was used as functional monomer since the acid functionality serves as both hydrogen donor and acceptor and forms hydrogen bonds with a variety of polar functionalities such as carboxylic acids, hetero atoms, amides and carboxylic esters of the template molecule (Sellergren 2001, Tunc et al., 2006). THP was used as a template as it is rigid; possesses hydrogen donor and acceptor sites and forms cyclic hydrogen bond with the carboxyl group of MAA (Tunc et al., 2006, Li et al., 2005).

The compositional analysis of all copolymers produced, closely matched the monomer feed ratio (Table 6.1). The functional copolymers lower in multivinyl monomer content are soluble in MeOH and polymers higher in multivinyl monomer content are soluble in THF. This indicates that no cross-linking occurred during polymerization (Li et al., 2005).

6.3.2 Functional Copolymer: THP Interaction Study

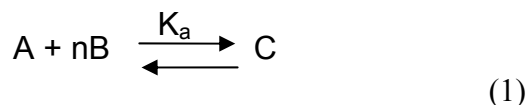
The enhanced binding capacity and selectivity of molecularly imprinted polymers depends on the strength of interactions as well as the disposition of the functional groups and template molecules during imprinting process (Li et al 2005, Tunc et al., 2006). In this study THP was selected as a template since the non-covalent binding between THP and MAA results from hydrogen bonding interactions between C=O of THP and MAA which act as hydrogen bond acceptors, while -OH of MAA and -NH of THP act as hydrogen bond donors (Vlatkis, 1993, Tunc et al., 2006). Chloroform is commonly used as solvent to study the interactions since it does not compete in hydrogen bonding (Norell et al., 1998; Li et al 2005; Tunc et al., 2006). But in the present study the imprinted nanoparticles were synthesized in DMF. It is therefore important to study the interactions between THP and the functional groups of the copolymer in DMF.

UV Analysis

The UV-*vis* spectrophotometric analysis revealed the shift in absorption maximum of THP (0.0275 mmol) in DMF in the presence of co-polymer and monomer in the range 0.24 to 4.0 mmol carboxylic groups. This demonstrated the presence of hydrogen bonding interactions in these systems (Tunc et al., 2006, Jie and Xiwen 1999). The

change in absorbance (ΔA) of THP at 288 nm with the addition of carboxyl groups was monitored to calculate the association constants (K_a) (Figure 6.1 Table 6.2).

Generally the formation of the complex C between template A and functional monomer B can be expressed by the following reaction:



Where $n = 1, 2, 3, \dots$ is the composition of the complex, and K_a refers to the association constant. If a_0 is a template concentration, c is complex concentration, and if the equilibrium concentration of B is approximated as b_0 , if further $b_0 \gg a_0$, K_a can be written as:

$$K_a = c / b_0 (a_0 - c) \quad (2)$$

After rearranging the equation (2), the concentration of complex, c can be calculated according to:

$$\begin{aligned} c &= a_0 b_0 K_a / 1 + b_0 K_a \\ c &= \Delta A / \Delta \epsilon l \end{aligned}$$

Where $\Delta A = A - A_0$ i.e. the absorbance difference. $\Delta \epsilon = \epsilon_C - \epsilon_A$ i.e. the difference between the molar absorptivities of A.

$$\begin{aligned} \Delta A / \Delta \epsilon l &= a_0 b_0 K_a / 1 + b_0 K_a \\ \Delta \epsilon l / \Delta A &= 1/a_0 b_0 K_a + 1/a_0 \\ 1 / \Delta A &= 1/a_0 b_0 K_a \Delta \epsilon l + 1/\Delta \epsilon l a_0 \end{aligned}$$

The plot of $1 / \Delta A$ versus $1/b_0$ was plotted to calculate the association constant.

Association constant $K_a = \text{Intercept} / \text{Slope}$.

Table 6.2. Association Constants

-COOH of polymer / monomer	K_a (Mol⁻¹)
Poly (EGDMA-co-MAA) (50:50)	4.94×10^2
(EGDMA+MAA) (50:50)	1.44×10^2
Poly (TMPTMA-co-MAA) (30:70)	4.25×10^2
(TMPTMA+MAA) (30:70)	2.89×10^2

The higher values of K_a for the copolymers confirmed enhanced association between THP and carboxyl group when the latter exists as a part of the polymer rather than as a free monomer. This is a result of the contributions from other interactions such as cooperative bonding and hydrophobic interactions between the functional copolymer and THP, which are stronger than hydrogen bonding alone. These result in higher selectivity over caffeine (CAF) as shown later.

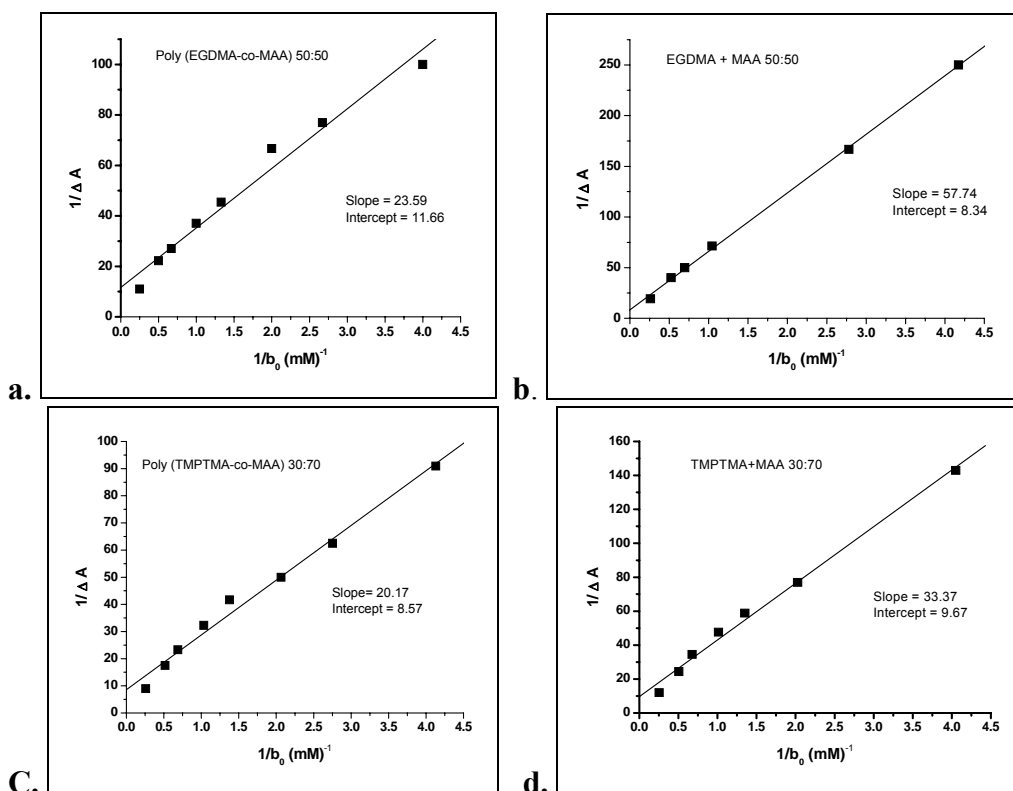


Figure 6.1: Plot of $1/\Delta A$ versus $1/b_0$ at 288 nm. a. poly (EGDMA-co-MAA) (50:50), b. (EGDMA+MAA) (50:50), c. poly (TMPTMA-co-MAA) (30:70), d. (TMPTMA+MAA) (30+70)

The polymer concentration used in the experiments above is greater than the critical overlap concentration. Also the functional group concentration was 8 to 150 folds higher than the template concentration. Since the nanoparticles were synthesized by cross-linking of the template bound polymer chains at concentrations 160 folds lower than the critical overlap concentration, and the functional group concentration was only

up to four folds higher than the template concentration, it was necessary to confirm that the interactions between the template and the functional monomer persisted under these conditions as well. To confirm this, the interactions between THP and carboxyl group of the copolymer in DMF were investigated at concentrations 16 times lower than the concentration used for intramolecular cross-linking. Even at these concentrations the absorbance of THP increased as the THP to carboxyl ratio was increased from 1:0.5 to 1:4 (Figure 6.2). This indicated that the interactions between THP and carboxyl group of polymer, persisted under conditions of nanoparticles synthesis.

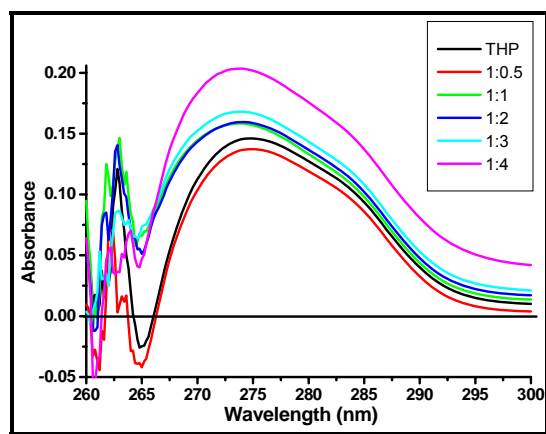


Figure 6.2: Spectral shifts due to interactions between THP and functional copolymer

FTIR Analysis

Table 6.3: FTIR of THP, Polymer and Their Stoichiometric Mixtures^a

Compound	N-H (THP)	C=O (THP)	C=N (THP)	C=O (Polymer, THP)
THP	3121.8	1678	1567	1714
Polymer	-	-	-	1728
1:1	3122.6	1672 (+6)	1566 (+1)	1718 (-4, +10)
1:2	3122.4	1670 (+8)	1562 (+5)	1720 (-6, +8)
1:3	3123.1 (very weak)	1668 (+10)	1557 (+10)	1723 (-9, +5)
1:4	3123.8 (very, very weak)	1667 (+11)	1556 (+11)	1725 (-11, +3)

^a(Difference in cm^{-1})

Infrared spectroscopy reflects the structure of the pre-organized complex comprising the template and functional monomers. When N-H, C=N, O-H, and C=O groups form hydrogen bonds with other hydrogen donors or acceptors, these bonds are weakened, and accordingly the stretching vibration bands shift. In the infrared spectra, all these bands are clearly distinguishable from other signals, and are useful probes to establish hydrogen-bonding interactions.

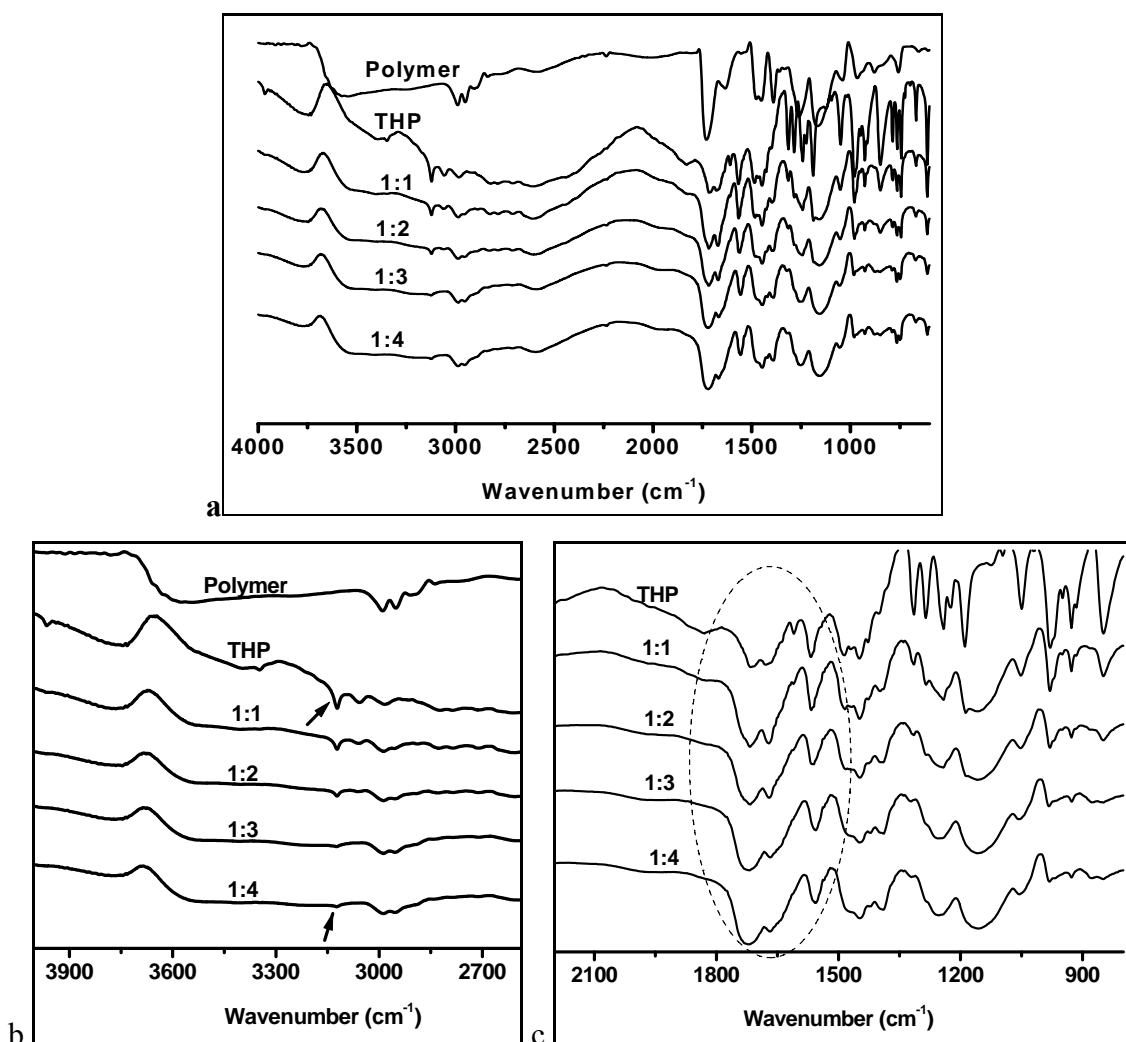


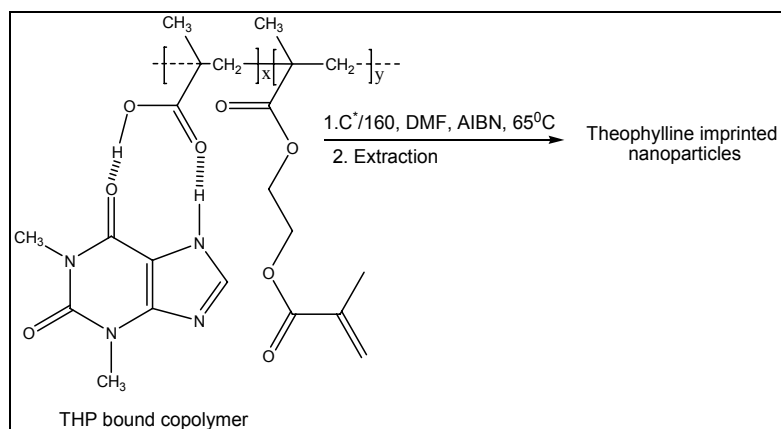
Figure 6.3: a. FTIR spectra of poly (EGDMA-*co*-MAA) (50:50), THP and different molar ratios of THP to -COOH of polymer, 1:1, 1:2, 1:3 and 1:4 b. spectra in N-H region c. spectra in C=O and C=N region

The FTIR spectrum of THP displayed peaks at 3122, 1714, 1678 and 1567 cm⁻¹, which were assigned to N-H stretching vibration, and vibrations of non-conjugated and

conjugated C=O group respectively and the imine group C=N in THP (I. M. Johnson et al 2003, Lin et al 1995). The FTIR spectrum of poly (EGDMA-co-MAA) (50:50) displayed peaks at 1728 and 1633 cm^{-1} for the stretching vibration of C=O and C=C respectively (Figure 6.3a). To study the interactions between functional groups of THP and carboxyl groups of the copolymer, both were mixed in stoichiometric ratios 1:1 to 1:4 in DMF. DMF was evaporated before FTIR analysis. The peak assignments and the shift in peak positions of THP, polymer and their mixture are summarized in Table 6.3. The peak at 3122 cm^{-1} assigned to the N-H stretching vibration of THP decreased in intensity with increasing carboxyl content and eventually disappeared indicating the participation of N-H in hydrogen bonding with the C=O group of the copolymer (Figure 6.3b) (Li et al 2006). The peak at 1678 cm^{-1} assigned to the conjugated C=O stretching vibration of THP decreased in intensity and also shifted to 1672 cm^{-1} , 1667 cm^{-1} and 1657 cm^{-1} for the THP: COOH ratio 1:1, 1:2 and 1:4. The peak at 1567 cm^{-1} assigned to the stretching vibration of C=N shifted to 1566 cm^{-1} and 1556 cm^{-1} for the THP: COOH ratio 1:1 and 1:4. This indicated only limited participation of imine group in interactions with the carboxyl group in the former case (shift 1 cm^{-1}) and enhanced participation in the later case (shift 11 cm^{-1}) (Figure 6.3c). This shift in peak positions of THP with increase in molar ratio indicated continuous increase in interactions between THP and the copolymer. Initially N-H and C=O groups in THP participated in the interaction. As the THP: COOH ratio increased, imine group also participated in the interactions. The interactions in the carbonyl region of the copolymer are described in the section 6.3.4.2. Thus both the UV and FTIR analyses showed complex formation between the functional groups of THP and the copolymer due to hydrogen bonding and also an increase in the degree of interactions with increase in molar ratio of functional copolymer.

6.3.3 THP Imprinted Nanoparticles: Synthesis

The functional copolymer and THP formed a non-covalent complex by hydrogen bonding as shown earlier. THP-imprinted nanoparticles were prepared by intramolecular cross-linking of pendant double bonds of THP bound functional copolymer in dilute solution (Scheme 6.2).



Scheme 6.2: Synthesis of THP imprinted nanoparticles

The nanoparticles were characterized by FTIR spectroscopy to confirm the extent of cross-linking reaction and by dynamic light scattering particle size measurements. The FTIR spectrum of the imprinted nanoparticles prior to THP extraction showed the presence of un-reacted double bonds even after cross-linking, especially in the nanoparticles prepared from the precursor polymer containing higher percentage of cross-linker. The FTIR spectrum of the nanoparticles after extraction of THP displayed complete absence of double bonds (Figure 6.4A) (Li et al., 2005, 2006). The FTIR spectrum of extracted nanoparticles displayed a peak at 3534 cm^{-1} which shifted to 3221 cm^{-1} after rebinding (Figure 6.4B). This indicates the presence of free carboxyl groups in imprinted nanoparticles, which interact with THP through hydrogen bonding during rebinding (Dong et al., 2005, Kobayashi et al., 1998).

The particle size of nanoparticles varied between 36 to 178 nm depending on the comonomer composition and the extent of cross-linking. The size of the imprinted nanoparticles after extraction was greater than that before extraction as well as the non-imprinted nanoparticles. This could be attributed to the presence of small amount of un-reacted pendant double bonds in the nanoparticles (Figure 6.4Aa), which undergo intermolecular cross-linking during the extraction of THP as confirmed by FTIR analysis (Figure 6.4Ab) Irrespective of inter and intramolecular reactions occurring during various stages of synthesis of nanoparticles, the particle size obtained was smaller than that obtained by precipitation polymerization (200 nm to $1\mu\text{m}$) (Ciardelli et al., 2004, Puoci et al., 2004

Table 6.4: Poly (EGDMA-*co*-MAA) and poly (TMPTMA-*co*-MAA) Nanoparticles

Comonomer composition	Precursor polymer (nm)	Imprinted Nanoparticles (after extraction) (nm)	Non-imprinted nanoparticles (nm)
EGDMA: MAA			
10:90	47.8	103.8	65.4
30:70	50.0	177.2	133.7
50:50	27.0	72.9 (C*/160)	94 (C*/160)
		139.5 (C*/80)	67.9 (C*/80)
		36.0 (1:2)	
		39.8 (1:3)	
		178.3 (1:4) (32.5*)	
70:30	31.6	61.8 (1:1)	33.5
		68.8 (1:2)	
90:10	59	X-linked after extraction (54.8 [#] , 70.6*)	70.2 (57.7 [#])
TMPTMA: MAA			
30:70	92	126.4 (C*/160) (86.6*)	84.2
		151.3 (C*/80) (102.5*)	93 (C*/80)
		110.9 (1:2) (89.1*)	
		126.2 (1:3) (90.5*)	
		122.7 (1:4) (88.2*)	
70:30	89	X-linked after extraction (117.4*)	109.3

[#] The data collected prior to concentration of nanoparticles reaction mixture

* The data collected prior to extraction of THP from the imprinted nanoparticles

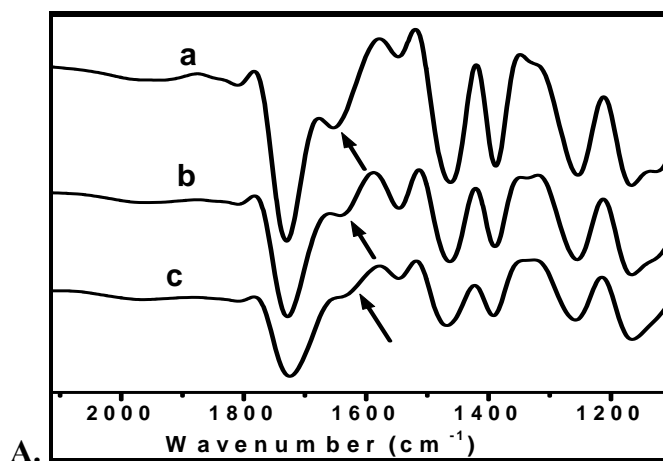


Figure 6.4 A. a. Poly (EGDMA-co-MAA) b. NIP nanoparticles
c. MIP nanoparticles after extraction of THP.

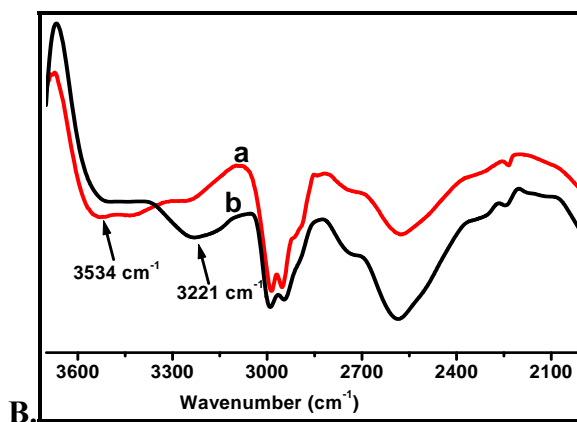


Figure 6.4B. a. MIP nanoparticles after THP extraction,
b. MIP nanoparticles after THP rebinding.

6.3.4 THP Imprinted Nanoparticles: Rebinding

THP imprinted nanoparticles were obtained by intramolecular cross-linking of THP bound functional copolymers. The co-monomer compositions as well as the imprinting conditions were varied.

Solvent choice governs the performance of molecularly imprinted polymers during rebinding. Polar solvents weaken the interactions between the template and the functional monomers (Tunc et al., 2006). Chloroform is widely used during imprinting because of its non-polar nature and low hydrogen-bonding tendency (Li et al., 2005).

However, size of the synthesized nanoparticles in the range 36 to 178 nm and good dispersibility in chloroform, posed difficulties in the recovery of nanoparticles from the rebinding media by centrifugation (Li et al., 2006). In contrast the nanoparticles could easily be separated by centrifugation from the rebinding media when they were suspended in acetonitrile. Therefore all rebinding experiments were carried out in acetonitrile, although it is a more polar solvent than chloroform.

6.3.4.1 Effect of Cross-link Density

Table 6.5: THP Rebinding on Nanoparticles

Nanoparticles		mg of THP / g polymer	Specific binding (MIP-NIP) mg	Recognition factor (MIP/NIP)
EGDMA: MAA				
10:90	MIP 1	0.656	0.323	1.97
	NIP 1	0.333		
30:70	MIP 2	1.380	0.516	1.59
	NIP 2	0.864		
50:50	MIP 3	1.246	0.716	2.35
	NIP 3	0.530		
70:30	MIP 4	1.432	0.702	1.96
	NIP 4	0.730		
90:10	MIP 5	1.057	0.526	1.99
	NIP 5	0.531		
TMPTMA: MAA				
10:90	MIP 6	1.0000	0.082	1.08
	NIP 6	0.9180		
30:70	MIP 7	1.4712	1.089	3.86
	NIP 7	0.3815		
70:30	MIP 8	2.1912	1.714	4.59
	NIP 8	0.4774		

The imprinted nanoparticles containing higher percentage of MAA showed low recognition factor (MIP / NIP) as well as lower specific binding (MIP-NIP). In particular MIP 1 obtained from poly (EGDMA-*co*-MAA) (10:90) and MIP 6 from poly (TMPTMA-*co*-MAA) (10:90) exhibited recognition factor of 1.97 and 1.08 respectively. This was due to the high percentage of polar groups and low cross-linking density in the imprinted polymers, which led to high swelling of the imprinted matrix and distorted the shape of the imprinted cavity (Wulff, 1995). Also an increase in polar groups in nanoparticles causes an increase the interchain interactions between MAA-MAA units of the copolymer and decreased their availability for hydrogen bonding with THP during rebinding experiments (Yoshimatsu et al., 2006). Thus non-specific interactions responsible for rebinding of THP result in lower recognition factor for the nanoparticles containing higher percentage of MAA units.

The imprinted matrices are generally prepared as to contain very high cross-linking density to retain the cavity size and shape (Kanekiyo et al., 2003). The recognition factors of MIP 2 and MIP 7 poly (EGDMA-*co*-MAA) and poly (TMPTMA-*co*-MAA) nanoparticles containing 30 % cross-linker were 1.59 and 3.86. TMPTMA contains two pendant double bonds per repeat unit, which at the same cross-linker concentration results in a greater cross-link density as compared to nanoparticles containing EGDMA (Ye et al., 2001).

Increasing EGDMA content from 10 to 50 % resulted in increase in the recognition factor of imprinted poly (EGDMA-*co*-MAA) nanoparticles from 1.97 to 2.35. Further increase in cross-linker content from 50 and 90 % led to lower recognition factor *viz* 1.99. Biffis et al., observed similar behavior for imprinted microgels obtained by the copolymerization of methyl methacrylate with EGDMA in dilute solutions. In contrast, for the imprinted nanoparticles of TMPTMA copolymers, MIP 6 (poly (TMPTMA-*co*-MAA), 10:90), MIP 7 (poly (TMPTMA-*co*-MAA), 30:70), MIP 8 (poly (TMPTMA-*co*-MAA), 70:30), the recognition factor as well as the specific binding increased from 1.08 to 4.59 and 0.082 to 1.714 mg respectively. Thus an optimal level of functional groups and the cross-link density are needed to achieve the enhanced rebinding capacity (Wulff, 1995, Ye et al., 2000).

Imprinted nanoparticles based on poly (TMPTMA-co-MAA) 30:70 synthesized by us exhibited a recognition factor of 3.86, as against 1.18 exhibited by a polymer of identical composition prepared by precipitation polymerization of monomers in the presence of template. Thus synthesis of imprinted nanoparticles by intramolecular cross-linking of template bound functional copolymer leads to nanoparticles, which exhibit enhanced rebinding (Biffis et al., 2001, Ciardelli et al., 2004).

Though THP-imprinted and non-imprinted nanoparticles were synthesized from the same precursor polymer, the imprinted nanoparticles exhibited higher binding capacity for THP. This confirms that the enhanced binding between THP and carboxyl groups and generation of THP specific binding cavities under conditions of nanoparticles synthesis results in greater rebinding in imprinted polymers as against non imprinted polymers.

6.3.4.2 Effect of THP to Carboxyl Ratio

Table 6.6: THP Rebinding on Nanoparticles: Effect of THP to Carboxyl Ratio

Nanoparticles	THP: COOH of polymer	mg THP / g of polymer	Recognition factor (MIP/NIP)
Poly (EGDMA-co-MAA) (50:50)	1:1	5.95	2.99
	1:2	2.83	1.42
	1:3	2.11	1.06
	1:4	2.22	1.12
	NIP	1.99	-
Poly (TMPTMA-co-MAA) (30:70)	1:1	3.21	2.94
	1:2	2.26	2.07
	1:3	1.90	1.74
	1:4	2.19	2.01
	NIP	1.09	-

The ratio of the template to functional monomer during imprinting has a critical influence on the performance of molecularly imprinted polymers (Tunc et al., 2006, Andersson et al., 1999). Low template to monomer ratio yields non-selective polymer

matrix. For the imprinted polymers containing THP and MAA monomer and EGDMA as cross-linker, THP to MAA ratio 1:4 resulted in higher selectivity (Vlatakis et al., 1993, Tunc et al., 2006). In contrast, in the case of the polymer, 1:2 ratio resulted in highest selectivity (Li et al., 2005).

Poly (EGDMA-*co*-MAA) and poly (TMPTMA-*co*-MAA) nanoparticles synthesized using THP to carboxyl ratio 1:1 of the polymer exhibited the highest recognition factor 2.99 and 2.94 respectively. The recognition factor decreased as this ratio was increased to 1:4 (Table 6.6)

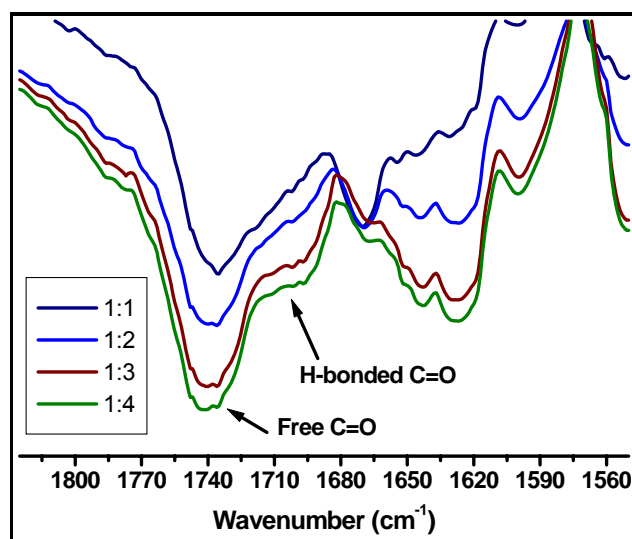


Figure 6.5: The FTIR spectra in the carbonyl region after subtracting the THP spectra from the THP to carboxyl mixture 1:1 to 1:4.

To understand the reasons for the observed behavior, the interactions between and the precursor polymer containing 50 % EGDMA and template to carboxyl ratio 1:1 to 1:4 were investigated by FT-IR spectroscopy. Figure 5 represents the difference spectra.

As the ratio of THP to carboxyl group increased from 1:1 to 1:4, the broad peak centered at 1735 cm⁻¹ split into two peaks, one around 1740 and the other around 1701 to 1698 cm⁻¹. This indicated participation of the carbonyl groups in hydrogen bonding interactions (Yoshimatsu et al., 2006). The carboxylic groups of poly (MAA) are well known to form MAA-MAA bridging interaction due to dimerization or self-association with other carboxyl groups in the polymer chains (Yoshimatsu et al., 2006). Increase in

the concentration of carboxyl groups increases the probability of these bridging interactions between the carboxyl units along with increase in hydrogen bonding interactions with the template molecules. This would create non-specific binding sites on the imprinted nanoparticles prepared using higher concentration of carboxyl groups and thus result in lower rebinding capacity.

6.3.4.3 THP Imprinted Nanoparticles: Binding Isotherm

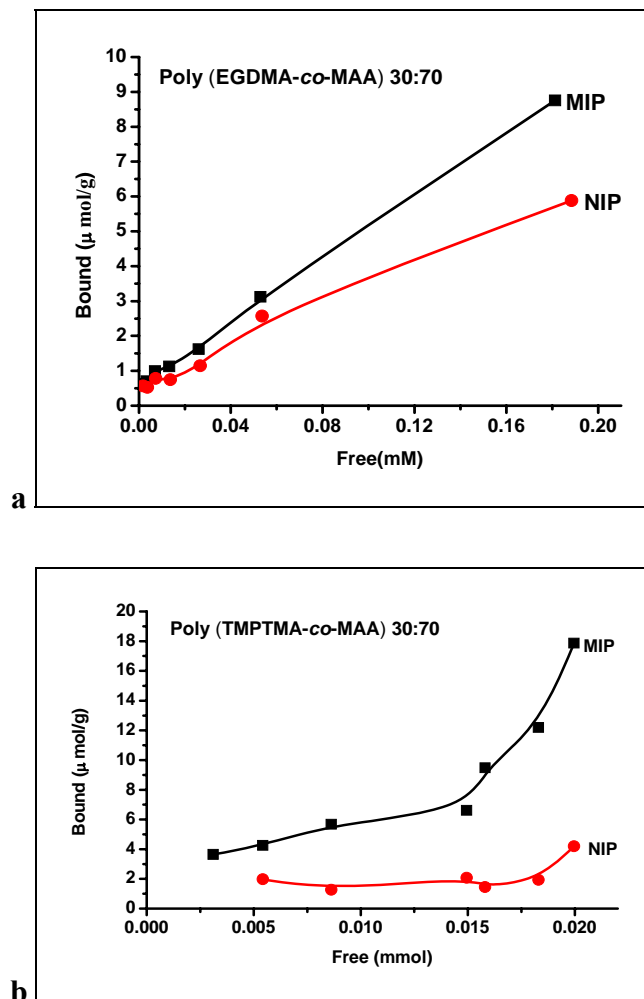


Figure 6.6. THP binding on a. poly (EGDMA-co-MAA) (30:70),
b. poly (TMPTMA-co-MAA) (30:70) nanoparticles

Freundlich isotherm provides a good fit for non-covalent MIP (Umpleby et al., 2001, Sellergren, 2001). Therefore the binding parameters of imprinted nanoparticles were evaluated by Freundlich isotherm (Rampey et al., 2004). In the Freundlich isotherm;

$$B(F) = \alpha F^m$$

B and F are the concentrations of the bound and free THP. The nanoparticles were suspended in 1×10^{-4} - 8.67×10^{-6} M THP in acetonitrile. The values of median binding affinity (K_0) and heterogeneity index (m) were estimated from the plot of log F vs log B.

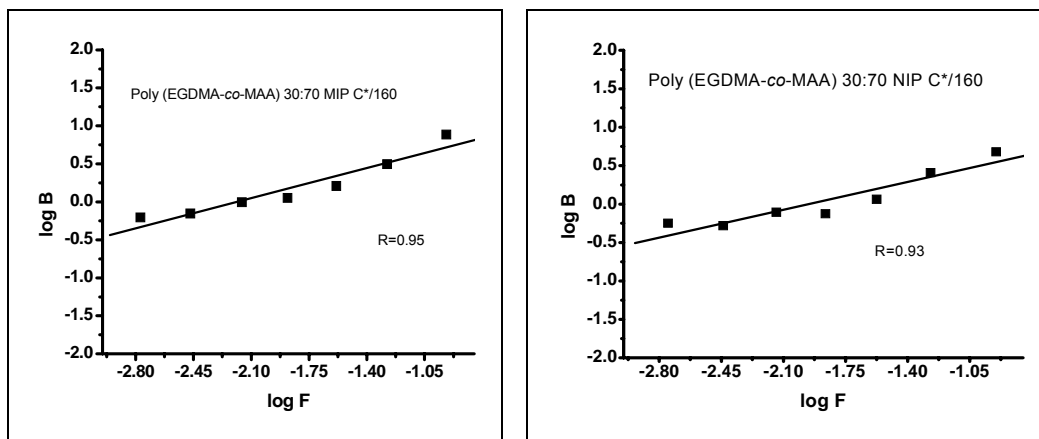


Figure 6.7: Freundlich fit for poly (EGDMA-co-MAA) (30:70) nanoparticles

Table 6.7: Effect of Cross-linking Density on Heterogeneity Index (m) and Median Binding Affinity (K_0) of Nanoparticles

Nanoparticles		Heterogeneity index (m)	Median binding affinity ($K_0 = \alpha^{1/m}$) ($\mu\text{molg}^{-1}\text{mmol}^{-1}$)
Poly (EGDMA-co-MAA) (30:70)	MIP	0.45	147.32
	NIP	0.42	77.77
Poly (EGDMA-co-MAA) (50:50)	MIP	0.68	1206.95
	NIP	0.77	256.50
Poly (EGDMA-co-MAA) (70:30)	MIP	0.72	167.07
	NIP	0.90	146.75
Poly (TMPTMA-co-MAA) (30:70)	MIP	0.69	649.48
	NIP	0.23	960.94

Heterogeneity index of poly (EGDMA-*co*-MAA) nanoparticles increased from 0.45 to 0.72 as EGDMA content increased in the precursor polymer from 30 to 70 %. This effect is more pronounced in the non-imprinted nanoparticles wherein the value increased from 0.41 to 0.90 for the same cross-linker content. This is obvious since in the case of non-imprinted polymer all binding sites have same type of interaction with THP. The heterogeneity index for poly (EGDMA-*co*-MAA) (70:30) reported by Li et al., (2005) was 0.69 for imprinted and 1 for the non-imprinted polymer.

A comparison of the heterogeneity index values for imprinted nanoparticles synthesized from the poly (EGDMA-*co*-MAA) and poly (TMPTMA-*co*-MAA) containing 30 % cross-linker, showed a value of 0.45 for the former vs 0.69 for the later. The imprinted poly (EGDMA-*co*-MAA) (50:50) nanoparticles exhibited the highest median binding affinity as well as the recognition factor.

Table 6.8: Effect of THP to Carboxyl Ratio on Rebinding Parameters

Nanoparticles	Ratio of THP: COOH group	Heterogeneity index (m)	Median binding affinity $K_0 = \alpha^{1/m}$ ($\mu\text{molg}^{-1}\text{mmol}^{-1}$)
Poly (EGDMA- <i>co</i> -MAA) (50:50)	1:1	0.68	1206.95
	1:2	0.64	664.144
	1:3	0.42	3096.4
	1:4	0.57	615.13
	NIP	0.77	256.50
Poly (TMPTMA- <i>co</i> -MAA) (30:70)	1:1	0.67	649.48
	1:2	0.70	431.21
	1:3	0.63	481.63
	1:4	0.74	509.73
	NIP	0.23	960.94

In the case of the nanoparticles synthesized from poly (EGDMA-*co*-MAA) (50:50), the heterogeneity index decreased from 0.68 to 0.42 as the THP to carboxyl ratio was varied from 1:1 to 1:3 during nanoparticles synthesis. Further increase in THP: carboxyl ratio to 1:4 resulted in increase in heterogeneity index value to 0.57. This could be attributed to increase in inter/ intrachain bridging interactions between – carboxyl groups of the polymer along with intermolecular hydrogen bonding interactions between THP and the carboxyl groups during nanoparticles synthesis. Cross-linking during the extraction resulted in increase in particle size from 32.5 to 178 nm indicating extensive interchain cross-linking was responsible for the heterogeneity of the sites generated. These nanoparticles are more heterogeneous as compared to those obtained using THP to carboxyl ratio of 1:1 and 1:2.

The nanoparticles synthesized from the copolymers containing TMPTMA exhibited higher heterogeneity index than the copolymers containing EGDMA but did not show any trend (0.63, 0.74). In these copolymers, two double bonds per TMPTMA unit are free to react under conditions of nanoparticle synthesis. They could react in variety of ways. The polymer chains could react intramolecularly or intermolecularly with only one of its double bond and the second double bond could participate in cross-linking during extraction step. Alternatively both double bonds could participate in cross-linking during nanoparticle synthesis. These pathways would result in nanoparticles containing varying cross-linking density and hence would exhibit diverse rebinding characteristics (Shea and Sasaki, 1991).

6.3.5 THP Imprinted Nanoparticles: Selectivity

Selectivity of THP imprinted and non-imprinted nanoparticle towards THP and CAF was investigated by heterogeneous rebinding experiments. The results are summarized in Table 6.9. THP has higher affinity than CAF for polyacrylates containing free carboxyl groups (Ye et al., 2000). In our case nanoparticles did bind to THP exclusively (Figure 6.8). The presence of hydrogen at 7th nitrogen THP results in strong hydrogen bonding through cyclic structure formation with the carboxyl group in the functional copolymer (Scheme 6.1) (Tunc et al., 2006, Li et al., 2005). Li et al., (2005) reported similar results. The imprinted poly (MAA-MMA-TMPTMA) nanoparticles synthesized by precipitation polymerization method exhibited a selectivity of 5.1 (Andersson et al.,

1996). The higher selectivity of the nanoparticles formed by cross-linking of THP bound polymer *vis a vis* the imprinted polymers formed by simultaneous polymerization / cross-linking approach is result of stronger binding between the template with a polymeric substrate as compared to the monomer.

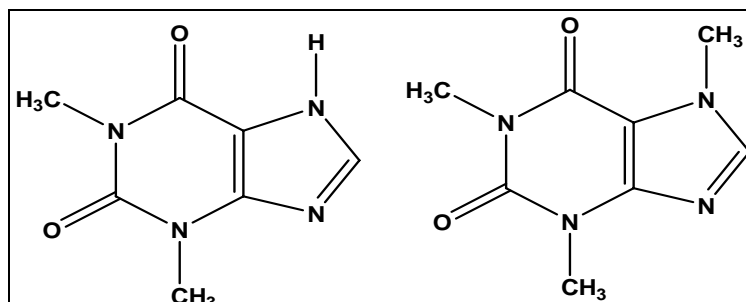


Figure 6.8: Structure of Theophylline and Caffeine

Table 6.9: THP-Imprinted Nanoparticles: Selectivity

Nanoparticles	Template molecule	Bound template mg/g of polymer	
		MIP	NIP
Poly (EGDMA-co-MAA) (30:70)	THP	1.380	0.864
	CAF	0.000	0.541
Poly (EGDMA-co-MAA) (50:50)	THP	1.245	0.530
	CAF	0.000	0.548
Poly (TMPTMA-co-MAA) (70:30)	THP	2.191	0.477
	CAF	0.000	0.044

6.3.6 THP Imprinted Nanoparticles: Release Study

6.3.6.1 Effect of Cross-link Density

Poly (EGDMA-co-MAA) nanoparticles containing 90 and 70 % MAA released THP within 30 min. This was because of high concentration of ionizable carboxyl groups and lower cross-linking density present in nanoparticles. This results in higher swelling of the imprinted matrix and thus distorts the shape of the cavity. Higher ionization limits

the hydrogen bonding interactions between THP and carboxyl groups resulting in its rapid release in buffer (Katime et al., 2004, Wulff, 1995).

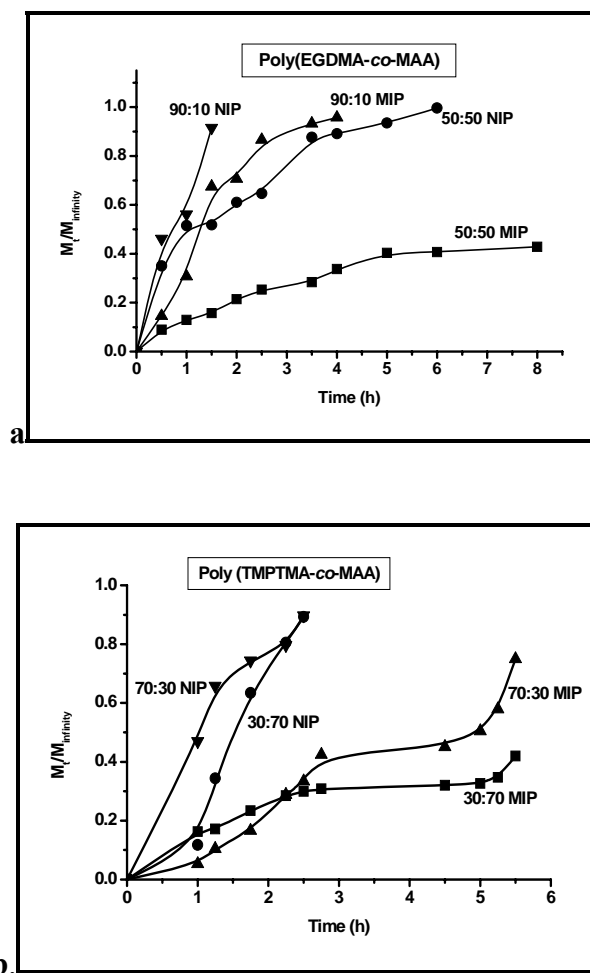


Figure 6.9: Fractional release of THP from a. poly (EGDMA-co-MAA) 50:50 and 90:10, b. poly (TMPTMA-co-MAA) 30:70 and 70:30 nanoparticles

Increase in cross-link density should sustain THP release by decreasing the swelling and distortion of the imprinted cavity. Poly (EGDMA-co-MAA) and poly (TMPTMA-co-MAA) nanoparticles containing 50 and 30 % cross-linker exhibited sustained release and only upto 40 % of THP was released in 6 h. In contrast, imprinted poly (TMPTMA-co-MAA) nanoparticles containing 30 % TMPTMA released 55 % THP in 4 h (Ciardelli et al., 2004). Further increase in the cross-link density of the imprinted nanoparticles increased the THP release. In particular imprinted poly (EGDMA-co-

MAA) (90:10) nanoparticles showed complete release of THP within 4 h and imprinted poly (TMPTMA-*co*-MAA) (70:30) nanoparticles released upto 75 % of THP in 6 h.

Thus the release from the imprinted nanoparticles containing higher cross-link density (90 % in poly (EGDMA-*co*-MAA) and 70 % in poly (TMPTMA-*co*-MAA) nanoparticles) was slower as compared to THP released from the imprinted nanoparticles containing lower cross-link density (10 to 30 % in poly (EGDMA-*co*-MAA) nanoparticles). This could be attributed to the increase in rigidity and thus low swelling of the imprinted cavity with increase in cross-link density, which suppresses the effective diffusivity of the template from the matrix (Puoci et al., 2004). But the more sustained release observed in the nanoparticles of intermediate cross-link density (50 % in poly (EGDMA-*co*-MAA) and 30 % in poly (TMPTMA- *co*-MAA) nanoparticles) indicated that the enhanced interactions between THP and the polymer bound functional groups override the cross-linking effects in the release of THP from the nanoparticles.

Thus an optimal balance between the functional group and cross-linker content is necessary to sustain the release of THP from the imprinted nanoparticles. The results showed that poly (EGDMA-*co*-MAA) and poly (TMPTMA-*co*-MAA) containing 30 and 50 % cross-linker respectively offer sustained release of THP from the imprinted nanoparticles.

6.3.6.2 Effect of THP loading

Poly (EGDMA-*co*-MAA) nanoparticles containing 50 % EGDMA, imprinted using THP to carboxyl ratio 1:1 and containing 6 mg /g THP, released 80 % THP in 6 h (Table 10). In contrast the same nanoparticles containing 1.2 mg / g THP released only 40 % THP in 6 h. This is because in the former case both high and low affinity-binding sites were occupied by THP during rebinding. THP bound on low affinity sites was released rapidly (Hiratani et al., 2005). Similar observations were also reported by Norell et al., (1998) for the release of THP from the imprinted poly (EGDMA-MAA) matrix, loaded with 50 mg / g to 0.1 mg / g of THP on dry polymer. The polymers containing 2.0 and 0.1 mg / g loading released 85 % and 75 % THP respectively in 6 h as compared to the polymer containing 10.0 mg / g THP, which released 95 % THP in 6 h. The imprinted nanoparticles synthesized by us containing 1.2 mg /g THP released

only 41 % THP in 6 h in contrast to 75 % release reported by Norell et al., (1998) for similar THP loading.

6.3.6.3 Effect of THP to Carboxyl Ratio

The release of THP from the imprinted nanoparticles obtained by varying THP to carboxyl ratio during the nanoparticles synthesis was studied and the results are summarized in Table 6.10.

Table 6.10: THP Release from Poly (EGDMA-*co*-MAA) (50:50) Nanoparticles

Time (h)	% of THP released from nanoparticles with stoichiometry of THP: carboxyl gr of polymer				
	1:1	1:2	1:3	1:4	NIP
2	16	12	30	27	53
3	61	26	50	38	67
6	80	46	74	61	82

The release of THP decreased as the ratio of THP to carboxyl group increased from 1:1 to 1:2. Further increase in the ratio upto 1:4 led to enhanced THP release. This indicated increase in the interactions between THP and carboxyl groups of the copolymer as the concentration of carboxyl increased during the synthesis of nanoparticles from 1:1 to 1:2. Further increase in the ratio of carboxyl groups, increased inter / intrachain bridging interactions with the polymer and THP supported by FTIR studies discussed in previous section. This created heterogeneous binding sites as evidenced from the lower value for the heterogeneity index and thus results in faster THP release.

6.4 Conclusions

Functional copolymers comprising both recognition and cross-linking functionality reorganize themselves around the template molecules through non-covalent interactions such as hydrogen bonding to form stable complex. The intramolecular single chain cross-linking of these complexes lead to soluble imprinted nanoparticles with good rebinding and selectivity properties as well as drug delivery properties demonstrated using THP as a model template molecule. These nanoparticles would find applications in controlled drug delivery systems.

Chapter 7

**Conclusions and Recommendations for
Future Research**

7.1 Introduction

Present investigation was undertaken to explore if the reactivity of hydrophobic multivinyl monomers could be controlled by exploiting host-guest chemistry of cyclodextrins (CD). Inclusion complex (IC) mediated polymerization of multivinyl monomers leads to latent cross-linkable polymers comprising pendant vinyl unsaturations. Subsequent reactions of the pendant unsaturations (intermolecular / intramolecular) yield cross-linked materials of varying properties. The research work further demonstrates the application of these polymers in nanotechnology, molecular imprinting and controlled drug delivery.

This chapter summarizes significant findings of the present investigation followed by the recommendations for future research.

7.2 Significant Findings

1. Divinyl monomers always formed 1:1 IC with CD whereas in case of trivinyl monomers the presence and absence of intramolecular hydrogen bonding resulted in the formation of 1:1 and 1:2 IC respectively.

(Chapter 3, Section 3.3.2.1, Table 3.1, Pages 54-55).

2. CD showed selectivity during formation of an IC with unsymmetrical multivinyl monomers. Unequivocal inclusion of methacrylate or acrylate in CD cavity was observed during the IC formation of EGMAVB or TMPDAVB.

(Chapter 4, Section 4.3.2.2, Figures 4.8, 4.9 and 4.13, Pages 76-77 and 80).

3. Intermolecular hydrogen bonding interactions between the ester carbonyl of multivinyl monomer and the hydroxyl of CD rim was observed by FTIR and thus resulted in the formation of stable IC.

(Chapter 3, Section 3.3.2.2, Table 3.2, Page 57)

4. Computational analysis of IC of divinyl monomers-CD confirmed the stability of bent conformation over stretched conformation of divinyl monomers after their inclusion in CD cavity. This explains the formation of exclusively 1:1 IC with CD independent of the feed ratio of divinyl monomer: CD.

(Chapter 3, Section 3.3.3.1, Page 59)

5. Computational analysis supported observed stoichiometry of trivinyl monomers. In TMPTA, the presence of intramolecular hydrogen bonding interactions between two acrylate groups ($C-H \cdots O=C$) brings them in close

vicinity and results in 1:1 IC formation. Such intramolecular hydrogen bonding interactions are absent in TMPTMA and TMPDAVB molecules, which results in formation of 1:2 ICs.

(Chapter 3, Section 3.3.3.2, Pages 60-62)

6. Inclusion complex mediated homo and copolymerization of divinyl and trivinyl monomers led to the formation of latent cross-linkable polymers since the vinyl groups included in CD cavity did not participate in radical polymerization.

(Chapter 4, Section 4.3.2.2, Pages 74-80 and Chapter 5, Section 5.3.2.2, Pages 97-98)

7. Comparable molecular weights obtained by GPC and MALLS confirmed the linear nature of IC mediated polymers.

(Chapter 4, Section 4.3.2.4, Table 4.4, Pages 85-86)

8. Co-monomer reactivity ratio measurements indicated that the reactivity of multivinyl monomers decreased on their inclusion in CD cavity. As a result of complexation the multivinyl monomers behave as a monovinyl monomer and the formation of IC decreases their reactivity due to steric reasons.

(Chapter 5, Section 5.3.3, Table 5.2, Page 107)

9. The pendant vinyl groups of polymers can be subsequently cross-linked by intermolecular or intramolecular cross-linking reactions.

(Chapter 4, Section 4.3.3, Pages 86-89)

10. The intermolecular cross-linking of pendant vinyl groups resulted in the cross-linked materials with enhanced thermal stability as confirmed by TGA and DSC analysis.

(Chapter 4, Section 4.3.3.1, Pages 86-88)

11. The intramolecular cross-linking of pendant vinyl groups yielded self cross-linked nanoparticles. The cross-linking concentration, percentage and type of multivinyl monomer, molecular weight of precursor polymer as well as the competition between the intermolecular and intramolecular cross-linking reactions governs the particle size of resulting nanoparticles.

(Chapter 4, Section 4.3.3.2, Pages 88-89)

12. Theophylline imprinted nanoparticles could be synthesized by exploiting the principles of molecular imprinting and intramolecular cross-linking.

(Chapter 6, Section 6.3.3, Pages 125-128)

13. The particle size of the functional nanoparticles varied between 36 to 180 nm depending on the functional monomer and multivinyl monomer composition in precursor copolymer as well as inter and intramolecular cross-linking reactions during their synthesis.

(Chapter 6, Table 6.4, Page 127)

14. The imprinted nanoparticles exhibited enhanced affinity, binding capacity and exclusive selectivity towards theophylline as compared to the imprinted polymers obtained by simultaneous precipitation and cross-linking.

(Chapter 6, Section 6.3.5, Table 6.6, 6.7, and 6.9, Pages 131, 134, 137)

15. Enhanced interactions between the polymer matrix and theophylline resulted in its sustained release from the nanoparticles.

(Chapter 6, Section 6.3.6.1, Pages 137-139)

16. The imprinted nanoparticles sustained release of theophylline depending on the composition of nanoparticles and the molar ratio of theophylline to functional comonomer. Drug release for a period spanning over one h to twenty-one days was obtained.

(Chapter 6, Section 6.3.6.3, Page 140)**7.3 Recommendations for Future Research**

A research investigation of this kind cannot address all the issues raised, within the limited time period available. The validation of the concept and its application demonstrated in this work opens new opportunities for future research, which are summarized below.

1. The immediate extension of the present investigation is to evaluate the inclusion complex formation ability of hydrophilic multivinyl monomers with CD and study their homo and copolymerization behavior. The hydrophilic divinyl monomer, methylene bis acrylamide (MBAM) is extensively used for biosensors preparation. The current approaches face the difficulties such as shrinkage of polymer due to uncontrolled cross-linking and presence of entrapped monomers that are toxic to the immobilized biomaterial. In contrast the inclusion complex mediated polymers of hydrophilic monomers will result

in the formation of soluble, latent cross-linkable and pure polymers and thus can use directly for these applications.

2. CDs are selective towards the inclusion complex formation with the unsymmetrical monomers. It will be very interesting to synthesize the multivinyl monomers differing in types of double bonds present in the same molecule e.g. methacrylate, acrylate, acrylamide or methacrylamide as well as allyl and styrenic double bonds and study their IC formation with CD. This will help to tailor the performance as well as properties of the final cross-linked materials. The IC mediated polymerization of amphiphilic cross-linker i.e. divinyl monomer comprising the hydrophobic methacrylate and hydrophilic methacrylamide double bonds in the same molecule will lead to the formation of latent cross-linkable polymers with pendant methacrylate groups. These polymers will be useful in processable molecular imprinting, as they will combine the properties and advantages of hydrophobic and hydrophilic moieties in the same molecule. The polymerized hydrophilic methacrylamide group will bind to the template molecules and the pendant methacrylate groups will cross-link to impart the rigidity to the imprinted cavity.
3. The copolymers, poly (MMA-*co*-EGDMA), poly (MMA-*co*-TMPTMA) and poly (MMA-*co*-EGMAVB) can directly be utilized for the integrated optical applications. The current approach utilizes multi-step synthetic methodology. This involves the synthesis of linear copolymers of HEMA and MMA and subsequent methacryloylation of pendant hydroxyl. The incomplete functionalization of pendant hydroxyl is one of the limitations of this method. The presence of hydroxyl groups in the polymer limits their optical applications as they have absorbance in near IR region, which lead to the optical loss. This problem could be overcome by exploiting IC mediated polymerization of multivinyl monomer and MMA.
4. The methodology can be utilized for the synthesis of latent cross-linkable polymers for lithography applications. Lithography requires the formation of pattern on the substrate using negative or positive photoresists. The critical selection of functional monomers and their copolymerization with suitable

multivinyl monomers by the methodology demonstrated herein will yield the polymers meeting the need of new materials for the lithography.

5. The methodology of synthesis of latent cross-linkable poly (MMA) can easily be extended to obtain the latent cross-linkable poly (MMA) layered clay nanocomposites. The recent developments in polymer clay nanocomposites synthesis are aimed at the preparation of highly exfoliated, thermally stable and processable nanocomposites. This can be easily achieved by the polymerization methodology described herein. The first step will be the modification of clay with a suitable functional monomer, copolymerization of the clay complexed monomer with MMA and the CD complexed multivinyl monomers. The resulting nanocomposites will be soluble in organic solvents; will have exfoliated clay and latent cross-linkable groups. These materials will find potential applications in anticorrosive coating as well as in microlithography.
6. The polymers used for the synthesis of theophylline-imprinted nanoparticles can also be utilized and evaluated for other template molecules depending on the applications. The functional nanoparticles synthesized in the present investigation exhibit exclusive selectivity towards theophylline as compared to its structural analogue caffeine. Polymers that can bind the template molecule exclusively will have enormous applications in chiral separations.

References

- Alvarez-Lorenzo, C.; Guney, O.; Oya, T.; Sakai, Y.; Kobayashi, M.; Enoki, T.; Takeoka, Y.; Ishibashi, T.; Kuroda, K.; Tanaka, K.; Wang, G.; Grosberg, A. Y.; Masamune, S.; Tanaka, T.; *Macromolecules* **2000**, *33*, 8693.
- Andersson, L. J. *Chromatogr. B* **2000**, *739*, 163.
- Andersson, H. S.; Karlsson, J. G.; Piletsky, S.A.; Koch-Schmidt, A.C.; Mosbach, K.; Nicholls, I. A. *J. Chromatogr. A* **1999**, *848*, 39.
- Andersson, L.I., Nicholls, I.A., Mosbach, K., *Adv. Mol. Cell Biol.* **1996**, *15B*, 651.
- Ansell R.J.; Mosbach K. *J. Chromatogr. A* **1997**, *787*, 55.
- Ansell R.J.; Mosbach K. *Analyst* **1998**, *123*, 1611 Aso, C. *J. Polym. Sci.* **1959**, *39*, 475.
- Bajaj, P.; Sreekumar, T. V.; Sen, K. *J Appl. Polym. Sci* **2001**, *79*, 1640.
- Barse, B.; Kaul, P.; Banerjee, A.; Kaul, C. L.; Banerjee, U. C. *Chemistry Today* **2003**, *48*.
- Bernhardt, S.; Glöckner, P.; Theis A.; Ritter, H.; *Macromolecules* **2001**, *34*, 1647
- Biffis, A.; Graham, N. B.; Siedlaczek, G.; Stalberg, S.; Wulff, G.; *Macromol. Chem. Phys.* **2001**, *202*, 163.
- Born, M.; Ritter, H. *Macromol. Rapid Commun.* **1991**, *12*, 471.
- Bortolus, P.; Monti, S. *Adv. Photochem.* **1996**, *21*, 1.
- Breslow, R; Campbell, P. *J. Am. Chem. Soc.* **1969**, *91*, 3085.
- Caro, E.; Masque, N.; Marce, R. M.; Borrull, F.; Cormack, PAG, Sherrington. D.C.; *J. Chromatogr. A*, **2002**. 963, 169.
- Carter, S.; Lu S.Y.; Rimmer, S. *Supramol. Chem.* **2003**, *15*, 213.
- Case, D. A.; Pearlman, D. A.; Caldwell, J. W.; Cheatham, T. E. III; Wang, J.; Ross, W. S.; Simmerling, C. L.; Darden, T. A.; Merz, K. M.; Stanton, R. V.; Cheng, A. L.;

- Vincent, J. J.; Crowley, M.; Tsui, V.; Gohlke, H.; Radmer, R. J.; Duan, Y.; Pitera, J.; Massava, I.; Seibel, G. L.; Singh, U. C.; Weiner, P. K.; Hornak, V.; Cui, G.; Schafmeister, C.; Gohlke, J.; Kollman, P. A. AMBER 8.0, University of California: San Francisco, CA, **2004**.
- Chen, L.; Zhu, X.; Yan, D.; Chen, Y.; Chen, Q.; Yao, Y. *Angew. Chem., Int. Ed.* **2006**, *45*, 87.
- Chronakis I.S.; Jakob, A.; Hagstrom B.; Ye L.; *Langmuir* **2006**, *22*, 8960.
- Ciardelli, G.; Cioni, B.; Cristallini, C.; Barbani, N.; Silvestri, D.; Giusti, P. *Biosensors and Bioelectronics* **2004**, *20*, 1083.
- Cramer, F. *Einschlussverbindungen (Inclusion Compounds)*; Springer-Verlag: Berlin, **1954**
- Cunliffe, D.; Kirby, A.; Alexander, C. *Advanced Drug Delivery Reviews* **2005**, *57*, 1836.
- Czarnik, A. W. *J. Org. Chem.* **1984**, *49*, 924.
- Das, K.; Penelle, J.; Rotello, V. M. *Langmuir* **2003**, *19*, 3921
- Dong, W.; Yan, M.; Zhang, M.; Liu, Z.; Li, Y. *Analytica Chimica Acta* **2005**, *542*, 186.
- Elliott J. E.; Bowman C. N., *Polymer Reaction Engineering*, **2002**, 10(1&2), 1.
- Elliott, J. E.; Macdonald, M.; Nie, J, Bowman, C.N. *Polymer* **2004**, *45*, 1503.
- Finemann, M; Ross, S. *J. Polym. Sci. A* **1964**, *2*, 1687.
- Flores, A.; Cunliffe, D.; Whitcombe, M.J.; Vulfson, E. N.; *J. Appl. Polym. Sci.* **2000**, *77*, 1841.
- Flory, P. J. "Principles of polymer Chemistry", Cornell Univ. Press, Ithaca, N. Y., **1953**, 384.

- Fornasier, R.; Marcuzzi, F.; Parmagnani, M.; Tonellato, U. *Carbohydr. Res.* **1991**, *217*, 245.
- Freudenberg K.; Rapp W. *Ber. Dtsch. Chem. Ges.* **1936**, *69*, 2041.
- French, D. *Adv. Carbohydr. Chem.* **1957**, *12*, 189.
- Freudenberg, K.; Blomquist G.; Ewald, Lisa; Soff, K. *Ber. Dtsch. Chem. Ges.* **1936**, *69*, 1258.
- Freudenberg, K.; Boppel, H. Meyer-Delius, M. *Naturwissenschaften* **1938**, *26*, 123.
- Freudenberg K.; Meyes-Delius, M. *Ber. Dtsch. Chem. Ges.* **1938**, *71*, 1596.
- Freudenberg, K.; Cramer, F. *Z. Naturforsch.* **1948**, *3b*, 464.
- Freudenberg, K.; Cramer, F.; Plieninger, H. Ger. Patent 895,769, **1953**
- Frisch, M. J.; Trucks, G. W.; Schlegel, H. B.; Scuseria, G. E.; Robb, M. A.; Cheeseman, J. R.; Montgomery, Jr., J. A.; Vreven, T.; Kudin, K. N.; Burant, J. C.; Millam, J. M.; Iyengar, S. S.; Tomasi, J.; Barone, V.; Mennucci, B.; Cossi, M.; Scalmani, G.; Rega, N.; Petersson, G. A.; Nakatsuji, H.; Hada, M.; Ehara, M.; Toyota, K.; Fukuda, R.; Hasegawa, J.; Ishida, M.; Nakajima, T.; Honda, Y.; Kitao, O.; Nakai, H.; Klene, M.; Li, X.; Knox, J. E.; Hratchian, H. P.; Cross, J. B.; Adamo, C.; Jaramillo, J.; Gomperts, R.; Stratmann, R. E.; Yazyev, O.; Austin, A. J.; Cammi, R.; Pomelli, C.; Ochterski, J. W.; Ayala, P. Y.; Morokuma, K.; Voth, G. A.; Salvador, P.; Dannenberg, J. J.; Zakrzewski, V. G.; Dapprich, S.; Daniels, A. D.; Strain, M. C.; Farkas, O.; Malick, D. K.; Rabuck, A. D.; Raghavachari, K.; Foresman, J. B.; Ortiz, J. V.; Cui, Q.; Baboul, A. G.; Clifford, S.; Cioslowski, J.; Stefanov, B. B.; Liu, G.; Liashenko, A.; Piskorz, P.; Komaromi, I.; Martin, R. L.; Fox, D. J.; Keith, T.; Al-Laham, M. A.; Peng, C. Y.; Nanayakkara, A.; Challacombe, M.; Gill, P. M. W.; Johnson, B.; Chen, W.; Wong,

- M. W.; Gonzalez, C.; Pople, J. A.; Gaussian 03, Revision C.02; Gaussian, Inc., Wallingford CT, **2004**.
- Fyfe M. C. T.; Stoddart J. F. *Acc. Chem. Res.*, **1997**, 30(10), 393.
- Gidley, M. J.; Bociek, S. M.; *J. Am. Chem. Soc.*, **1988**, 110, 3820.
- Glockener, P.; Ritter, H. *Macromol. Rapid Commun.* **1999**, 20, 602
- Griffiths, D. W.; Bender, M. L. *J. Am. Chem. Soc.* **1973**, 95, 1679.
- Guan Z. *J. Am. Chem. Soc.* **2002**, 124, 5616.
- Harada, A. *Coordination Chemistry Reviews* **1996**, 148, 115.
- Harada, A.; Kamachi, M. *Macromolecules* **1990**, 23, 2821.
- Harada, A.; Li, J.; Kamachi, M. *Macromolecules* **1993**, 26, 5698.
- Harada, A.; Li, J.; Suzuki, S.; Kamachi, M. *Macromolecules* **1998**, 26, 5267-5268.
- Harada, A.; Nishiyama, T.; Kawaguchi, Y.; Okada, M.; Kamachi, M. *Macromolecules* **1997**, 30, 7115.
- Haupt, K. *React. Funct. Polym.* **1999**, 41, 125.
- Haupt, K.; Mayes, A. G.; Mosbach, K. *Anal. Chem.* **1998**, 70, 3936.
- Haupt, K.; Mosbach, K. *Chem. Rev.* **2000**, 100, 2495.
- Heatley, F.; Lovel, P.A.; McDonald, J. *Eur. Polym. J.* **1993**, 29, 255.
- Hedge, A. *Chem. Rev.* **1998**, 98, 2035.
- Hirai, H.; Mihori, H.; Terakado, R. *Macromol. Rapid Commun.* **1993**, 14, 439.
- Hirai, H.; Shiraishi, Y.; Mihori, H.; Saito, K. *Polym. J.* **1996**, 28, 91.
- Hirai, H.; Shiraishi, Y.; Shirai, H. *Macromol. Rapid Commun.* **1995**, 16, 697.
- Hirai, H.; Shiraishi, Y.; Saito, K. *Macromol. Rapid Commun.* **1995**, 16, 31.
- Hiratani, H.; Alvarez-Lorenzo, C., *Journal of Controlled Release*, **2002**, 83, 223.
- Hiratani, H.; Alvarez-Lorenzo C., *Biomaterials*, **2004**, 25(6), 1105.

- Hiratani, H.; Fujiwara, A.; Tamiya, Y.; Mizutani, Y.; Alvarez-Lorenzo, C. *Biomaterials*, **2005**, 26(11), 1293.
- Hiratani, H.; Mizutani, Y.; Alvarez-Lorenzo, C. *Macromol. Biosci.* **2005**, 5, 728.
- Huang, L.; Allen, E.; Tonelli, A. E.; *Polymer* **1998**, 39, 4857.
- Hu, H.; Uno, A.; Harada, A.; Takahashi, S. *Chem. Lett.* **1990**, 797.
- Hu, H.; Uno, A.; Harada, A.; Takahashi, S. *Bull. Chem. Soc. Jpn.* **1991**, 64, 1884.
- Isaure, F.; Cormack, P. A. G.; Graham, S.; Sherrington, D. C.; Armes, S. P.; Butun, V. *Chem. Commun.* **2004**, 1138.
- Jeromin J., Ritter H. *Macromol. Rapid Commun.* **1998**, 19, 377.
- Jeromin J.; Noll O.; Ritter H. *Macromol. Chem. Phys.* **1998**, 199, 2641.
- Jeromin, J.; Ritter, H. *Macromolecules* **1999**, 32, 5236.
- Jiao, H.; Goh, S.H.; Valiyaveetil, S. *Macromolecules* **2001**, 34, 8138.
- Jiang, J.; Thayumanavan, S. *Macromolecules*, **2005**, 38, 5886.
- Jie, Z.; Xiwen, H. *Anal Chim. Acta* **1999**, 381, 85.
- Joshi VP, Karode SK, Kulkarni MG, Mashelkar RA. **1998**. *Chem. Eng. Sci.* 53: 2271.
- Joshi VP, Karmalkar RN, Kulkarni MG, Mashelkar RA. **1999** *Ind. Eng. Chem. Res.* 38: 4417.
- Joshi VP, Kulkarni MG, Mashelkar RA. **2000**. *Chem. Eng. Sci.* 55, 1509.
- Johnson, I. M.; Bhuvan Kumar, S.G.; Malathi, R. *Journal of Biomolecular Structure & Dynamics*, **2003**, 20(5), 687.
- Kanekiyo, Y.; Naganawa, R.; Tao, H. *Angew. Chem. Int. Ed.* **2003**, 42, 3014.
- Katime, I.; Novoa, R.; Diaz De Apodaca, E.; Rodriguezm, E.; *J. Polym Sci. Polymer Chemistry* **2004**, 42, 2756.
- Karmalkar, R.N.; Kulkarni, M.G.; Mashelkar, R.A.; *J. Control. Release* **1997**, 43, 235.

- Karrer, P.; Nageli, C. *Helv. Chim. Acta* **1921**, *4*, 169.
- Kelen, T.; Tudos, F. *J. Macromol. Sci A* **1975**, *9*, 1.
- Kobayashi, T. Wang, H. Y. Fujii, N. *Analytica Chimica Acta* **1998**, *365*, 81.
- Komiyama, M. Takeuchi, T. Mukawa, T. Asanuma H. "Molecular imprinting from fundamentals to applications" , VCH, Weinheim, **2002**.
- Koo, J-S.; Smith, P. G. R.; Williams, R. B.; Grossel, M. C.; Whitcombe, M.; *J. Chem. Mater.* **2002**, *14*, 5030.
- Landin, D. T.; Macosko C. W., *Macromolecules* **1988**, *21*, 846.
- Lanza, F. Sellergren, B. *Anal. Chem.* **1999**, *71*, 2092.
- Lau, W., Rohm and Haas Company: Eur. Pat. Appl., 1996; Vol. 125, 59402 CA
- Lehn J. M., *Supramolecular Chemistry*, VCH. Weinheim **1995**
- Leyer, R.j.; Wildburg, G.; Haunschild, A. BASF A. G., Ger. Offen. **1996**; 129, 68159.CA
- Li, J.; Ni, X.; Leong, K. *Angew chem. Int. ed.* **2003**, *42*(1) 69.
- Lin, S-H.; Shih, J-C. *Journal of Applied Polymer Science*, **2001**, *80*, 328.
- Lin, S-Y.; Liao C-M.; b, Hsiue G-H.; Liang, R-C. *Thermochimica Acta*, **1995**, *245*, 153.
- Liu, J-H.; Sato, T.; Hashimoto, M.; Seno, M.; Hirano, T. *European Polymer Journal* **2004**, *40*, 273.
- Li, J.; Yan, D.; Jiang, X.; Chen, Q. *Polymer* **2002**, *43*, 2625.
- Li, P., Rong F., Yuan C.W., *Polym. Int.* **2003**, *52*, 1799.
- Liu, J-H.; Lin, S-H.; Shih, J-C.; *J. Appl. Polym. Sci.* **2001**, *80*, 328.
- Li, Z.; Day, M.; Ding, J.; Faid K., *Macromolecules* **2005**, *38*, 2620.
- Maciejewski M.M., *J. Macromol. Sci. Chem.*, **1979**, *A13*, 77.

- Maciejewski, M.; Gwizdowski, A.; Peczak, P.; Pietrzak, A. *J. Macromol. Sci. Chem.* **1979**, A13, 1, 87-109.
- Magbitang, T. Huang, E.; Miller, R. D. *Adv. Mater.* **2001**, 13 (3), 204.
- Mao, R.; Liu, Y.; Huglin, M. B.; Holmes, P. A.; *Macromolecules* **1995**, 28, 6739.
- Mathew-Krotz, M.; Mahadevan, V.; *Macromol. Chem. Phys.* **1997**, 198, 1597.
- Matsui, J.; Nicholls, I. A. Karube, I.; Mosbach K. *J. Org. Chem.* **1996**; 61(16), 5414.
- Mecerreyes, D.; Lee, V.; Hawker, C. J.; Hedrick, J. L.; Wursch, A.; Volksen, W.;
- Miekeley, A. *Ber. Dtsch. Chem. Ges.* **1932**, 65, 69.
- Morris, G. M.; Goodsell, D. S.; Halliday, R. S.; Huey, R.; Hart, W. E.; Belew, R. K.;
- Olson, A. J. *J. Comput. Chem.* **1998**, 19, 1639.
- Mosbach, K.; Ramstrom, O. *Bio/Technology* **1996**, 14, 163.
- Nagelsdiek R., Mennicken M., Maier B., Keul H. and Hocker H. *Macromolecules*, **2004**, 37 (24), 8923.
- Nickel, A. L.; Seker, F.; Ziemer, B. P.; Ellis, A. B. *Chem. Mater.* **2001**, 13, 1391.
- Norell, M.C. Andersson, H. S. Nicholls, I. A. *J. Mol. Recogn.* **1998**, 11, 98.
- Odian, G. "Principles of polymerization", John Wiley and Sons Inc. New York, **1991**.
- Ogata N., Sanui K. Wada J., *J. Polym. Sci. Polym. Lett.*, **1976**, 14, 459.
- Okumura, H.; Okada, M.; Kawaguchi, Y.; Harada, A. *Macromolecules*, **2000**, 33(12), 4297.
- Patel A., Fouace S. and Steinke J. H. G. *Chem. Commun.* **2003**, 88.
- Perez N., Moral, A.G. Mayes, Langmuir **2004**, 20, 3775.
- Perez, N.; Whitcombe M. J.; Vulfson, E. N., *Journal of Applied Polymer Science*, **2000**, 77, 1851.
- Perez N., Whitcombe M.J., Vulfson E.N., *Macromolecules* **2001**, 34, 830.

- Pringsheim, H. *A Comprehensive Survey of Starch Chemistry*; Walton, R. P., Ed.; Chemical Catalogue Co., Inc.: New York, NY, **1928**; 35.
- Puoci, F. Iemma E., Muzzalupo R., Spizzirri U.G., Trombino S., Cassano R., Picci N., *Macromol. Biosci.* **2004**, *4*, 22.
- Rampey, A. M.; Umpleby, R. J.; Rushton, G. T.; Iseman, J. C.; Shah, R. N.; Shimizu, K. *D. Anal. Chem.* **2004**, *76*, 1123.
- Rao C.N.R. *Chemical applications of infrared spectroscopy*, Academic press, New York, **1963**, pp 209, 244-252.
- Rimmer, S.; Tattersall, P. *Polymer* **1999**, *40*, 6673.
- Ritger, P. L.; Pepps, N. A. *J. Controlled Release* **1987**, *5*, 23.
- Ritter H., Tabatabai M, *Prog. Polym. Sci.* **2002**, *27*, 1713.
- Ritter, H.; Tabatabai, M. *Prog. Polym. Sci.* **2002**, *27*, 1713.
- Rusa, C. C.; Bullions, T. A.; Fox, J.; Porbeni, F. E.; Wang, X.; Tonelli, A. E. *Langmuir* **2002**, *18*, 10016.
- Rusa, C. C.; Luca, C.; Tonelli, A. E. *Macromolecules* **2001**, *34*, 1318.
- Rusa, C. C.; Tonelli, A. E. *Macromolecules* **2000**, *33*, 5321.
- Saenger, W. *Angew. Chem. Int. Ed. Engl.* **1980**, *19*, 344.
- Saito, R.; Yamaguchi, K. *Macromolecules* **2005**, *38*, 2085.
- Sarvothaman, M. K.; Ritter, H. *Macromol. Rapid Commun.* **2004**, *25*, 1948.
- Satav, S. S.; Karmalkar, R. N.; Kulkarni, M. G.; Nagaraju, M.; Sastry. G. N. *J. Am. Chem. Soc.* **2006**, *128*, *24*, 7752.
- Satav, S. S.; Karmalkar, R. N.; Kulkarni, M. G.; Nagaraju, M.; Sastry. G. N. *Macromolecules* **2007**, *40*, 1824.
- Sato, T.; Hashimoto, M.; Seno, M.; Hirano, T. *Eur. Polym. J.* **2004**, *40*, 273.

- Sato, T.; Ihara, H.; Hirano, T.; Seno, M. *Polymer* **2004**, *45*, 7491.
- Schardinger, F. *Z. Unters. Nahr. u. Genussm.* **1903**, *6*, 865.
- Schardinger, F. *Zentralbl. Bakteriol. Parasitenk. Abt. 2* **1911**, *29*, 188.
- Schneider, H.-J.; Hacket, F.; Rudiger, V. *Chem. Rev.* **1998**, *98*, 1755-1785
- Schmid, G. *Trends Biotechnol.* **1989**, *7*, 2.
- Sellergren B, Andersson L. *J. Org. Chem.* **1990**. *55*, 3381.
- Sellergren, B. *Makromol. Chem.* **1989**, *190*, 2703.
- Sellergren B, *Anal. Chem.* **1994**, *66*, 1678.
- Sellergren, B. *J. Chromatogr A* **2001**, *906*, 227.
- Serra, L.; Domenech, J.; Pepas, N. *Biomaterials* **2006**, *27*, 5440.
- Shiraishi, Y.; Kojima, S.; Tomita, H.; Ohsuka, H.; Kawamura, T.; Toshima, N.; Hirai, H. *Polym. J.* **1996**, *28*, 619.
- Shea, K. J.; Dougberty, T. K. *J. Am. Chem. Soc.* **1986**, *108*, 1091
- Shea, K.J.; Sasaki, D.Y. *J. Am. Chem. Soc.* **1991**, *113*, 4109.
- Sibrian-Vazquez, M.; Spivak, D. A. *J. Org. Chem.* **2003**, *68*, 9604.
- Sibrian-Vazquez, M.; Spivak, D. A. *Macromolecules* **2003**, *36*, 5105.
- Sneshkoff, N.; Crabb, K.; BelBruno, J.; *J. Appl. Polym. Sci.* **2002**. *86*, 3611.
- Southard, G. E.; Houten, K. A. V.; Murray, M. *Macromolecules* **2007**, *40*, 1395.
- Soykan, C.; Erol, I. *European Polymer Journal* **2003**, *39*, 2261.
- Sreenivasan, K. *J. Appl. Polym. Sci.* **1999**, *71*, 1819.
- Srichana, T.; Suedee, R. *Drug Dev. Ind. Pharm.* **2001**, *27*, 457.
- Storsberg, J.; Ritter, H.; Pielartzik, H.; Groenendaal, L. *Adv. Mater.* **2000**, *12*, 567.
- Stockmayer, W. *J. Chem. Phys.* **1944**, *12*, 125.
- Stergiou, G.; Dousikos, P.; Pitsikalis, M. *European Polymer Journal* **2002**, *38*, 1963.

- Suedee, R.; Srichana, T.; Chotivatesin, R.; Martin, G.P. *Drug Dev. Ind. Pharm.* **2002**, *28*, 545.
- Suedee, R.; Srichana, T.; Rattananont, T.; *Drug Deliv.* **2002**, *9*, 19.
- Szejtli, J. *Chem. Rev.* **1998**, *98*, 1743-1753
- Szejtli, J., Osa, T., Eds. *Comprehensive Supramolecular Chemistry*; Pergamon: Oxford, **1996**; Vol. 3 (Cyclodextrins), p 693.
- Takahashi K. *Chem. Rev.* **1998**, *98*, 2013
- Takashima, Y.; Osaki, M.; Harada A. *J. Am. Chem. Soc.* **2004**, *126*, 13588.
- Takeuchi, T.; Mukawa, T.; Matsui, J.; Higashi, M.; Shimizu, K. D. *Anal. Chem.* **2001**, *73*(16), 3869.
- Tian, X. Q.; Holick, M. F. *J. Biol. Chem.* **1995**, *270*, 8706
- Tunc, Y.; Hasirci, N.; Yesilada, A.; Ulubayram, K. *Polymer* **2006**, *47*, 6931.
- Umpleby, R. J.; Baxter, S.C.; Chen, Y.; Shah, R. N.; Shimizu, K. D. *Anal. Chem.* **2001**, *73*, 4584.
- Vaihinger, D. Landfester, K.; Krauter, I. Brunner, H.; Gunter, E. Tovar, M. *Macromol. Chem. Phys.* **2002**, *203*, 1965.
- Van Nostrum Drug Discovery Today: Technologies, **2005**, *2* (1), 119.
- Villiers, A. *Compt. Rend.* **1891**, *112*, 536.
- Vlatakis, G.; Andersson, L. I. Muller, R. Mosbach, K. *Nature* **1993**, *361*, 641.
- Vulfson, E. N.; Alexander, C.; Whitcombe, M. J. *Chem Br* 1997, *33*, 23.
- Wang J.F., Cormack P.A.G., Sherrington D.C., Khoshdel E., *Angew. Chem., Int. Ed.* **2003**, *42*, 5336.
- Wen, X.; Liu, Z.; Zhu, T. *Chemical Physics Letters* **2005**, *405*, 114.

- Whitcombe, M. J.; Rodriguez, M. E.; Villar, P.; Vulfson E. N.; *J. Am. Chem. Soc.* **1995**, *117*(27),7105.
- Wulff, G. *Angew. Chem., Int. Ed. Engl.* **1995**, *34*, 1812.
- Wulff, G.; Gross, T.; Schonfeld, R. *Angew. Chem., Int. Ed. Engl.* **1997**, *36*, 1962.
- Wulff, G.; Vietmeier, J.; Poll, H.-G.; *Makromol. Chem.* **1987**, *188*, 731.
- Wulff, G.; Vietmeier, J. *Makromol. Chem.* **1989**,*190*, 1727.
- Yang, H-H Zhang, S-Q, Yang, W.; Chen, X-L.; Zhuang, Z-X.; Xu, J-G.; Wang, X-R.; *J. Am. Chem. Soc.* **2004**, *126*, 4054.
- Ye, L., Cormack, P.A.G., Mosbach, K., *Anal. Chim. Acta* **2001**, *435*, 187.
- Ye L., Mosbach K., *React. Funct. Polym.* **2001**, *48*, 149.
- Ye, L.; Cormack, P. A.G.; Mosbach, K., *Anal. Commun.*, **1999**, *36*, 35.
- Ye, L.; Weiss, R.; Mosbach, K.; *Macromolecules*, **2000**, *22*, 8239.
- Yoshimatsu, K.; Reimhult, K.; Krozer, A.; Mosbach, K.; Sode, K.; Ye, L. *Analytica Chimica Acta*, **2007**, *584*, (1), 112.
- Zhang Z.H., Liu Y.J., Long Y.M., Nie L.H., Yao S.Z., *Anal. Sci.* **2004**, *20*, 291
- Zhao T. and Beckham H.W., *Macromolecules* **2003**, *36*, 9859
- Zhu S. and Hamielec A. E., *Macromol. Chem. Macromol. Symp.* 1993, *69*, 247.
- Ziaee, F.; Nekoomanesh, M. *Polymer*, **1998**, *39*, 203.
- Zimmerman, S. C.; Lemcoff, N. G. *Chem. Commun.* **2004**, *5*.

List of Publications

Communications

1. Formation of linear polymers with pendant unsaturations via inclusion complex mediated polymerization of divinyl monomers. *J. Am. Chem. Soc.* **2006**, 128, 24, 7752-7753
2. Hydrogen bonding in trivinyl monomers: implications for inclusion complexation and polymerization. *Macromolecules*, **2007**, 40, 1824-1830
3. Template mediated binding enhancement overrides cross-linking effects in release from nanoparticles (Manuscript communicated)
4. Comonomers reactivity ratio : effect of inclusion complexation on the reactivity of multivinyl monomers. (Manuscript in preparation)

Patent Applications Published / Filed

1. Inclusion complexes of cyclic macromolecular organic compounds and polymerization thereof. **US20050032995**
2. Soluble polymers comprising unsaturation and process for preparation thereof. **US20050096443**
3. Imprinted nanotraps for sustained release. (Application filed)

Sunita Suryakant Satav

Institution Address

Room no. 937,
Polymer Science & Engg. Division,
National Chemical Laboratory (CSIR),
Homi Bhabha Road,
Pune 411 008, India.
Tel: +91-20-25902188/2186
Fax: + 91-20-25902618

Residential Address

Survey No. 14, Trupti Garden,
F-2, B-wing, Anand Nagar,
Wadgaon Budruk,
Pune 411 051, India.
Tel : +91-20-24345744
Mobile : 09850828044
Email : ss.satav@ncl.res.in
sssatav@gmail.com

Educational Background

Ph.D. (Polymer Science)

Thesis: Studies in polymerization comprising
supramolecular complexes July, 2007
Advisor: Dr. Mohan G. Kulkarni.
Head, Polymer Science & Engineering Division,
National Chemical Laboratory (CSIR), India.

Master of Science (Organic Chemistry)

S. P. College, Pune University, India July, 2001
First Class with Distinction

Bachelor of Science (Chemistry)

H. V. Desai College, Pune University, India April, 1999
First Class with Distinction

Awards and Fellowships

- **Second Prize** in "**Chemiad**" from Pune center in Pune University 1997.
- **National Merit Scholarship** for year 1999 - 2001 from Pune University.
- **Second Prize** in girls from Pune University in **Master of Science** (Organic chemistry) 2001.
- **Qualified** in Council of Scientific and Industrial Research (CSIR) **Junior research fellowship** (Conducted in July 2001).
- **First Prize** for "**Best Business Plan**" Competition organized by Human Resource Development Group, CSIR India and Indian Institute Management (IIM), Bangalore, 2004.

Research Interests

- Synthesis of novel polymer architectures
- Supramolecular host - guest chemistry
- Nanotechnology
- Molecular imprinting
- Drug delivery

Strengths

- A broad, interdisciplinary scientific background in organic, polymer, supramolecular chemistry, molecular imprinting and nanotechnology.
- A quantitative and analytical approach to synthesis of novel monomers, functional polymers and their characterization by instrumental techniques such as UV, NMR, FTIR, DSC, MALLS and GPC etc.
- Conversant with patent search, reading and drafting
- Excellent interpersonal skills and enjoy working with teams.

Technical Skills

1. Area of Expertise

Design and synthesis of functional monomers and polymers for molecular imprinting, optoelectronics, microlithography, nanocomposites, controlled drug delivery and nanotechnology.

2. Experimental Techniques

Acquainted with basic organic and polymer synthesis techniques. Hands on experience in handling equipments and analysis using FTIR, UV-Visible spectroscopy, DSC, TGA, GPC, MALLS and XRD.

3. Computer Proficiency

Skilled in the MS Office, Well acquainted with soft wares like Chem Draw, ACD specview.

Workshop Attended

Technology Entrepreneurship

Conducted by: Human Resource Development Group CSIR, India, and Indian Institute Management Bangalore (IIM) (2004) Venue: NCL, Pune, India.

Publications

Communications

- 1) **Sunita S. Satav**, Rohini N. Karmalkar, Mohan G. Kulkarni, M. Nagaraju, G. Narhari Sastry. "Formation of linear polymers with pendant unsaturations via inclusion complex mediated polymerization of divinyl monomers."
J. Am. Chem. Soc. 2006,128, 24, 7752-7753.
- 2) **Sunita S. Satav**, Rohini N. Karmalkar, Mohan G. Kulkarni, M. Nagaraju, G. Narhari Sastry. "Hydrogen bonding in trivinyl monomers: Implications for inclusion complexation and polymerization."
Macromolecules 2007, 40, 1824-1830.
- 3) **Sunita S. Satav**, Mohan G. Kulkarni, "Template mediated binding enhancement overrides cross-linking effects in diffusion of drug from nanoparticles." (Communicated)
- 4) **Sunita S. Satav**, Mohan G. Kulkarni, "Co-monomers reactivity ratio effect of inclusion complexation on the reactivity of multivinyl monomers." (Manuscript in preparation)

Patent Applications Published / Filed

- 1) Mohan G. Kulkarni, Rohini N. Karmalkar, **Sunita S. Satav**, "Inclusion complexes of cyclic macromolecular organic compounds and polymerization thereof." **US20050032995**
- 2) Mohan G. Kulkarni, Rohini N. Karmalkar, **Sunita S. Satav**, "Soluble polymers comprising unsaturation and process for preparation thereof."
US20050096443

- 3) Mohan G. Kulkarni, **Sunita S. Satav**, Satish C. Biradar, "Imprinted Nanotraps for sustained release." (Patent filed)

Conference Presentations

- 1) "Novel method for the synthesis of soluble polymers from divinyl monomers" presented in "Macro 2002" at IIT Kharagpure, India.
- 2) "Soluble polymers from divinyl monomers: methods and applications" invited at Society of Polymer Science (SPS) symposium 2003, NCL, Pune, India.
- 3) "Functional soluble polymers from cross-linkers via cyclodextrin host guest chemistry" invited at NCL-IITB meet 2006, NCL, Pune, India.

Poster Presentations

- 1) "Synthesis of novel cross-linked polymers: Mechanistic studies and applications" presented at Society of Polymer Science symposium 2003, NCL, Pune, India.
- 2) "Reactivity in free radical polymerization: Role of inclusion complexes" presented at "Macro 2006", NCL, Pune, India.
- 3) "Demystifying the supramolecular complexes: Switching reactivity in free radical polymerization" poster presented on National Science Day, 2007 at NCL, Pune, India.